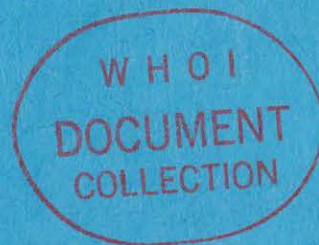


WHOI-81-91

copy 1

Woods Hole

*Oceanographic
Institution*



ACOUSTICALLY AND VISUALLY TRACKED DROGUE
MEASUREMENTS OF NEARSURFACE WATER VELOCITIES
IN LAKE HURON, PLUS OBSERVATIONS
OF A COASTAL UPWELLING

by

J. H. Churchill
and
B. H. Pade

October 1981

*Prepared for the Department of Energy under
Contract DE-AC02-79EV10005 and the National
Oceanic and Atmospheric Administration under
Contract 03-5-022-26.*

WOODS HOLE, MASSACHUSETTS 02543

copy 1

WHOI-81-91

ACOUSTICALLY AND VISUALLY TRACKED DROGUE MEASUREMENTS
OF NEARSURFACE WATER VELOCITIES IN
LAKE HURON, PLUS OBSERVATIONS OF A
COASTAL UPWELLING

by



J. H. Churchill
and
B. H. Pade



WOODS HOLE OCEANOGRAPHIC INSTITUTION
Woods Hole, Massachusetts 02543

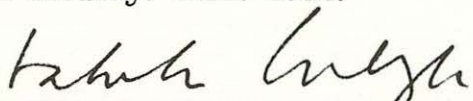
October 1981

TECHNICAL REPORT

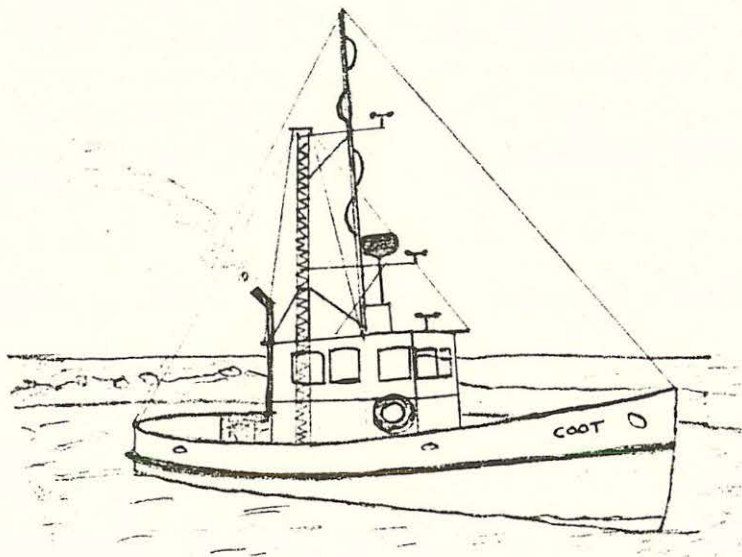
*Prepared for the Department of Energy under Contract
DE-AC02-79EV10005 and the National Oceanic and Atmos-
pheric Administration under Contract 03-5-022-26.*

*Reproduction in whole or in part is permitted for any
purpose of the United States Government. This report
should be cited as: Woods Hole Oceanog. Inst. Tech.
Rept. WHOI-81-91.*

Approved for Distribution:


Valentine Worthington, Chairman
Department of Physical Oceanography

BOTTOM PINGER ACOUSTIC DROGUE
LAKE HURON
EXPERIMENT



1980

B P A D E

ABSTRACT

During July and August of 1980 our research group measured nearsurface water velocities near the eastern coast of Lake Huron by tracking drogues using acoustic travel time and compass sighting techniques. The velocity fields appeared to consist of two components. These have been termed: a sub-current, which varied slowly with depth (compared to the deepest drogue depth of 5.2 m) and, in most cases, was apparently in geostrophic balance with the cross shore pressure gradient; and, a surface layer-current (defined by the relative velocity from deeper to shallower drogues) which decayed rapidly with depth and was directed nearly parallel with the wind and waves. There was no discernable relationship between wind speed and relative velocity. There was, however, a direct dependence of relative velocity with estimated surface roughness, suggesting that Stokes drift may have been primarily responsible for the shear. The magnitudes of the observed relative velocities were approximately equal to Stokes drift magnitudes calculated from representative wave energy spectra. Also reported are measurements of current and temperature structure made prior to and following a coastal upwelling.

TABLE OF CONTENTS

	Page
Abstract	2
1. INTRODUCTION	6
2. SIGHTED DROGUE EXPERIMENTS	6
2a. Measurement Technique	6
2b. Drogue Position and Velocity Calculation	11
2c. Correction of the Magnetic Bias of the Grebe	13
2d. Experimental Error	15
2e. Uncertainty in Drogue Speed Due to Baseline Length Error and Sighting Angle Error	17
2f. Averaging Speed, Direction and ERR2 Values of a Particular Cluster	20
2h. Results	21
2i. Discussion	36
3. ACOUSTIC DROGUE EXPERIMENTS	47
3a. Introduction	47
3b. Acoustic Navigation System	47
3c. Acoustic Drogue Assembly	50
3d. Wind Measurement	54
3e. Effects of Ray Bending	56
3f. Determination of Transponder Position	58
3g. Data Analysis	59
3h. Results	61
3i. Discussion	80
4. MEASUREMENTS OF WATER VELOCITY AND TEMPERATURE STRUCTURE PRIOR TO AND FOLLOWING A COASTAL UPWELLING	81
Acknowledgements	94
References	95
Appendix	

LIST OF TABLES

	Page
Table 1: Estimates of Errors Contributing to Drogue Velocity Uncertainty	16
Table 2: Key to Labels of Drogue Vectors in Figures 7-14 and 39	23
Table 3: 1.2 cm and 1.8 m Drogue Velocities, Relative Velocities (1.8 m to 1.2 cm), with Corresponding Wind Velocities and Estimated Surface Roughness of all Processed Sighted Drogue Runs	38
Table 4: Rotation Periods of Acoustic Drogues which Curved Clockwise, Calculated by Equation 19	73

LIST OF FIGURES

	Page
Figure 1: Field project site.	7
Figure 2: Sighted drogues.	9
Figure 3: Geometry of a drogue sighting	12
Figure 4: Geometry of a post retrieval sighting for compass bias calibration.	12
Figure 5: Compass correction data for August 14.	14
Figure 6: Drogue and ship positions for July 31, run 2.	19
Figure 7: Hodographs of drogue velocities and concurrent wind velocities.	24
Figure 8: Hodographs of drogue and wind velocities.	25
Figure 9: Hodographs of drogue and wind velocities.	26
Figure 10: Hodographs of drogue and wind velocities.	27
Figure 11: Hodographs of drogue and wind velocities.	28
Figure 12: Hodographs of drogue and wind velocities.	29
Figure 13: Hodographs of drogue and wind velocities.	30
Figure 14: Hodographs of drogue and wind velocities.	31
Figure 15: Hourly averages of wind velocity measured at a height of 10 m at Baie Du Doré.	32
Figure 16: Hourly averages of wind velocity measured at a height of 10 m at Baie Du Doré.	33
Figure 17: Magnitudes of relative velocities between the 1.8 m drogue and the 1.2 cm drogue graphed as a function of wind speed at 3 m.	40
Figure 18: Magnitudes of relative velocities between the 1.8 m drogue and the 1.2 cm drogue graphed as a function of estimated surface roughness.	42

LIST OF FIGURES (continued)

	Page
Figure 19: Two examples of wave energy spectra.	44
Figure 20: Computed and measured velocity profiles.	46
Figure 21: Geometry of the acoustic tracking system used in Lake Huron.	48
Figure 22: Assemblies of submerged drogues.	51
Figure 23: Surface acoustic drogue assemblies.	53
Figure 24: R/V Coot as equipped during the experiments.	55
Figure 25: Drogue and ship positions of the August 12 experiment.	63
Figure 26: Drogue and wind velocities of the August 12 experiment.	64
Figure 27: Drogue and ship positions of the August 14 experiment.	65
Figure 28: Drogue and wind velocities of the August 14 experiment.	66
Figure 29: Drogue and ship positions of the August 15 experiment.	67
Figure 30: Drogue and wind velocities of the August 15 experiment.	68
Figure 31: Drogue and ship positions of the August 20 experiment.	69
Figure 32: Drogue and wind velocities of the August 20 experiment.	70
Figure 33: Drogue and ship positions of the August 21 experiment.	71
Figure 34: Drogue and wind velocities of the August 21 experiment.	72
Figure 35: Wind data recorded during the August 20 drogue tracking experiment.	77
Figure 36: Wind data recorded during the August 21 drogue tracking experiment.	78
Figure 37: Temperature profile and horizontal velocities from measurements taken on August 17.	83
Figure 38: Temperature profile and horizontal velocities from measurements taken on August 17.	84
Figure 39: Hodographs of sighted drogue velocities (August 17).	85
Figure 40: Convergence of 10.2 cm slabs on the slick.	86
Figure 41: Temperature profile and horizontal velocities from measurements taken on August 18	87
Figure 42: Temperature profile and horizontal velocities from measurements taken on August 19.	88
Figure 43: Temperature profile and horizontal velocities from measurements taken on August 22.	89
Figure 44: Temperature profile and horizontal velocities from measurements taken on August 23.	90
Figure 45: Temperature profile and horizontal velocities from measurements taken on August 26.	91
Figure 46: Temperature profile and horizontal velocities from measurements taken on August 27.	92
Figure 47: Temperature profile and horizontal velocities from measurements taken on August 28.	93

1. INTRODUCTION

The nearsurface dynamics of the ocean and inland waters has been a topic of much attention in recent years. The importance of the nearsurface region cannot be understated. It is the path by which many pollutants, oil spills, deep ocean waste dumps, etc. enter the aquatic environment. Of equal significance are the exchange heat and momentum with the atmosphere. A physical comprehension of this region requires, along with other information, a knowledge of the velocity structure. Velocity measurement in very nearsurface water using conventional current meters is hampered by surface waves and, if deployed from a ship, by the effect of the ship. Typically very nearsurface currents are measured in a Lagrangian fashion by following a tracer such as dye or drogues.

During July and August of 1980, our research group conducted a series of drogue tracking experiments in Lake Huron offshore from the Bruce Nuclear Power Generating Station in Tiverton, Ontario (Figure 1). The project operated from the University of Toronto's Baie Du Doré Research Station and was run in conjunction with a field study by the Canada Centre for Inland Waters.

Two drogue tracking techniques were employed. One involved taking simultaneous compass bearings of drogues from two anchored vessels. The other method used an acoustic travel time navigation system to track drogues outfitted with hydrophones and VHF transmitting equipment. The use and results of each technique will be described in separate sections (2 and 3).

During mid-August a coastal upwelling event was studied using both types of drogues together with current meters. The results are discussed in section 4.

2. SIGHTED DROGUE EXPERIMENTS

2a. Measurement Technique

The basic procedure of these experiments was to take simultaneous bearings on drogues, submerged to various mean depths, from two anchored vessels which were separated by a measured distance. A set of similar experiments was carried out in Cape Cod Bay and is reported by Churchill and Pade (1980).

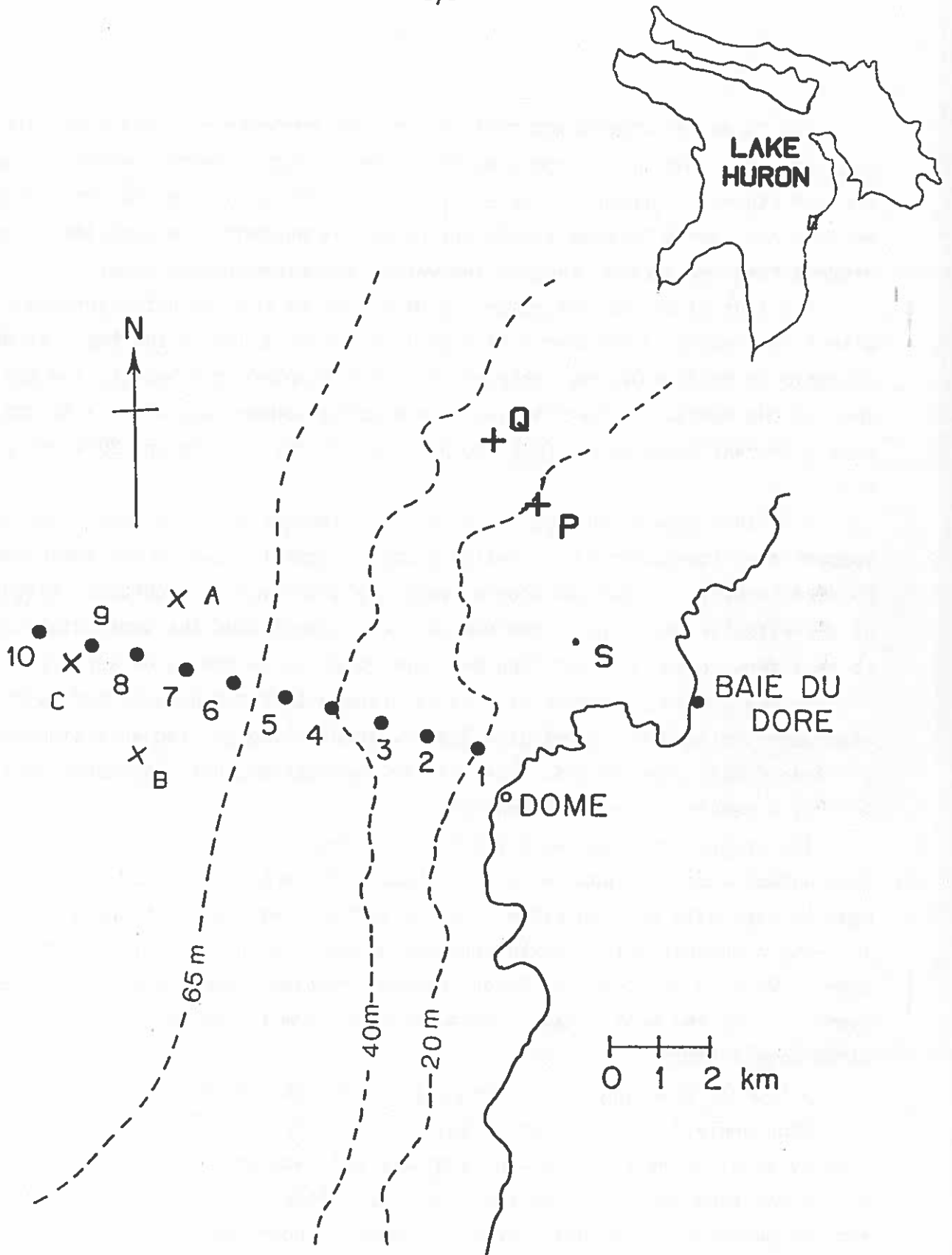


Figure 1: Field project site. Circles labeled 1-10 mark Flag stations; X's labeled A, B and C depict bottom transponder locations; +'s labeled P and Q show locations of sighted drogue experiments. Flag station numbers are equivalent to the distances of the stations, in km, from shore.

Two types of drogues and silicone treated confetti were tracked. The drogues were constructed from a material consisting of densely entwined rubberized strands, "synthetic horsehair", often used as packing matter. Such drogues can easily be made stable and neutrally buoyant. In addition, they offer a large contact surface to the water, ensuring minimum slip.

One type of drogue was comprised of a slab of the synthetic horsehair with a thin pad (~ 4 mm thick) of Dupont microfoam glued to the top. It was designed to drift with the horsehair material completely submerged and the pad just at the surface. The slab was of horizontal dimensions 20 cm x 20 cm; five different thicknesses (2.4 cm, 5.0 cm, 7.6 cm, 10.2 cm and 20.4 cm) were used.

The other type of drogue was a 40.5 cm diameter by 11 cm disk which was supported at the surface by a sealed plastic eggshell (5.5 cm maximum diameter by 8 cm length). These two drogue types are displayed in Figure 2. Drogues of a particular depth had microfoam pads or eggshells of the same unique color so that they could be identified by observation above the water surface.

In the ensuing analysis it will be assumed that the drogues followed the mean water motion at a particular depth without slippage, and were stable in all wave fields experienced. Qualitative observations have indicated that this is a reasonably good assumption.

The vessels involved were the Punt and Grebe II. The Punt is a low, 6 m long outboard powered boat with a 2 m beam. The Grebe II is a 8 m long by 3 m beam cruiser with an open cabin. It was equipped with a winch and davits for lowering a current meter and temperature sensor. Both boats are entirely steel. As will be discussed later, compass readings from the Punt were nearly unaffected by the boat's mass. Magnetic bias from the Grebe was, however, often significant.

A typical tracking session (run) proceeded as follows:

Upon arrival at the experimental site, the Grebe either set anchor or tied up to a moored flag station (stations are labeled 1-10 in Figure 1). A drogue was then deployed from the Grebe and, after sufficient time, its bearing was measured. The Punt's crew attempted to position the boat such that the baseline between the two vessels was 30° - 45° with respect to the drogue's

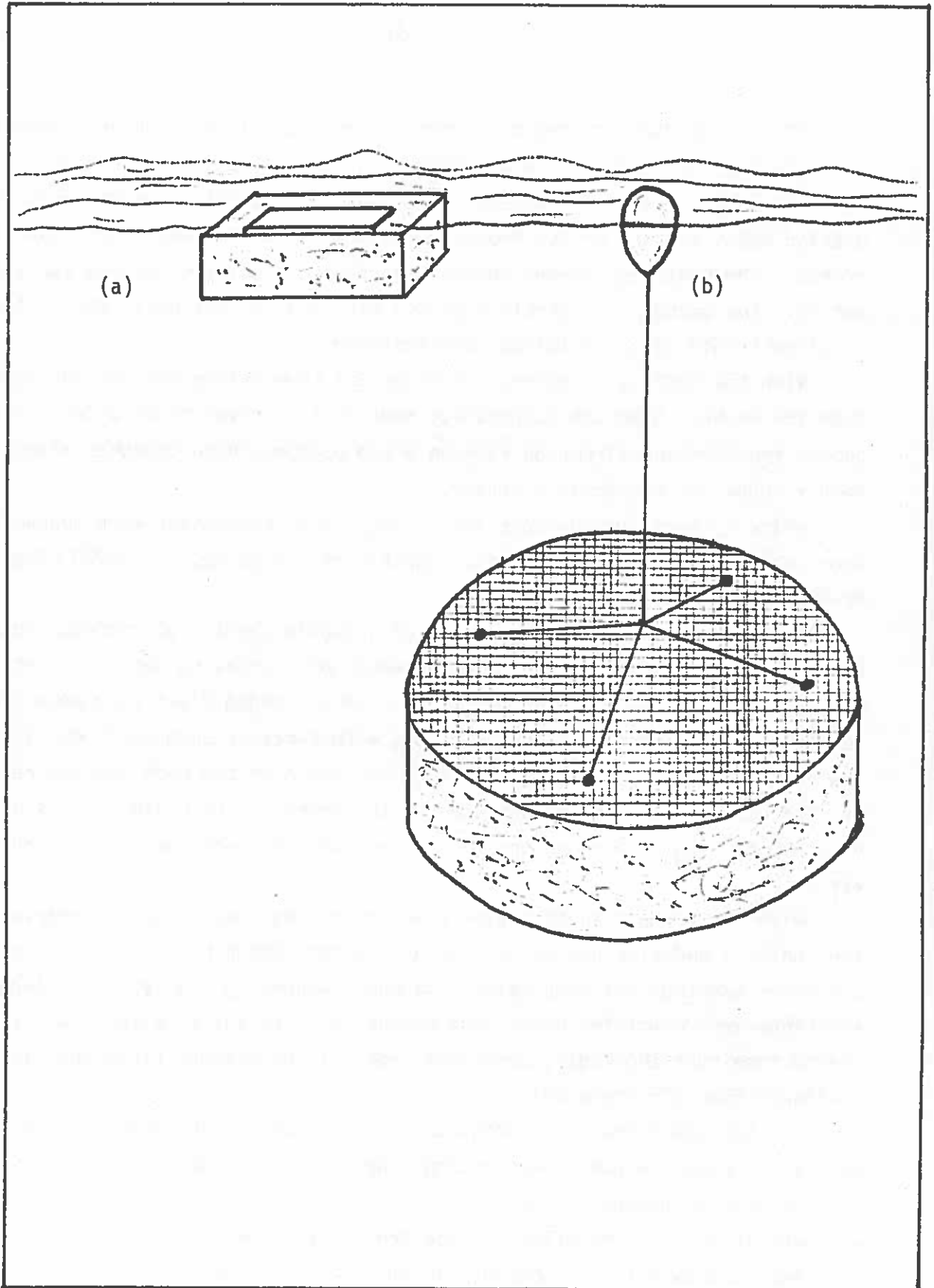


Figure 2: Sighted drogues: (a) surface slab; (b) submerged disk.

trajectory. As demonstrated by Churchill and Pade (1980) such an orientation is optimal for relatively low uncertainty of drogue position and velocity determination. To set the baseline the Punt motored away from the Grebe at a bearing opposite that of the drogue's trajectory for a distance of about 300 meters. The Punt then turned roughly 90° to the right and motored about 40 meters. The anchor was quickly deployed and line let out until the desired baseline length and orientation were achieved.

With the Punt so occupied, a current and temperature profile was taken from the Grebe. A Bendix Corporation model Q-15 current meter, which has a ducted impeller and direction vane on a 1 m boom, was used together with a Bendix model D-1 temperature sensor.

Prior to each run the baseline's length and orientation were measured from both boats using telescoping range finders (Ranging, Inc. 1000 Rangematic MK-5) and hand held compasses.

A run commenced with the release of a double handful of confetti from the Punt. The slabs were then released in order of increasing depth. Generally five slabs of each depth were deployed. The submerged disks were next released, again in increasing depth order, with three of each depth deployed. The drogues were generally set out from the stern of the Punt and the release of each depth group was communicated to the Grebe via CB radio. Times of deployment, read from synchronized digital watches, were recorded aboard both vessels.

With all drogues in the water simultaneous hand held compass bearings on the confetti and clusters of drogues of the same depth began. The confetti was never sighted more than twice in a run. Generally 2-5 cycles of drogue sightings were completed before the drogues drifted out of visual range. During some runs the Punt's crew lost sight of the drogues first and sightings continued from the Grebe only.

At the completion of tracking the baseline was again measured from both vessels. Drogue retrieval was accomplished using the Punt.

On some occasions, while the Punt returned to its anchor buoy, an attempt was made to measure the effect of the Grebe's mass on the compass bearings. This was done by motoring the Punt in approximately the same path as followed

by the drogues. At several locations simultaneous bearings were taken from each ship on the other. The values were used to correct the drogue bearings taken from the Grebe, as will be described in Section 2c, by assuming that bearings from the Punt were always magnetically correct.

Before and after each run wind speed and direction were measured from the Grebe. The speed was measured using a 3 cup anemometer mounted at a height of about 3 m above the water and 1 m above the cabin. The wind direction was taken as the boat's heading plus any difference noted from a vane held at the vessel's bow.

2b. Drogue Position and Velocity Calculation

Figure 3 diagrams the sighting of a cluster of drogues at location d by two ships at positions 1 and 2 (Punt and Grebe respectively). The baseline length (D12) and its orientation as measured by either ship (β_{12} and β_{21}) are taken as averages of the values measured before and after each run. The bearings α_1 and α_2 are taken simultaneously.

The distance the cluster has traveled since release, D1d, can be found by noting that:

$$\frac{D1d}{\sin(A2)} = \frac{D12}{\sin(A3)} = \frac{D12}{\sin(A1+A2)}$$

which gives:

$$(1) \quad D1d = D12 \frac{\sin(A2)}{\sin(A1+A2)}$$

where A1 and A2 are the drogue bearings from each ship with respect to the baseline.

If the sighting takes place at a time, T, after the drogues' release then the speed since release is simply:

$$(2) \quad SP = \frac{D1d}{T}$$

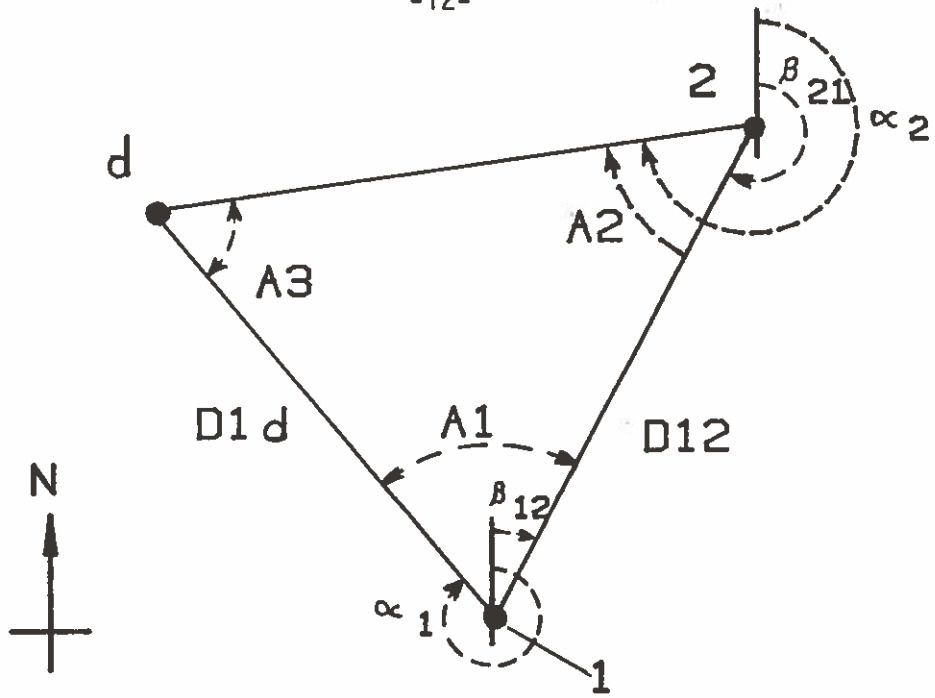


Figure 3: Geometry of a drogue sighting.

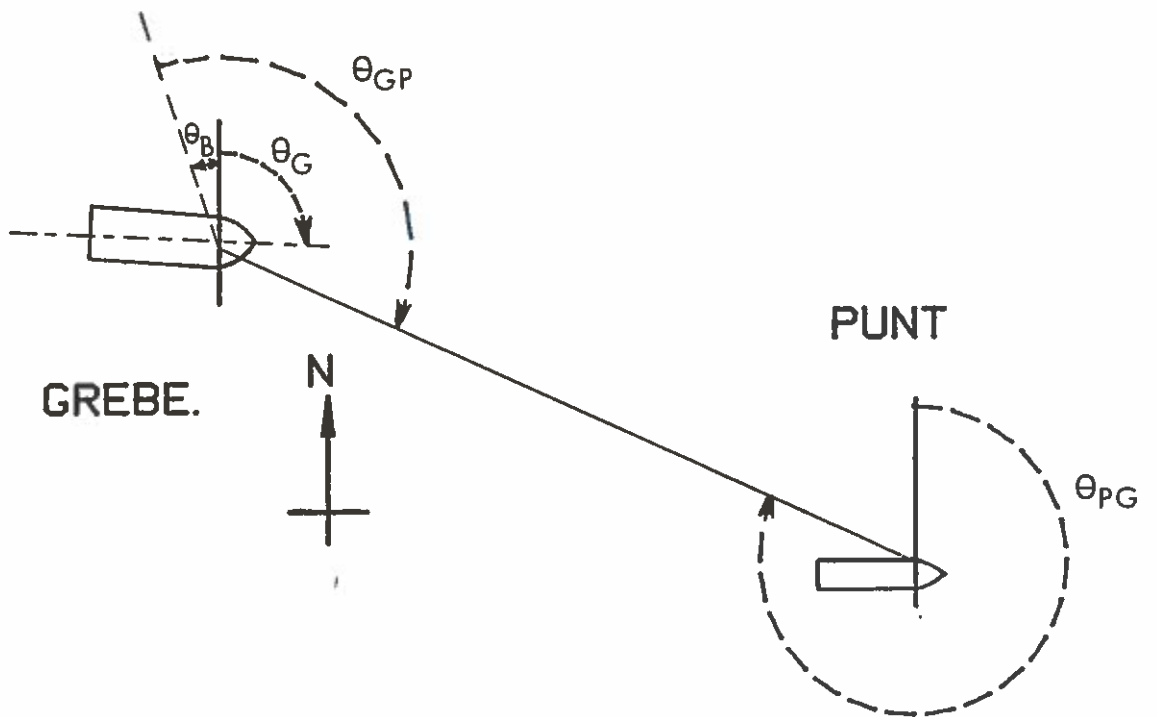


Figure 4: Geometry of a post-retrieval sighting for compass bias calibration.

The direction at which the drogue cluster has traveled is α_1 plus the local magnetic deviation (-6° at the project site).

It is worthwhile to note that prior to the experiments a method was devised to compute the position of a drogue simultaneously sighted from three vessels. The drogue position, which optimally satisfied an overdetermined set of equations, was calculated using a nonlinear regression technique. Sightings from three vessels were never conducted, however, because the necessary boats and personnel were never available at one time.

2c. Correction of the Magnetic Bias of the Grebe

For a few runs bearings taken from the Grebe were corrected for magnetic bias using the post retrieval compass correction data. Figure 4 depicts the geometry of a typical post-retrieval sighting. θ_{PG} and θ_{GP} are simultaneous bearings from the Punt and Grebe respectively. θ_G is the Grebe's heading as measured by the boat's compass (tests have shown that this bearing is magnetically correct). Assuming that the bearing from the Punt is unbiased, the bias in the bearing taken from the Grebe is:

$$\theta_B = \theta_{PG} + 180^\circ - \theta_{GP}$$

A set of these values, measured on August 14, is plotted against θ_2 in Figure 5; where θ_2 is the bearing of the Punt with respect to the Grebe, i.e. $\theta_2 = \theta_{GP} - \theta_G$. The piecewise linear function fit to these points was used to calculate A_2 , used in equation (1), according to:

$$(3) \quad A_2 = \alpha_2 + \text{FPL}(\alpha_2 - \theta_G) - [\beta_{21} + \text{FPL}(\beta_{21} - \theta_G)]$$

where FPL is the piecewise linear function, α_2 and β_{21} are as defined in Figure 3, and θ_G is the Grebe's heading which was recorded as part of the wind direction measurement. Simply stated, the above equation defines the angle of the drogue with respect to the baseline as the corrected drogue bearing minus the corrected baseline bearing.

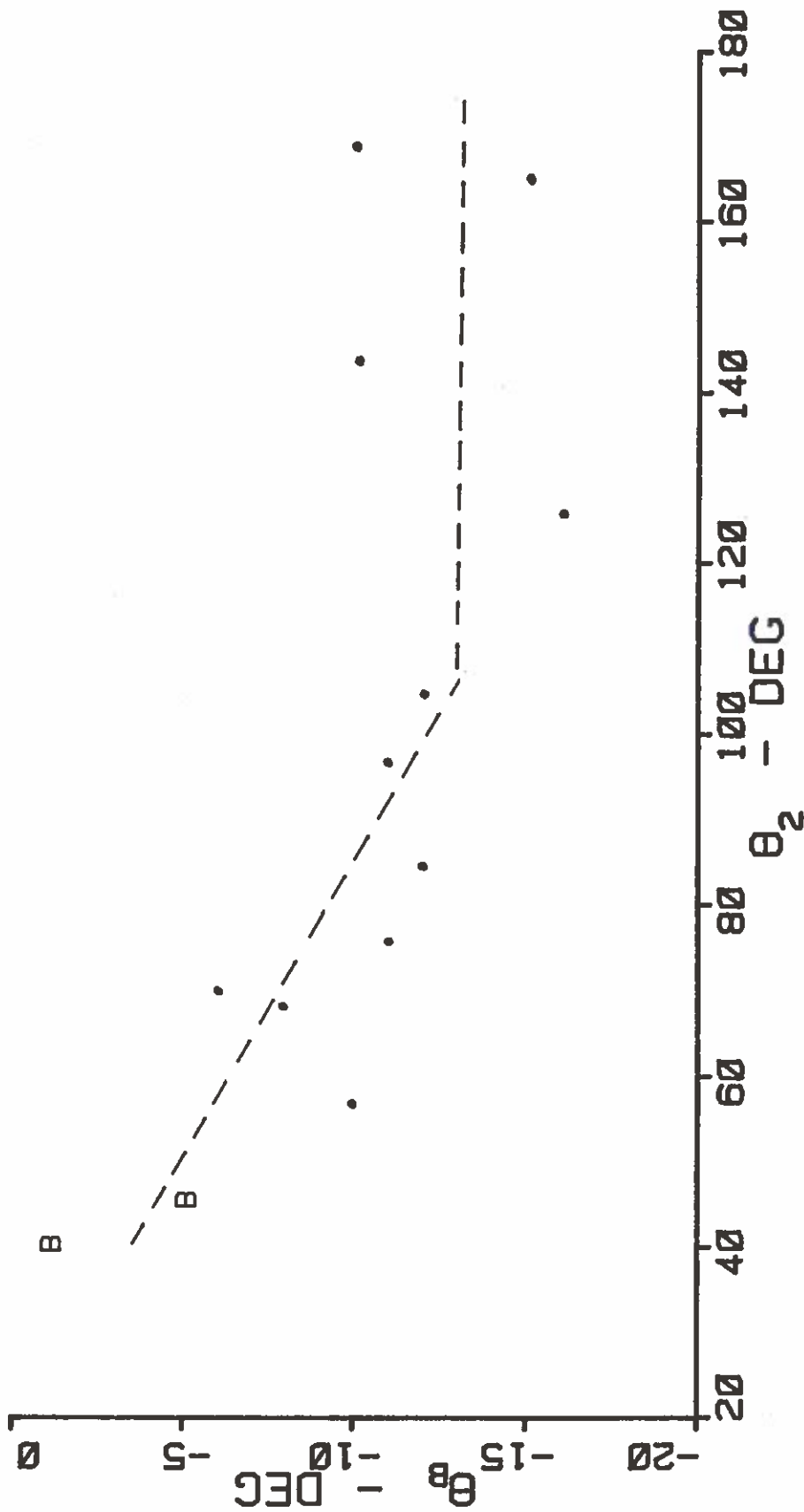


Figure 5: Compass correction data for August 14. Dots represent post-retrieval sightings, B's are baseline sightings. The dashed line is the piecewise linear correction function, $F_{PL}(\theta_2)$ of eq. (3).

2d. Experimental Error

The primary sources of error contributing to uncertainty in drogue position and velocity were compass errors and inaccuracy in measuring the baseline length.

A shorebased check of the range finders used to measure the baseline distance indicated an accuracy of about 10 percent.

The compass error was variable depending on the location from which the bearings were taken and the existing lake conditions. A major source of concern was the effect of the steel from which both boats were constructed.

An assembly was mounted aboard the Punt which allowed bearings to be taken while standing atop one of the seats. With the Punt at dockside, bearings were taken from this position to various points on shore, and from these shore locations to the Punt. The results indicated that bearings made from the Punt were not magnetically biased.

Drogue bearings from the Grebe were taken at three locations. On calm days sightings were made while standing atop the bow. Studies similar to that described above have indicated that such bearings had very little magnetic effect from the ship.

On rough days in August sightings were taken while standing atop a box mounted near the bow. The ship had a marked effect on bearings taken from this position as was shown in Figure 5. For all such runs, however, post retrieval correction data was used to correct for the magnetic bias.

In July rough weather bearings were taken while standing on the deck at the bow. The effect of the ship on these bearings was significant. Unfortunately, no post retrieval compass correction runs were conducted. In August attempts were made at collecting data to apply to the July runs. However, no satisfactory data was obtained with the Grebe at the same heading as during the July runs.

Table 1 tabulates magnitudes of the various errors discussed above.

Another source of bearings' error was a shift in baseline during a run. For all runs which were eventually processed this was very small, most commonly $\pm 1^\circ$ or $\pm 2^\circ$ about the average.

Table 1

Estimates of Errors Contributing to Drogue Velocity Uncertainty

Instrument	Location of Measurement	Errors		Comments
		Calm Weather	Rough Weather	
Range finder	Punt/Grebe	10° / °	10° / °	
Compass	Punt	±3°	±5°	No magnetic bias
Compass	Top of Grebe's bow	±3°	Not attempted	No magnetic bias
Compass	From atop box at Grebe's bow	±5°	±8°	Compass correction applied
Compass	From deck at Grebe's bow	±12°	±15°	Magnetically biased

Ship to shore and vice versa bearings have indicated that the Grebe's ship compass, used for the wind direction measurements, was unbiased by the ship's mass. The wind direction measurement has an estimated uncertainty of $\pm 10^\circ$. This figure would be slightly less on days when the Grebe's heading was steady, which was commonly the case when the wind and current were strong and in line. It would be slightly greater on days when heading varied erratically. The accuracy of the wind speed measurement was about 10 percent, with most of the uncertainty due to gustiness.

The speed and direction of the current meter measurements were accurate to about 5 cm/s and 10 deg. The temperature measurement had an uncertainty of 0.2 deg.

2e. Uncertainty in Drogue Speed Due to Baseline Length Error and Sighting Angle Error

As noted the baseline length has an uncertainty of about 10 percent. As can be seen from equations (1) and (2) this translates to a 10 percent error in drogue speed. This uncertainty has no effect on the drogues' heading; and, for a particular run, all speeds are affected in the same proportion.

The contribution to speed uncertainty due to an uncertainty of value $\Delta A2$ in the sighting angle $A2$ can be expressed as a Taylor series. A first term only approximation is:

$$(4) \quad (\Delta SP)_{A2} \approx \frac{\partial SP}{\partial A2} \Delta A2$$

The uncertainty estimate in speed due to a 1 degree uncertainty in $A2$ will be termed ERR2 and is given by:

$$ERR2 = \frac{\partial SP}{\partial A2} \frac{\pi}{180} = \frac{1}{T} \frac{\pi}{180} \frac{\partial D1d}{\partial A2}$$

Using equation (1):

$$(5) \quad ERR2 = \frac{\pi}{180} \frac{D12}{T} \frac{\sin(A1)}{\sin^2(A1+A2)}$$

This expression was examined as a function of A1, A2 and distance from point of release by Churchill and Pade (1980).

The estimate of speed uncertainty due to a 1° uncertainty in A1 is given by:

$$(6) \quad \text{ERR1} = \frac{\pi}{180} \frac{D12}{T} \frac{\sin(A2) \cos(A1+A2)}{\sin^2(A1+A2)}$$

A computer program has been developed which, for each sighting, calculates: the drogue's geographic position (coordinate origin at the Punt), the velocity since release, ERR1 and ERR2 by use of equations (1), (2), (5), and (6). A plot of drogue and ship positions, such as that of Figure 6, is also generated.

It was observed that, typically, ERR1 and ERR2 were proportional with ERR2 being greater. As demonstrated by Table 1 the uncertainties in bearings from the Grebe were greater than those from the Punt. The dominant contribution to speed uncertainty due to compass related error was thus that resulting from the uncertainty in bearings from the Grebe.

For cases where the magnetic bias of the Grebe is either poorly or not corrected, the uncertainty in relative velocity magnitude between drogues of different depths may be better than would be inferred by the uncertainty of the respective speeds.

Very commonly, all bearings from the Grebe during a cycle (this refers to a period during which all drogues are sighted in succession) have about the same value. This is demonstrated by Figure 6 which shows drogue positions during each cycle to form a cluster. The uncertainty in A2 can be separated into two parts: one due to magnetic bias, $\Delta A2_B$; and the other due to the accuracy at which the compass can be read, $\Delta A2_C$. Consider sightings during a particular cycle on drogues a and b. The possible range of the measured speed of a can be approximated by:

$$SP_{Ma} \approx SP_{Ta} + \text{ERR2}_a \Delta A2_{Ba} \pm \text{ERR2}_a \Delta A2_C \pm \Delta_a$$

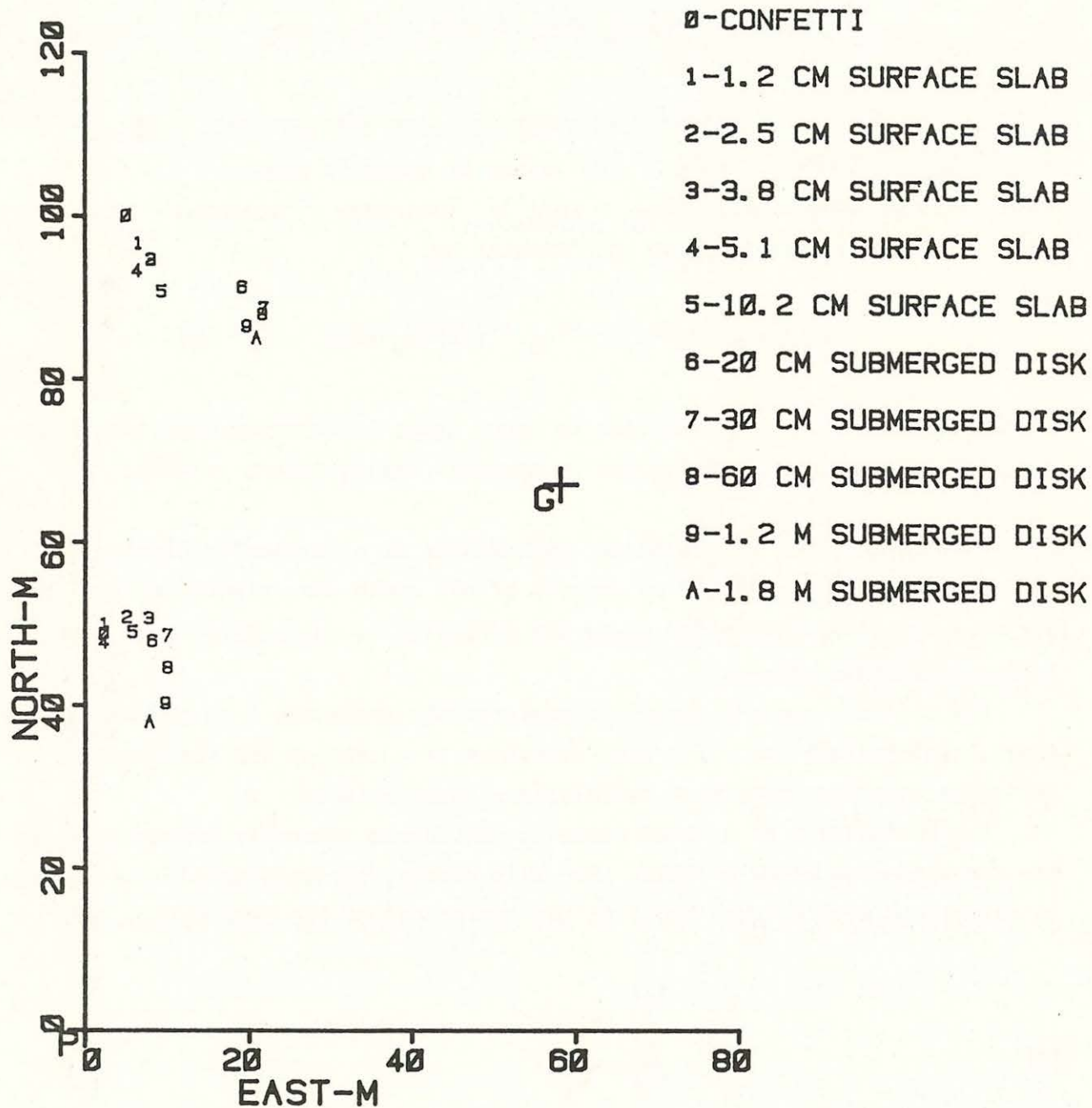


Figure 6: Drogue and ship positions for July 31 run 2. The coordinate origin is at the punt's location. The Grebe's position is marked by a cross labeled G.

where SP_{Ta} is the true speed since release and Δ_a is the uncertainty from sources other than errors in the bearing from the Grebe. Similarly for drogue b:

$$SP_{Mb} \approx SP_{Tb} + ERR2_b \Delta A2_{Bb} \pm ERR2_b \Delta A2_C \pm \Delta_b$$

If the drogues are sighted at about the same bearings ($A1_a \approx A1_b$, $A2_a \approx A2_b$) then $ERR2_b \approx ERR2_a$. The values of magnetic bias would also be about equal ($\Delta A2_{Bb} \approx \Delta A2_{Ba}$). The range of measured speed difference could thus be approximated by:

$$SP_{Ma} - SP_{Mb} \approx SP_{Ta} - SP_{Tb} \pm (2ERR2_b \Delta A2_C + \Delta_a + \Delta_b)$$

which states that the contribution to speed shear uncertainty resulting from the Grebe's bearings is mostly due to compass reading errors ($\sim \pm 5^\circ$).

2f. Averaging Speed, Direction and ERR2 Values of a Particular Cluster

As mentioned, a cluster of drogues of one depth were sighted up to 5 times during a run. Representative speed and direction of the cluster have been taken as averaged values.

For a single run all direction measurements (bearings from the Punt) have about equal reliability. The mean direction of a cluster and its standard deviation have therefore been calculated without weights.

The reliability of a speed value is considered inversely proportional to the corresponding value of ERR2. For this reason, the mean speed of a cluster is calculated with weights equal to the reciprocal of the ERR2 values, or:

$$(7) \quad SP = \frac{\sum_{i=1}^N SP_i W_i}{\sum_{i=1}^N W_i}$$

where N = number of sightings on the cluster during the run

SP_i = the speed since release at sighting No. i

$$W_i = \frac{1}{ERR2_i}$$

The standard deviation about this mean is [Brown, (1977)]:

$$(8) \quad (ST\ DEV)_{\overline{SP}} = \left[\frac{\sum_{i=1}^N W_i (SP_i - \overline{SP})^2}{(1-1/N) \sum_{i=1}^N W_i} \right]^{1/2}$$

The mean contribution of a 1 degree error in $A2$ to the uncertainty of \overline{SP} is approximated by the weighted mean of $ERR2$, which is:

$$\overline{ERR2} = \frac{\sum_{i=1}^N ERR2_i W_i}{\sum_{i=1}^N W_i}$$

or more simply

$$(9) \quad \overline{ERR2} = \frac{N}{\sum_{i=1}^N (1/ERR2_i)}$$

2h. Results

A total of 21 sighted drogue runs were processed. Run by run listings of averaged drogue speeds, directions and $ERR2$ values together with the standard deviations of speed and direction [calculated using equations (1), (2), (5), (7), (8), and (9)] are given in Tables A1-A21 of the Appendix. Also listed

are the location and starting time of each run, the position on the Grebe from which sightings were taken, the estimated wave height, and the measured wind velocity. Concurrent temperature and current meter profiles, measured from the Grebe, are listed in Table A22 of the Appendix. Unfortunately, because of instrument malfunction, the current meter profile is often missing. Drogue velocity vectors (labeled as described in Table 2) and wind vectors are displayed in Figures 7-14.

Figures 15 and 16 display a time series of wind for the period during which sighted drogue runs were conducted. This record was measured by an anemometer mounted 10 m above the water surface on a tower at the end of the causeway leading to the Baie Du Doré docking facility (Fig. 1). Speed and direction were recorded as hourly averages, with the direction given in 45° increments (N, NE, E, etc.). So that strong wind events can be easily identified, wind vectors with magnitude exceeding 20 km/hr are terminated with an arrowhead. The time of each sighted drogue run is indicated on the time axis. Rough agreement has been observed between the wind measured during the sighted drogue runs and the corresponding shore-base measurement.

An examination of each day of sighted drogue results with consideration of the wind history follows.

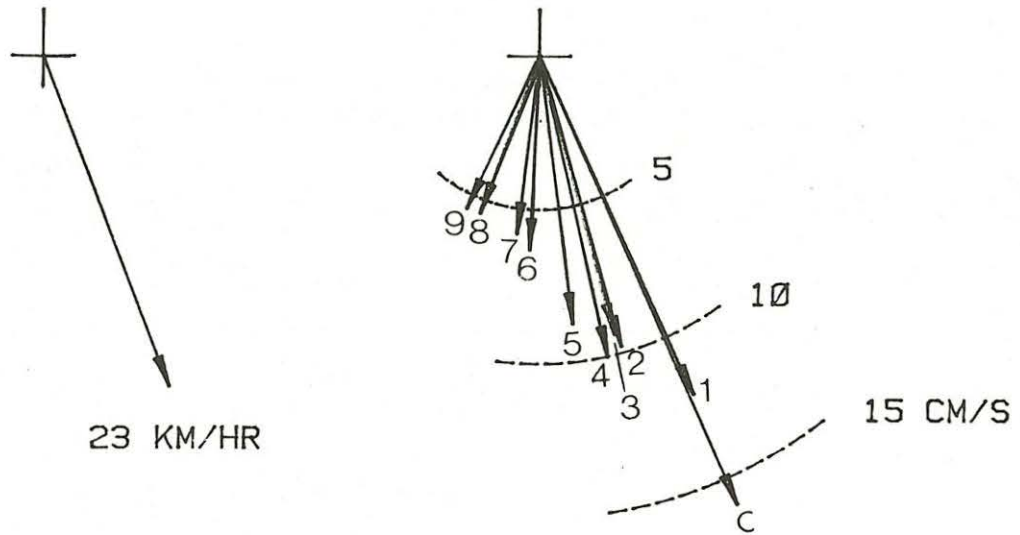
For a number of days prior to July 23, the first day of drogue tracking, strong winds were predominately from the south. During July 23, the wind dramatically shifted to a north wind. On the morning of that day our team attempted to track drogues at site P of Figure 1. The slabs had almost no motion; whereas, the submerged disks moved very slowly in a direction opposite to the wind. The current meter profile (Table A22a) showed a very weak current in the approximate wind direction at 2 m depth, and a stronger current, opposite to the wind, from 4 m to the thermocline (10 m). This deeper current was also in the direction of the strong winds during previous days.

When tracking resumed after lunch, the wind was noticeably stronger and the lake was extremely rough, which made sightings difficult. Results of the only processed run of this day are given in Table A1 and Figure 7. The shallowest velocities (1.2 cm drogue and confetti) were roughly in the wind direction. With increasing depth the velocity vectors rotated clockwise, towards

Table 2
Key to Labels of Drogue Vectors
in Figures 7-14 and 39

LABEL	DROGUE (MEAN DEPTH)
C	Confetti
1	1.2 cm Surface Slab
2	2.5 cm Surface Slab
3	3.8 cm Surface Slab
4	5.1 cm Surface Slab
5	10.2 cm Surface Slab
6	20 cm Submerged Disk
7	30 cm Submerged Disk
8	60 cm Submerged Disk
9	120 cm Submerged Disk
10	180 cm Submerged Disk

JULY 23 RUN 5



JULY 24 RUN 2

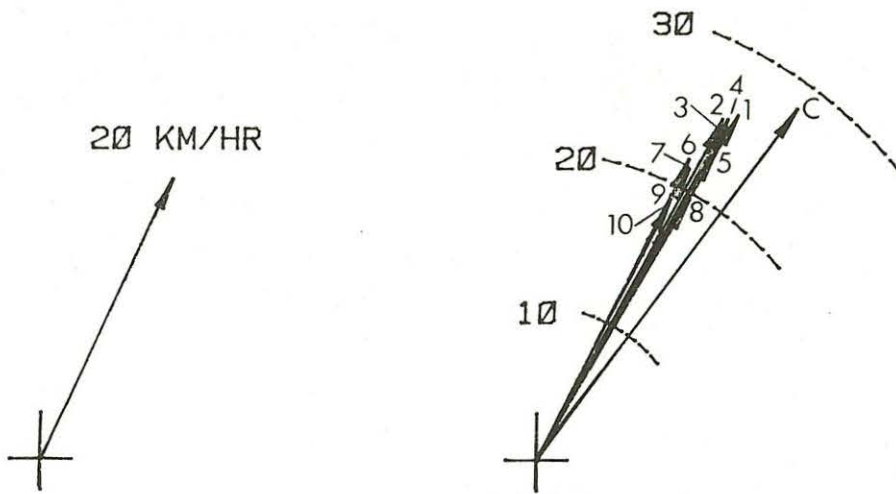
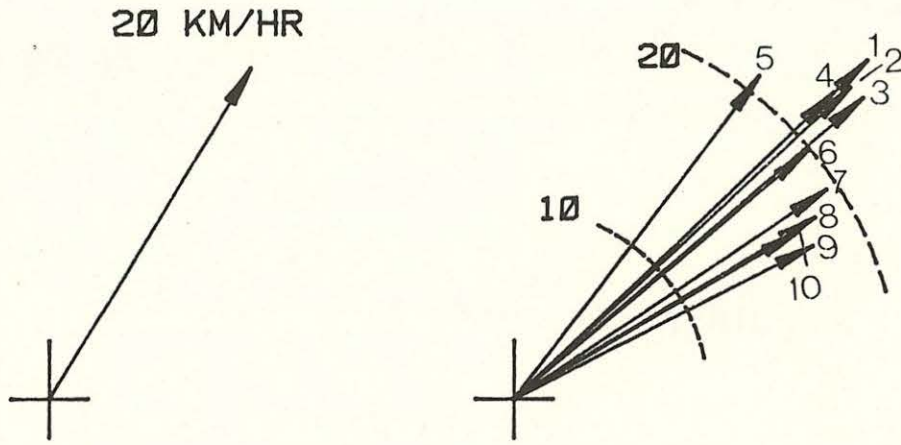


Figure 7: At right are hodographs of drogue velocities labeled according to Table 2 . The vectors at the left represent concurrent wind velocities.

JULY 25 RUN 2



JULY 25 RUN 3

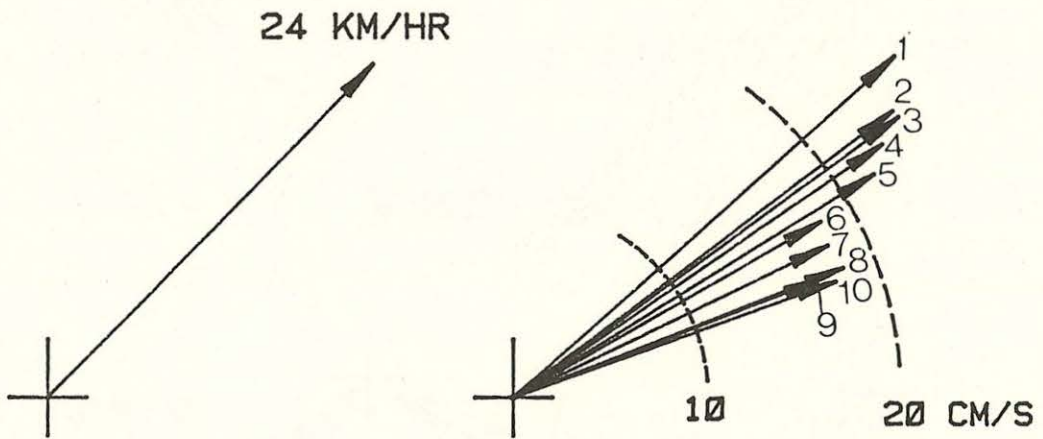
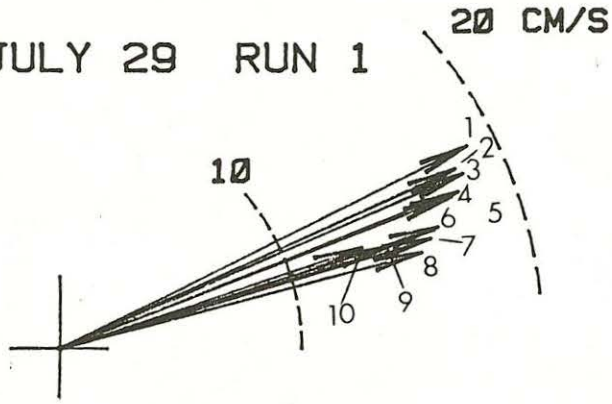
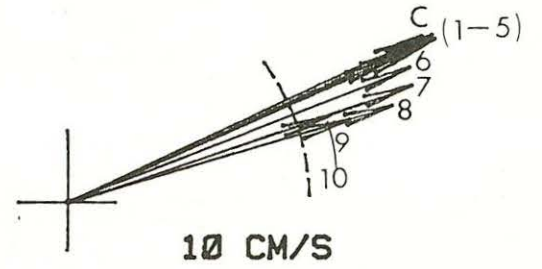


Figure 8: Hodographs of drogue and wind velocities.

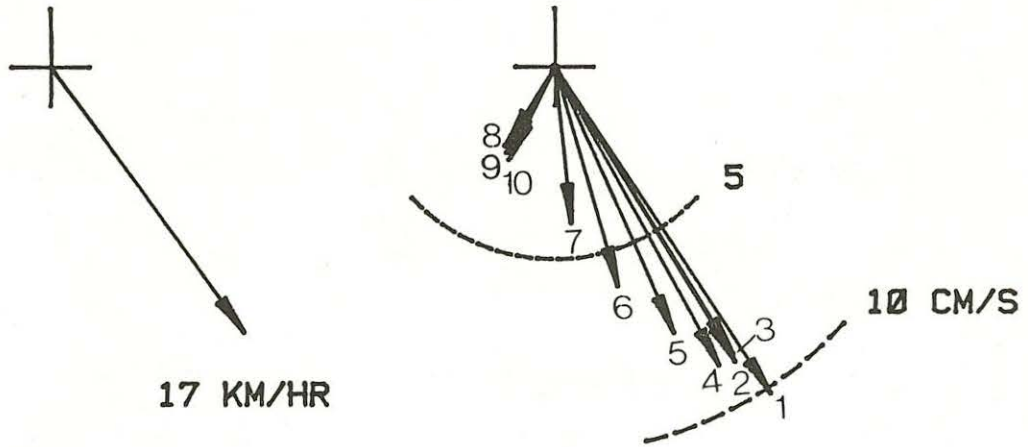
JULY 29 RUN 1



JULY 29 RUN 2



JULY 30 RUN 1



JULY 30 RUN 2

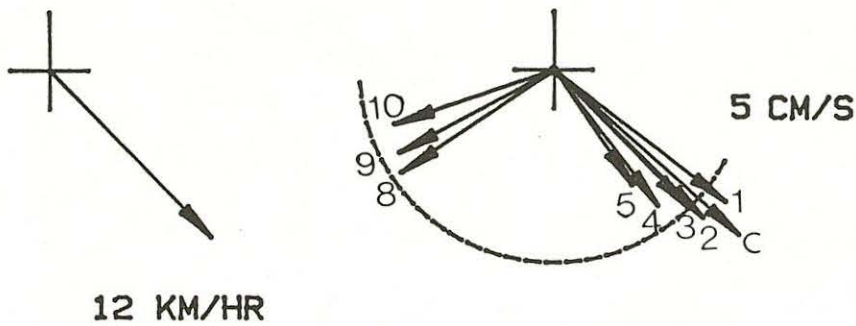
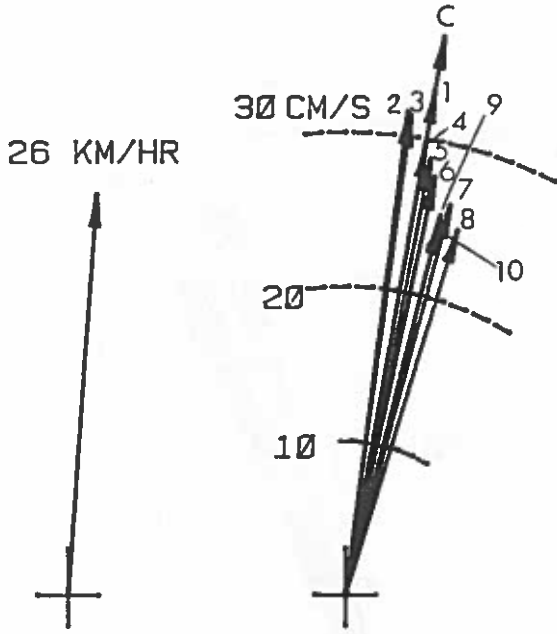
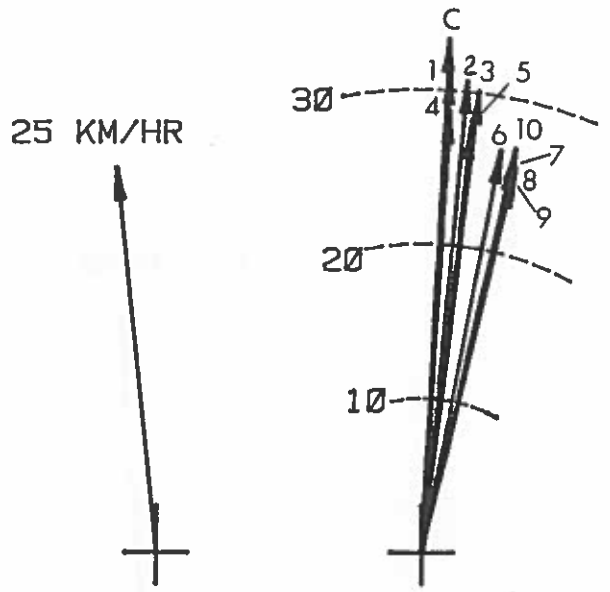


Figure 9: Hodographs of drogue and wind velocities.

JULY 31 RUN 1



JULY 31 RUN 2



JULY 31 RUN 3

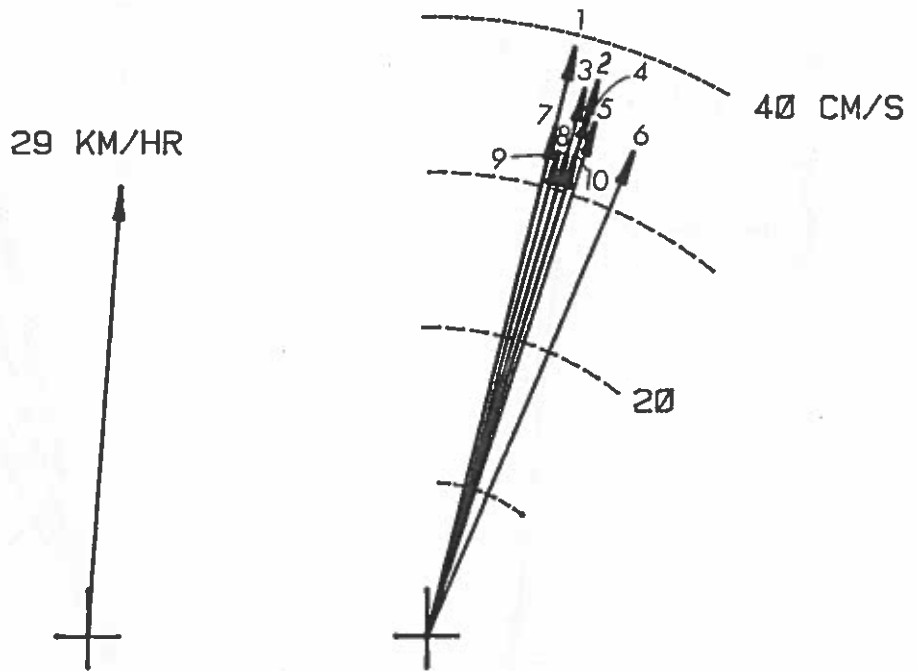
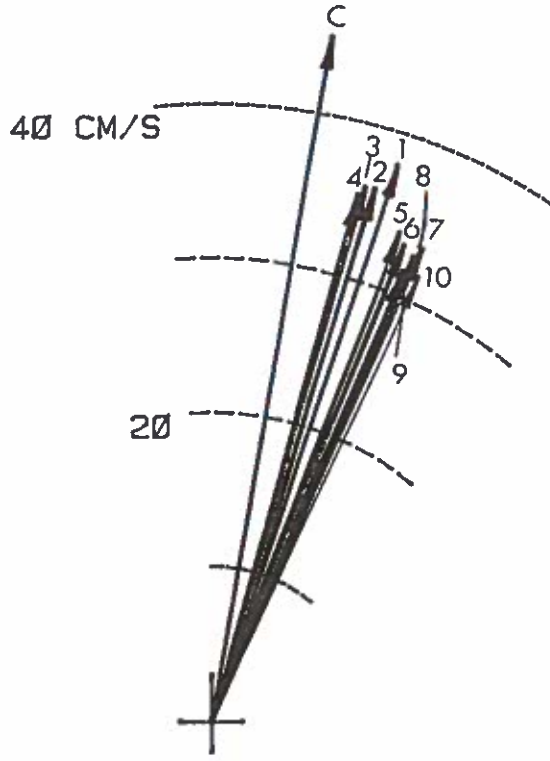


Figure 10: Hodographs of drogue and wind velocities.

JULY 31 RUN 4

25 KM/HR



JULY 31 RUN 5

28 KM/HR

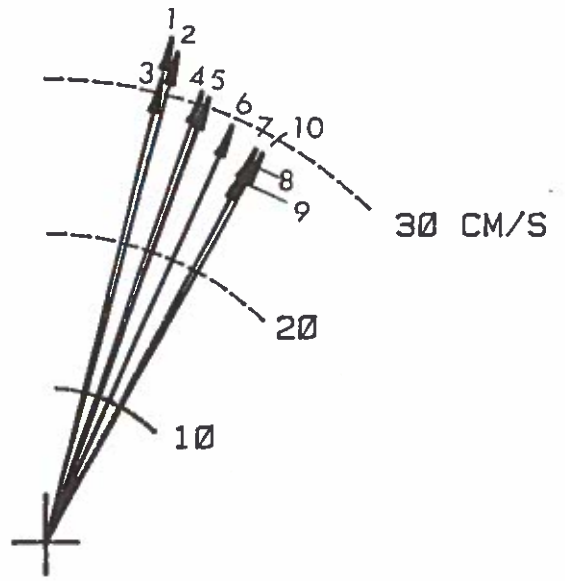
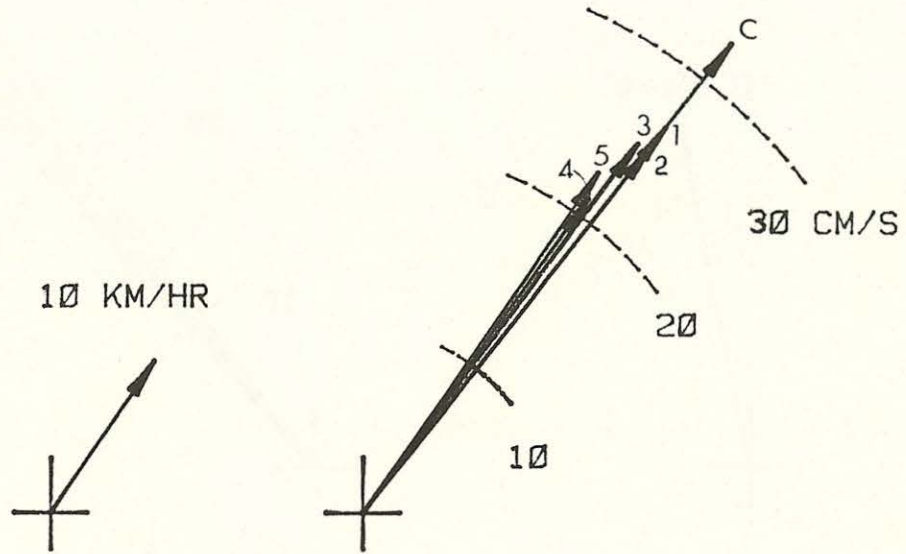
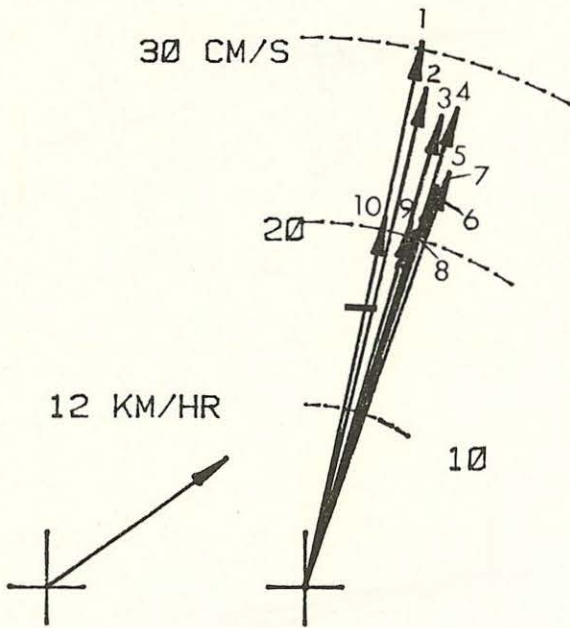


Figure 11: Hodographs of drogue and wind velocities.

AUG 6 RUN 1



AUG 6 RUN 2



AUG 6 RUN 3

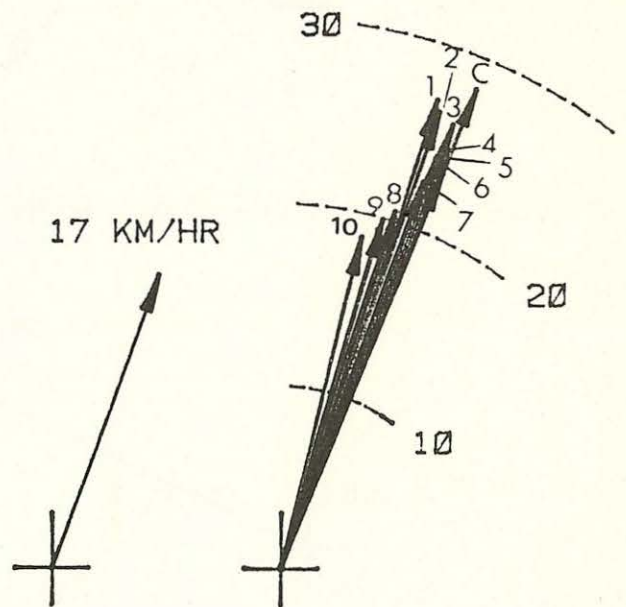


Figure 12: Hodographs of drogue and wind velocities.

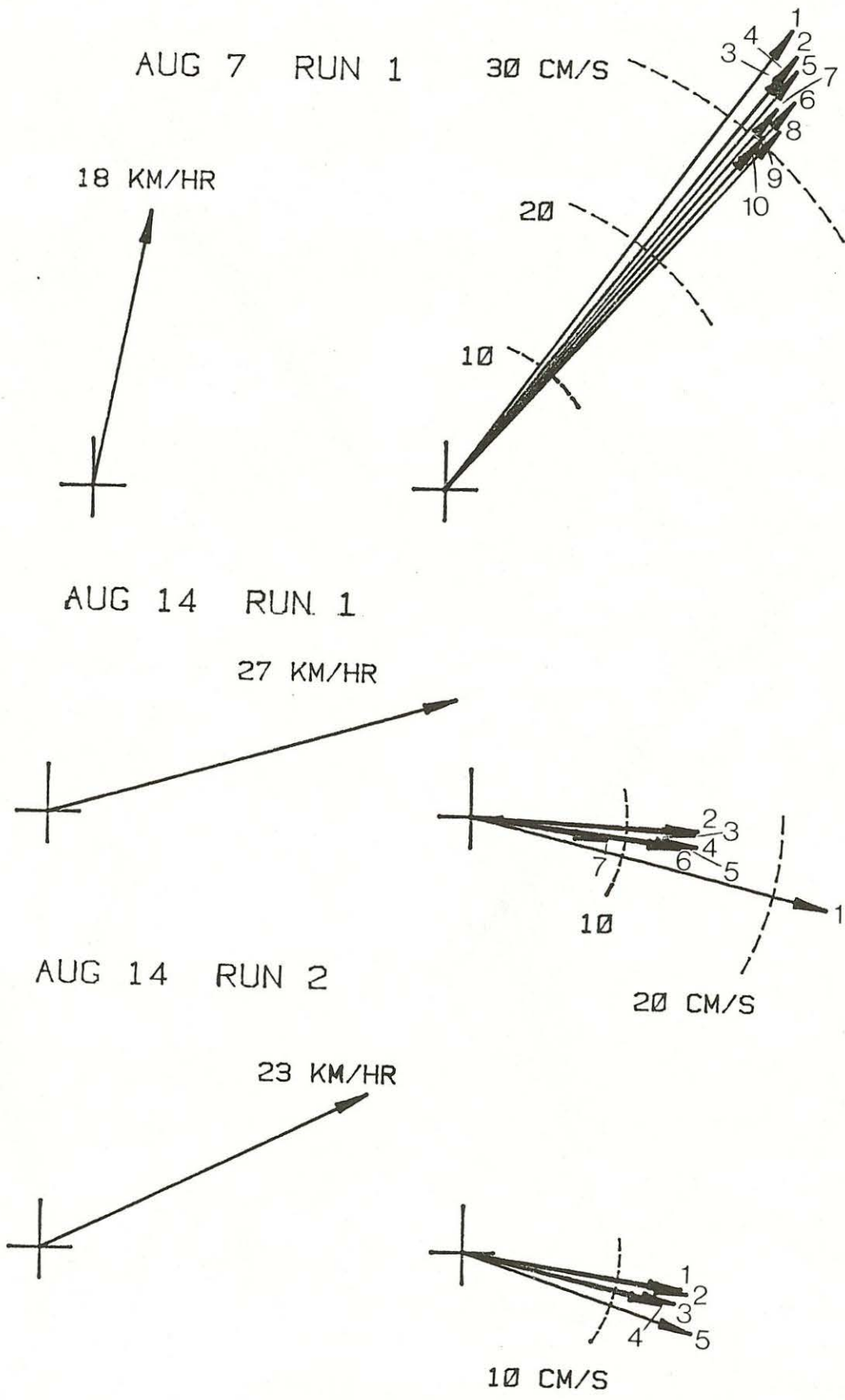
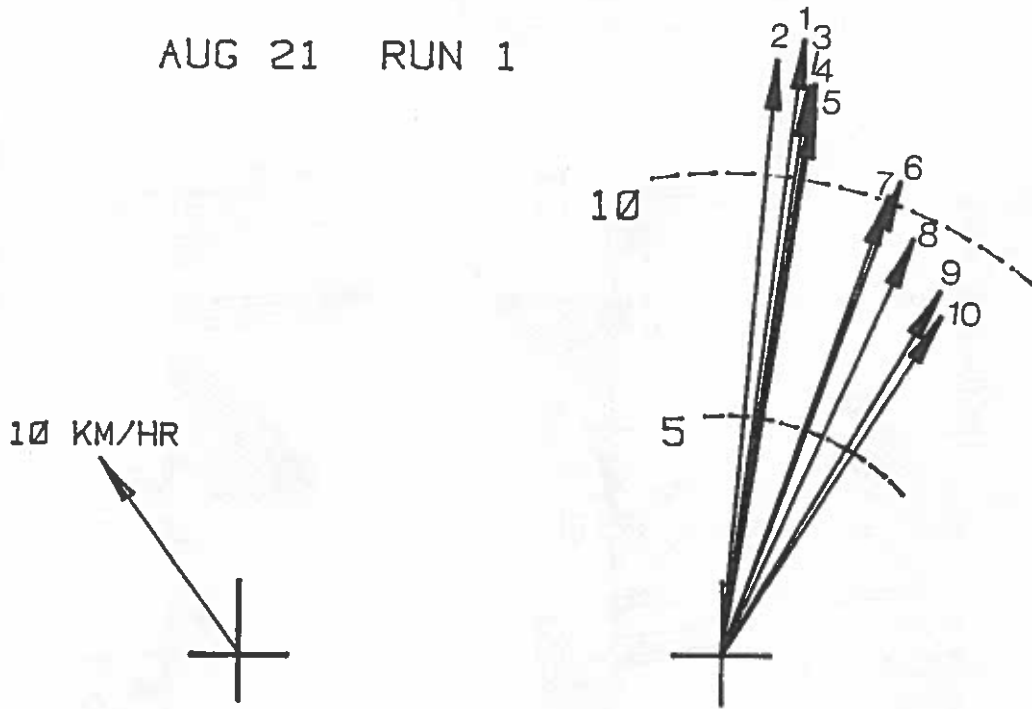


Figure 13: Hodographs of drogue and wind velocities.

AUG 21 RUN 1



AUG 21 RUN 2

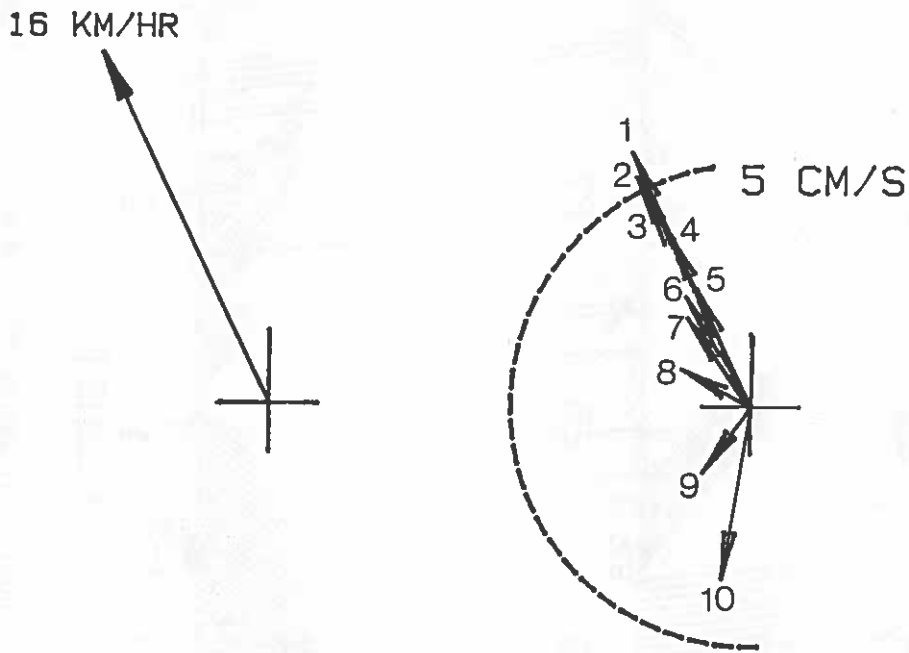


Figure 14: Hodographs of drogue and wind velocities.

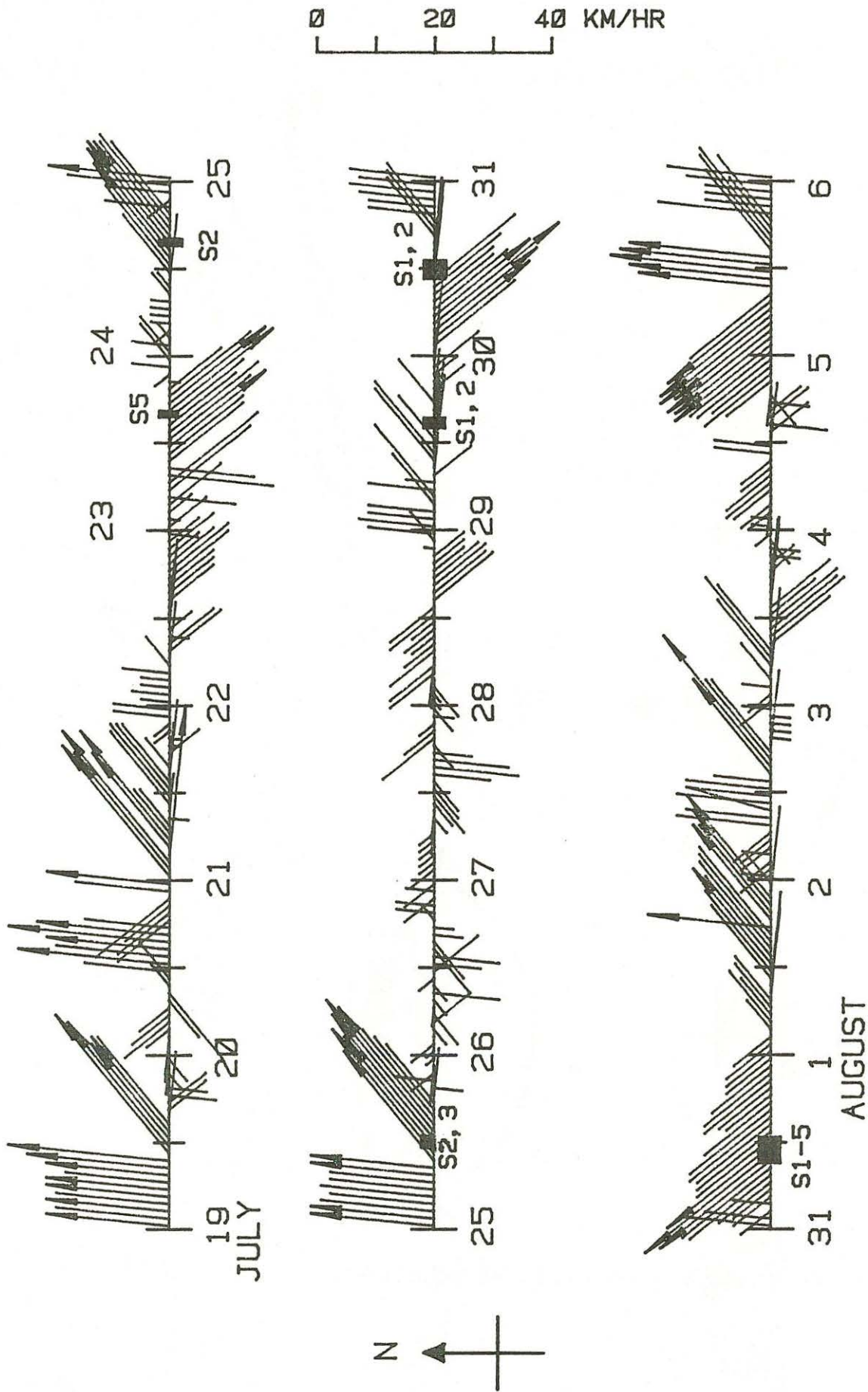


Figure 15: Hourly averages of wind velocities measured at a height of 10 m at Baie Due Doré. Vectors with magnitude exceeding 20 km/hr are terminated with an arrowhead. Date numbers mark the first hour of each day. Times of sighted drogue experiments are indicated by a closed box labeled by an 'S' followed by the run number(s).

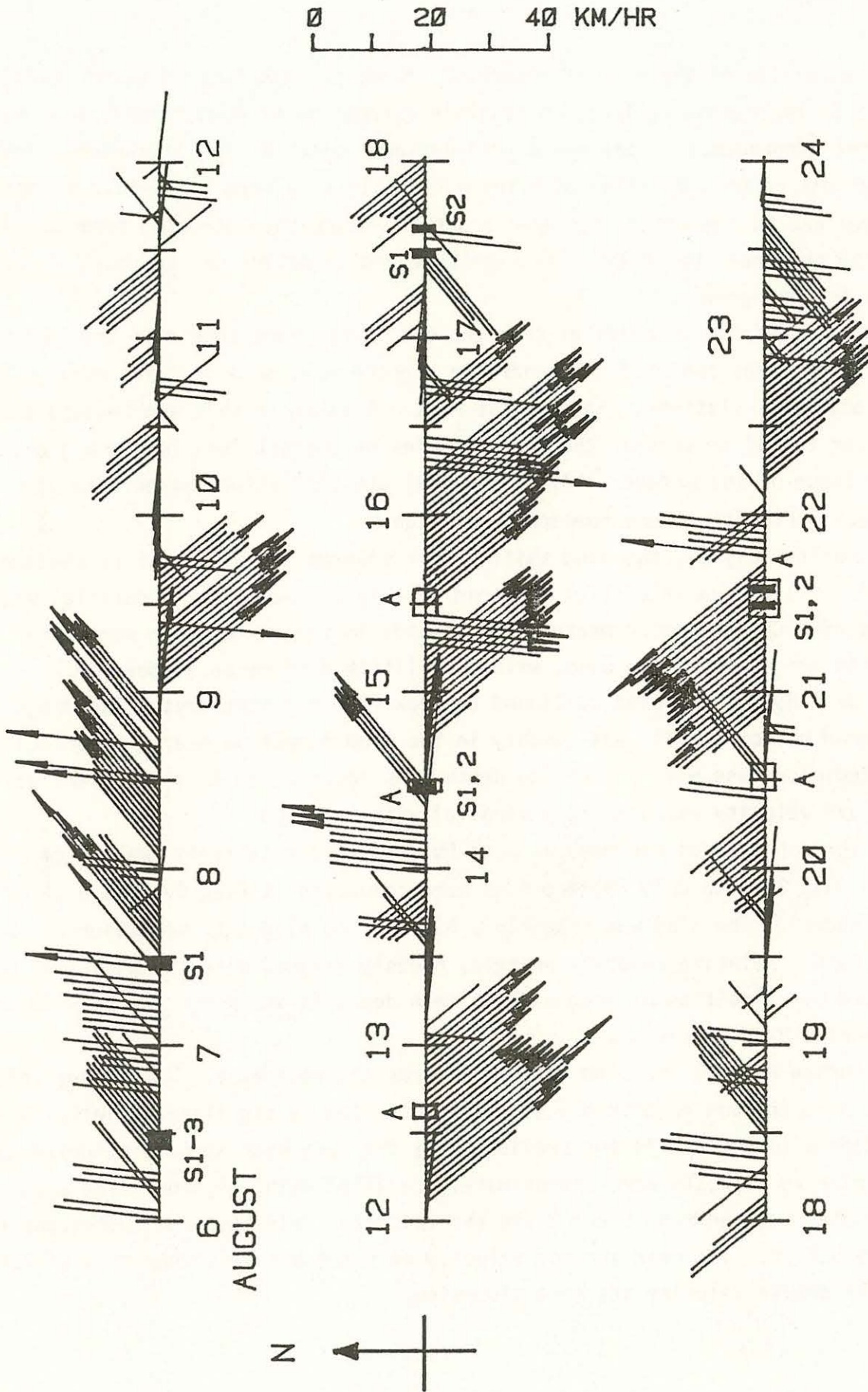


Figure 16: Same as Figure 15 except for a different time period. Times of acoustic drogue tracking are indicated by an open box labeled with an A.

the direction of the 4 to 10 m current of the morning current meter profile. (Due to instrument failure, no reliable current meter measurements were made in the afternoon.) There was a well-defined relative velocity between drogues which was roughly parallel with the wind. (In this report relative velocity is defined as the vector difference between velocities directed from the deeper to the shallower velocity. The magnitude and direction can be roughly deduced from the hodographs.)

The confetti velocity of this and most other runs should be treated with suspicion. The confetti was generally sighted only once or twice during a run at locations relatively close to the Punt. Because of this and because the cluster tended to spread, the uncertainties of confetti bearings are greater than those of the drogues. Also, the ERR1 and ERR2 values associated with confetti velocities were comparatively high.

During July 24, the wind shifted back towards the northeast (a southwest wind). All drogue velocities measured on this day were nearly parallel with the wind. Current meter measured velocities in the mixed layer were also roughly aligned with the wind, with very little difference in bearing.

On July 25, the wind continued to blow from the southwest. The drogue measured velocity field was roughly in the wind direction near the surface and rotated clockwise with increasing depth. As observed on July 23, there was a relative velocity approximately parallel with the wind.

The wind speeds recorded at Baie Du Doré were relatively small from July 26 to July 29. On July 29, two runs were conducted at Flag Station 4 (4 km from shore). The wind was from 226° ; but was too slight to be measured. For both runs a relative velocity profile, roughly aligned with the wind, can be deduced by velocities of drogues with mean depth in the range 1.2 m - 60 m (vectors 1-8 of Figure 9).

During July 30 the wind shifted towards the southeast. The drogue velocities of both runs on this day were characterized by significant clockwise rotation with depth. As for previous runs the very near surface velocity and the relative velocity were approximately parallel with the wind. The wind diminished between runs 1 and 2 and the velocity field appeared to respond to the reduction. The near surface velocity of run 2 was less than that of run 1 and the deeper velocity was more clockwise.

During July 31, all drogues moved with high velocity in the wind direction (northward). Submerged drogue velocities of run 5 were 10-15° clockwise of the corresponding velocities of run 1, which was 3 hours earlier (possibly a manifestation of inertial motion). Tracking was halted abruptly at 13:00 EDT due to an impending thunderstorm from the south.

The wind during the first run of August 6 was slight (10 km/hr) and towards the northeast. Despite the light wind there were long and high swells traveling towards the northeast, likely the result of the strong winds during August 5. During succeeding runs the wind increased slightly and the wave height decreased. All drogue velocities and mixed layer current meter measured velocities were approximately in the wind and wave direction. This day's results are particularly noteworthy because they represent a near surface current field under the influence of light but increasing winds and significant but decreasing waves.

On August 7, one run was completed just before the arrival of a violent storm from the south. Drogue and mixed layer current meter measured velocities were of high magnitude and towards the northeast.

On August 14, simultaneous acoustic and sighted drogue tracking experiments were conducted. Acoustic drogues were released and tracked from station 8, while sighted drogue tracking was done from station 7. The wind and all sighted drogue velocities were approximately onshore, eastward.

On August 21, two sighted drogue experiments were conducted at station 6 in conjunction with acoustic drogue tracking from station 8. As can be seen from Figure 14 the sighted drogue profiles were markedly different. Velocities of run 1 rotated clockwise, whereas those of run 2 rotated significantly counterclockwise. During both runs, however, the relative velocity was roughly parallel with the wind.

To summarize: from the results of most runs a well-defined relative velocity profile, roughly parallel with the wind direction, has been observed. The velocity of the shallowest drogue (1.2 cm) was also most often parallel with the wind. Drogue runs from July 23 to August 7 were all carried out within 4 km from shore. During this period and for a few weeks prior strong winds were predominantly from the south. Drogue velocities of runs conducted

during northward winds were all towards the north. For runs during southward winds the velocity of the shallowest drogue was approximately parallel with the wind, and velocities rotated clockwise, towards the north (the direction of previous strong winds), with increasing depth.

From August 12 to August 17, strong winds were predominantly towards the south. During the August 21 experiment, the wind was towards the north. The shallowest drogue's velocity was nearly parallel with the wind. Deeper velocities rotated towards the south with increasing depth.

2i. Discussion

The above summary suggests that the observed drogue velocities consisted of two components. One component varied slowly with depth and was nearly parallel with strong winds of previous days. For convenience this component will be referred to as the sub-current. Superimposed on this was a current which varied rapidly with depth (on the observation scale of 2 m) and was nearly parallel with the existing wind. This component will be called the surface layer-current.

The fundamental question to be addressed is: what were the causes of these two components

The sub-current was likely set up by previous winds and was presumably in geostrophic balance with the cross-shore pressure gradient. On the eastern shore of Lake Huron a persistent north wind generates a southward current near the coast. Geostrophic balance is maintained by the elevation of the isotherms close to shore. For a wind of sufficient strength and duration a coastal upwelling results. Conversely, a wind from the south produces a northward flow and downward tilt of the nearshore isotherms. Such currents have been observed at this location in Lake Huron [Csanady and Pade (1968)] and are manifested by the temperature and current meter data presented in section 4.

For currents generated on the time scale of one inertial period, transient inertial oscillations may be expected. It has been frequently noted that at large distances from shore, currents following a strong wind event generally oscillate at close to the inertial period (= 17 hrs at Baie Du Doré). Due to

the coastal constraint cross-shore inertial excursions are reduced close to shore. As a consequence there is a coastal zone, typically 5 to 10 km wide, where relatively high currents are forced to flow predominantly in a longshore direction (Csanady, 1981; Murthy and Blanton, 1975). Thus, within 4 km of shore (where most experiments were conducted) a current in geostrophic equilibrium with the coastal pressure field should be directed roughly parallel with the longshore component of strong winds during previous days; this was the case for the observed sub-currents.

The behavior and causes of the sub-currents should be further clarified when concurrently recorded data from current meter moorings of the Canada Centre for Inland Waters becomes available.

The surface layer-current may be defined as the relative velocity between drogues. Table 3 lists the relative velocities between the 1.8 m and 1.2 cm drogues together with the corresponding wind velocities. As can be noted from the Table, the relative velocities (surface layer-currents) were directed roughly parallel with the wind. (The relative velocity between the 1.8 m and 1.2 cm drogues was an average of 10° counterclockwise of the wind with a standard deviation of 18.5° .) These surface layer-currents were most likely driven by a combination of surface wind stress and wave action (Stokes drift), with one factor or the other possibly dominating.

Nearsurface currents produced by surface wind stress were first studied mathematically by Ekman (1905) in his classic paper. In Ekman's model momentum from the wind was transferred through the water column by turbulence, or more precisely, Reynolds stresses. The stresses were parameterized by an eddy viscosity coefficient which was considered everywhere constant. Ekman obtained a steady state solution describing the velocity field resulting from a constant wind blowing over an infinitely deep ocean with no horizontal bounds. Since Ekman's original paper a vast number of theoretical models have been advanced based on his general reasoning. Agreement with velocity profiles measured in the field, however, has been marginal at best. One problem is that there is no accepted value of the eddy viscosity coefficient or its dependence with depth. Another difficulty is the specification of the lower boundary condition (at the bottom and at the thermocline). Also, because the

Table 3

1.2 cm and 1.8 m Drogue Velocities,
Relative Velocities (1.8 m to 1.2 cm)
With Corresponding Wind Velocities and Estimated Surface Roughness
of all Processed Sighted Drogue Runs

DAY	RUN	WIND		VELOCITY 1.2 CM DROGUE		VELOCITY 1.8 M DROGUE		REL. VEL. 1.8 M-1.2 CM		ESTIMATED ROUGHNESS**
		SP M/S	DIR* DEG	SP CM/S	DIR DEG	SP CM/S	DIR DEG	SP CM/S	DIR DEG	
Jul 23	5	6.3	159	12.1	155	-	-	10.3	129 ^τ	R+
Jul 24	2	5.6	25	25.8	30	18.0	27	7.9	36	M
Jul 25	2	5.6	31	25.3	46	17.7	59	9.5	22	R
Jul 25	3	6.7	44	26.4	48	17.7	70	12.0	15	R+
Jul 29	1	-	46	18.8	63	13.2	71	6.1	46	C
Jul 29	2	-	46	16.5	65	11.4	71	5.3	51	C
Jul 30	1	4.7	144	10.2	147	2.7	206	9.1	132	R
Jul 30	2	3.3	136	5.6	128	4.3	251	8.8	104	R
Jul 31	1	7.2	4	33.1	10	24.9	14	8.5	-2	M
Jul 31	2	6.9	-6	31.2	3	26.8	13	6.6	-40	M
Jul 31	3	8.1	4	39.1	14	32.3	16	6.9	5	M
Jul 31	4	6.9	4	37.9	19	31.7	25	7.4	-11	M
Jul 31	5	7.7	-6	33.6	14	28.7	29	9.5	-38	M+
Aug 6	1	2.8	34	26.7	38	-	-			
Aug 6	2	3.3	54	30.4	12	20.7	12	9.7	12	M+
Aug 6	3	4.7	20	27.0	18	18.7	14	8.5	29	M
Aug 7	1	5.0	11	37.8	36	29.8	41	7.6	16	M+
Aug 14	1	7.5	74	23.5	104	-	-			
Aug 14	2	6.4	64	14.1	99	-	-			
Aug 21	1	2.8	-36	12.9	7	8.3	32	6.4	-27	C+
Aug 21	2	4.4	-26	5.8	335	3.6	189	9.0	-12	M

* Direction towards which the wind was blowing

** C - calm, M - moderate, R - rough

^τ Relative velocity at 1.8 m obtained by logarithmically extrapolating the relative velocity profile.

wind seldom blows at a constant speed and direction for a long time, the time dependence of the solution is important.

All solutions do have common features. All predict clockwise rotation of velocity vectors with depth, and a surface current directly related to the wind stress and to the right of the wind (northern hemisphere).

Very nearsurface wind driven flow has been considered by Jones and Kenney (1977) and Csanady (1979) to be analogous to wall layer flow over a rough surface. For such a model the surface shear is given by:

$$(10) \quad \left. \frac{du}{dz} \right|_0 = \text{func} (u_*, \gamma^{-1})$$

where: γ is a roughness length

u_* is the friction velocity = τ_0/ρ

τ_0 is the surface wind stress

ρ is the water density.

The simplest form of the above relationship is given by:

$$(11) \quad \left. \frac{du}{dz} \right|_0 = \text{const.} \frac{u_*}{\gamma}$$

In this model, as in all Ekman-like models, the nearsurface relative velocity is directly related to the wind stress. The relative velocities observed in these experiments (Table 3) are graphed as a function of wind speed in Figure 17. There is no apparent dependence of relative velocity with wind speed.

The roughness length of equation (10) can be considered proportional to the height of breaking surface waves (or waves more accelerated at the crest than at the trough). Due to the limited fetch in Lake Huron, a large proportion of waves observed during these experiments were breaking or clearly accelerated at the crest by the wind. For models in which Reynolds stresses are parameterized by the eddy viscosity coefficient the shear is inversely proportional to the eddy viscosity coefficient. It has been argued by Huang (1979)

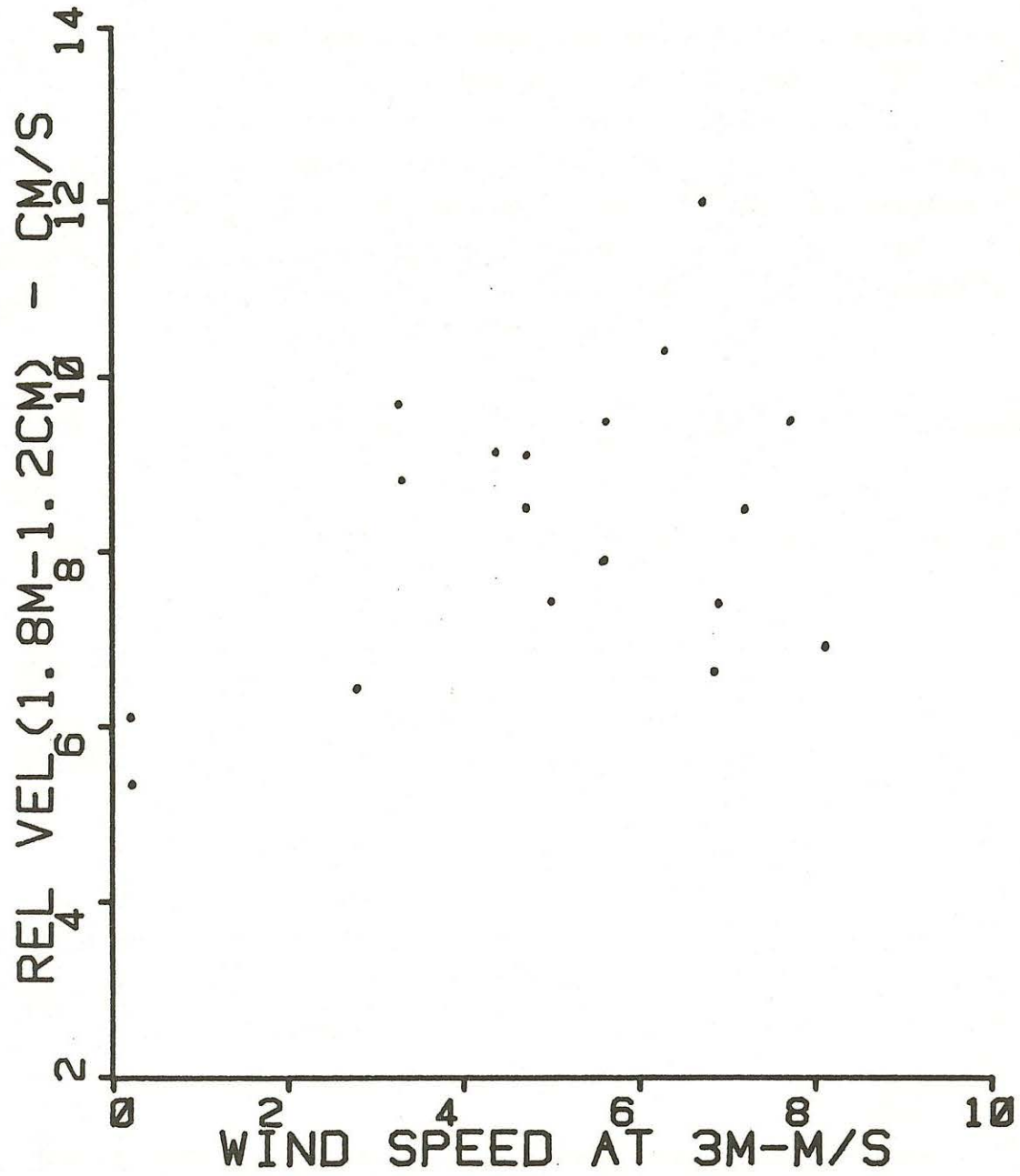


Figure 17: Magnitudes of relative velocities between the 1.8 m drogue and the 1.2 cm drogue graphed as a function of wind speed at 3 m.

and Csanady (1978) that eddy viscosity in nearsurface water is approximately proportional to surface roughness. Thus, for such models, as for equation (10), the nearsurface relative velocity is inversely related to surface roughness.

Unfortunately, no quantitative measurements of the wave fields during the sighted drogue experiments were made. However, qualitative assessments of the surface roughness during each run have been fit into the following categories:

- C = calm
- M = moderate
- R = rough

with '+' indicating the rough extreme of each category. The roughness estimate increased with increasing wave height and decreasing wave length. The roughness values of each run are listed in the last column of Table 3 and are graphed against relative velocity in Figure 18. Although the roughness scale is admittedly crude, there does appear to be a direct (rather than inverse) dependence of shear with surface roughness.

This dependence of relative velocity on roughness suggests that the observed relative velocity profiles may have been primarily a manifestation of Stokes drift, a second order effect of surface waves. Stokes drift for a one-dimensional, single frequency wave field [observed in the laboratory by Lange and Huhnerfuss (1978) and Alofs and Reisbig (1972)] is directed parallel to the wave motion and given by:

$$(12) \quad v_S = \left(\frac{\pi H}{\lambda}\right)^2 C \exp(-4\pi z/\lambda)$$

where:

- H = wave height
- λ = wave length
- C = phase speed.

Due to the limited fetch, the wind and wave directions during these experiments were approximately equal. As already noted the relative velocities were approximately in the wind direction; thus, the relative velocities were roughly aligned with the wave directions. According to (12) the surface

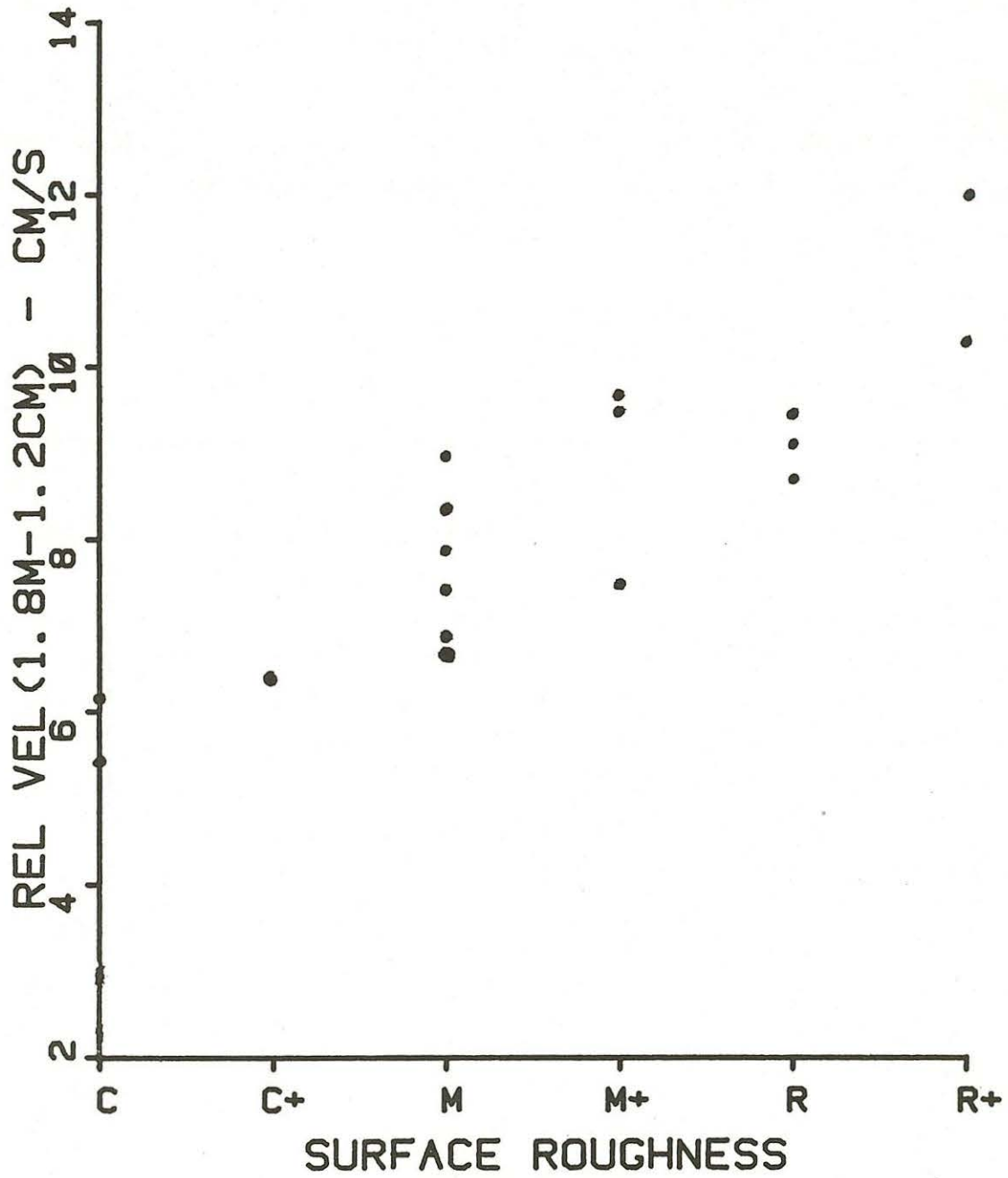


Figure 18: Magnitudes of relative velocities between the 1.8 m drogue and the 1.2 cm drogue graphed as a function of estimated surface roughness.

velocity is proportional to $(H/\lambda)^2$ and is thus approximately proportional to surface roughness.

Stokes drift is more accurately computed using the wave energy spectrum. For a 1-dimensional spectrum the Stokes drift is given by:

$$(13) \quad v_S = \frac{2}{g} \int_0^{\infty} \sigma^3 W(\sigma) \exp(-2 \sigma^2 z/g) d\sigma$$

where: σ is the frequency in rad/s
 W is the wave energy spectrum
 g is the gravitational acceleration.

(This equation is still only an approximation of Stokes drift because the effects of directional spreading and wave breaking are not included.)

Wave energy spectra, each computed from a 20 minute record of a waverider accelerometer buoy moored in 11.3 m of water off Port Elgin, Ontario (approximately 20 km from the project site), have been provided to us by the Marine Environmental Data Service of the Canadian government. Two of these spectra are shown in Figure 19. Stokes drift profiles have been computed from ten digitized spectra by numerically performing the integration of equation (13) from the Nyquist frequency of 0.5 hz (rather than infinity) to 0 hz. Also computed was the significant wave height of each spectrum, which is calculated as four times the square root of the area under the energy spectrum and, according to the analysis of Longuet-Higgins (1952), is approximately equal to the mean of the highest 1/3 number of the waves. The significant wave height roughly corresponds to the visual estimate of wave height.

The computed relative velocity was greater for spectra with higher significant wave height. For spectra with the same significant wave height the relative velocity increased with decreasing peak period (period of maximum spectral density). Thus, for the 10 digitized spectra the relative velocity due to Stokes drift increased with surface roughness.

The magnitude of the computed relative velocity between 1.8 m and 1.2 cm ranged from 0.6 cm/s to 12.6 cm/s. For most spectra, the calculated relative velocity magnitude was approximately 1/2 the magnitude observed during periods

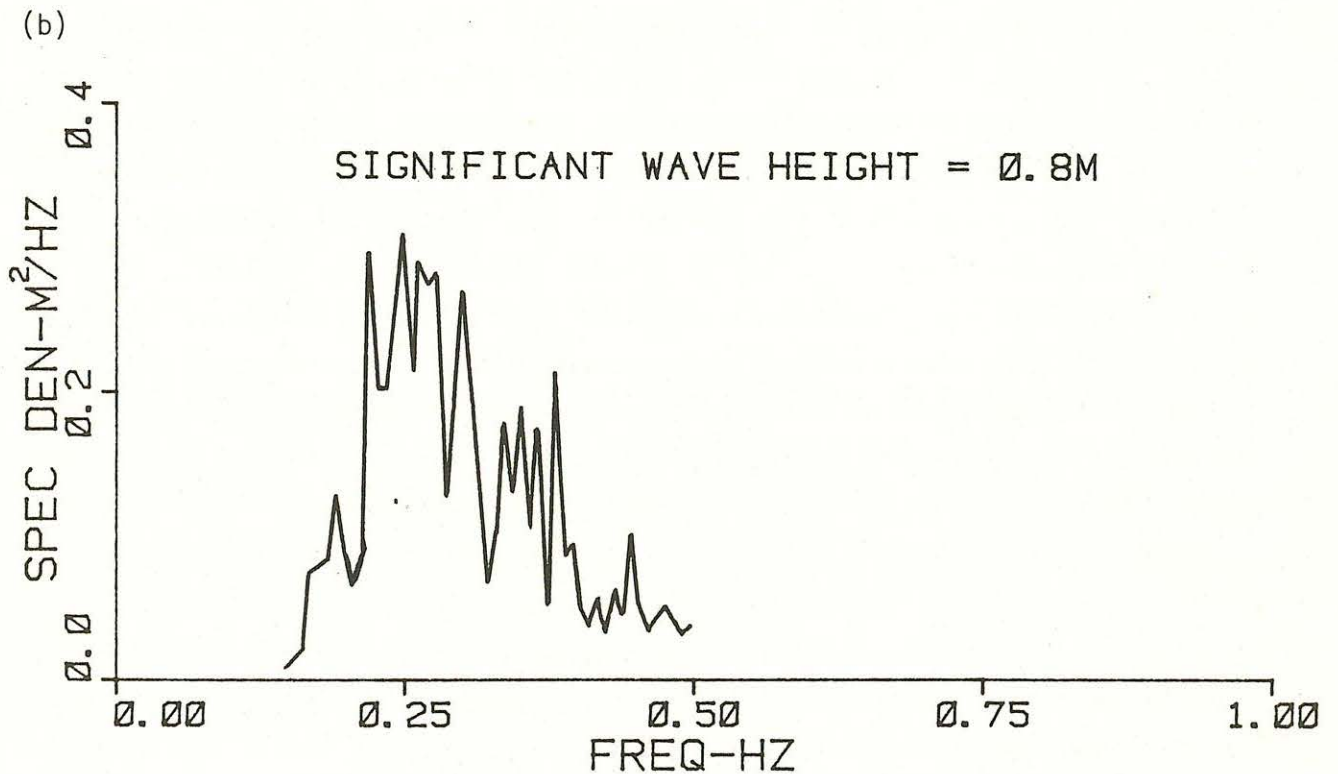
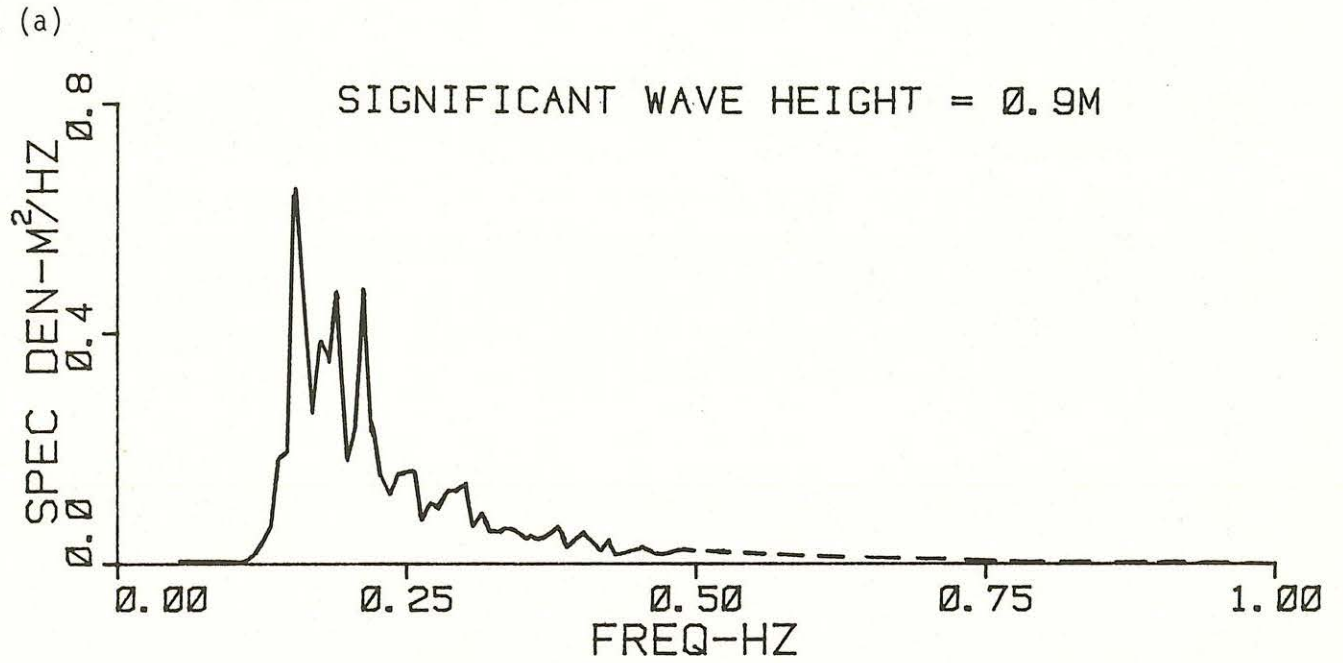


Figure 19: Two examples of wave energy spectra. The dashed line of spectrum (a) is a contrived extrapolation of the spectral density to 0 m²/hz at 1 hz.

of similar wave heights. For example, the relative velocity between 1.8 m and 1.2 cm calculated from spectra with 0.6 m to 0.8 m significant wave height ranged from 2.4 cm/s to 6.9 cm/s, as compared with a range of 6.6 cm/s to 9.5 cm/s observed during a lake state of approximately 0.6 to 0.8 m.

The computed Stokes drift was probably significantly lower than that given by equation (13) because the upper limit of integration was only 0.5 Hz. As indicated by Figure 19 there is appreciable wave energy at 0.5 Hz. The waverider spectra have been extrapolated to higher frequencies using two methods: extrapolation to $0 \text{ m}^2\text{s}$ at 1 Hz; and extrapolation using the Phillips (1958) form of the equilibrium spectrum, $W(\sigma) = \beta g^2 \sigma^{-5}$, with β calculated from spectral values near 0.5 Hz. Both techniques yielded Stokes drift profiles of nearly identical magnitude which were approximately equal to the observed profiles. Profiles of similar magnitude were also calculated using spectra from a wave capacitance recorder (Simpson, 1969) which included the frequency range 0.1 Hz to 1.0 Hz.

Figure 20 displays examples of calculated and observed profiles with nearly equivalent associated values of significant wave height and sea state. These profiles indicate that Stokes drift likely comprised a major portion of the near surface relative velocity.

It should be noted that for all digitized spectra the calculated Stokes drift was confined to the very near surface. For example, the Stokes velocity at 10 m computed from the spectra of Figure 19a was 0.07 cm/s.

Thus the magnitude and direction of the observed relative velocities as well as their dependence on surface roughness are all consistent with the notion that the surface layer-currents were primarily due to Stokes drift. The results of runs 2 and 3 on August 6 during which the shear decreased while the wave height lessened and the wind speed increased are also indicative of Stokes drift. In view of the uncertainties of the drogue velocities and the crudeness of the surface roughness estimates, these results cannot be considered conclusive. They are, however, supportive of studies by Bye (1967) and Kirwan et al. (1979) which construed Stokes drift as being the primary factor driving nearsurface currents.

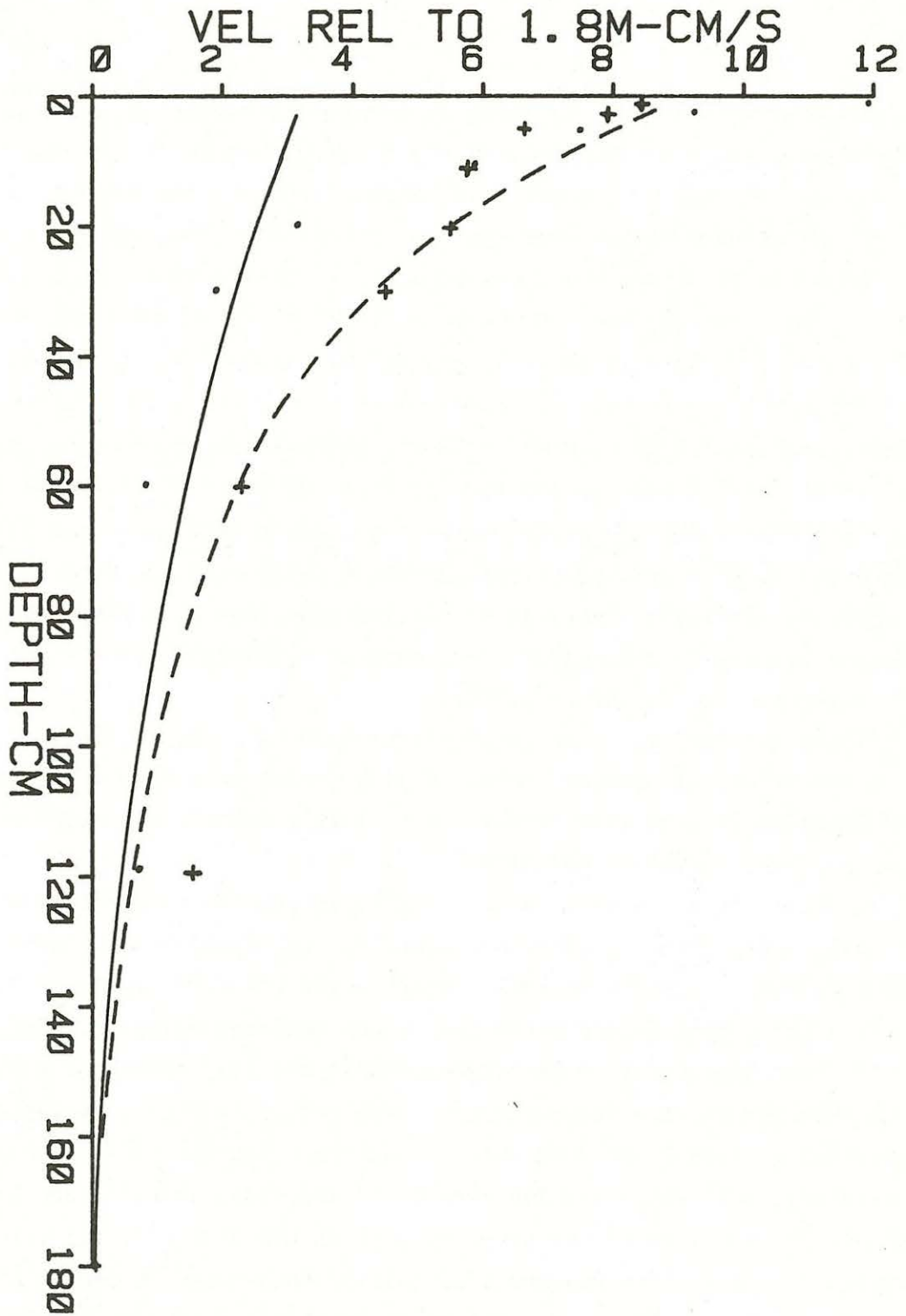


Figure 20: The solid line is the velocity profile relative to 1.8 m calculated using equation (13) and the spectrum of Figure 19a (solid line only). The dashed line is the profile calculated with the dashed line portion of Figure 19a included. The dots and +'s are relative velocity magnitudes from July 25 run 3 and August 6 run 3 respectively.

Ekman-like drift was not necessarily absent even if Stokes drift was predominantly responsible for the observed shear. Ekman currents may have decayed on depth scale greater than the depth of the deepest drogue, 1.8 m.

3. ACOUSTIC DROGUE EXPERIMENTS

3a. Introduction

In these experiments drogues, equipped with sonobuoys, were tracked using a shipboard acoustic navigation system which measured travel times of pulses transmitted from three bottom mounted transponders to a drogue attached hydrophone. Also recorded were simultaneous wind speeds at three levels and wind direction. A similar experiment which measured nearsurface velocities at deep water dumpsite No. 106 (DWD-106, ~ 200 km SE of New York City) was carried out in April of 1979 and is reported by Churchill *et al.* (1981). Multiple reflections caused by ray bending in the shallow, highly stratified water of Lake Huron made drogue tracking more troublesome than at DWD-106. The influence of multiple reflections on velocity determination and acoustic tracking range will be briefly discussed in this report. A detailed examination is given by Churchill (1981).

3b. Acoustic Navigation System

The acoustic navigation system used in these experiments has been employed by Woods Hole Oceanographic Institution investigators for a number of years and is well documented. Hunt *et al.* (1974) and Peal (1974) have provided an overall description of the system's design and operation. In addition to the study at DWD-106, sonobuoy tracking has been reported by Spindel and Porter (1974) and Spindel, Davis, MacDonald, Porter and Phillips (1974). The system will be briefly described in this report.

The geometry of the system as used in Lake Huron is diagrammed in Figure

21. The fundamental components are:

- a transducer lowered from the tracking ship (R/V Coot)
- three bottom-mounted transponders
- a drogue connected to a listening hydrophone and transmitting VHF antenna

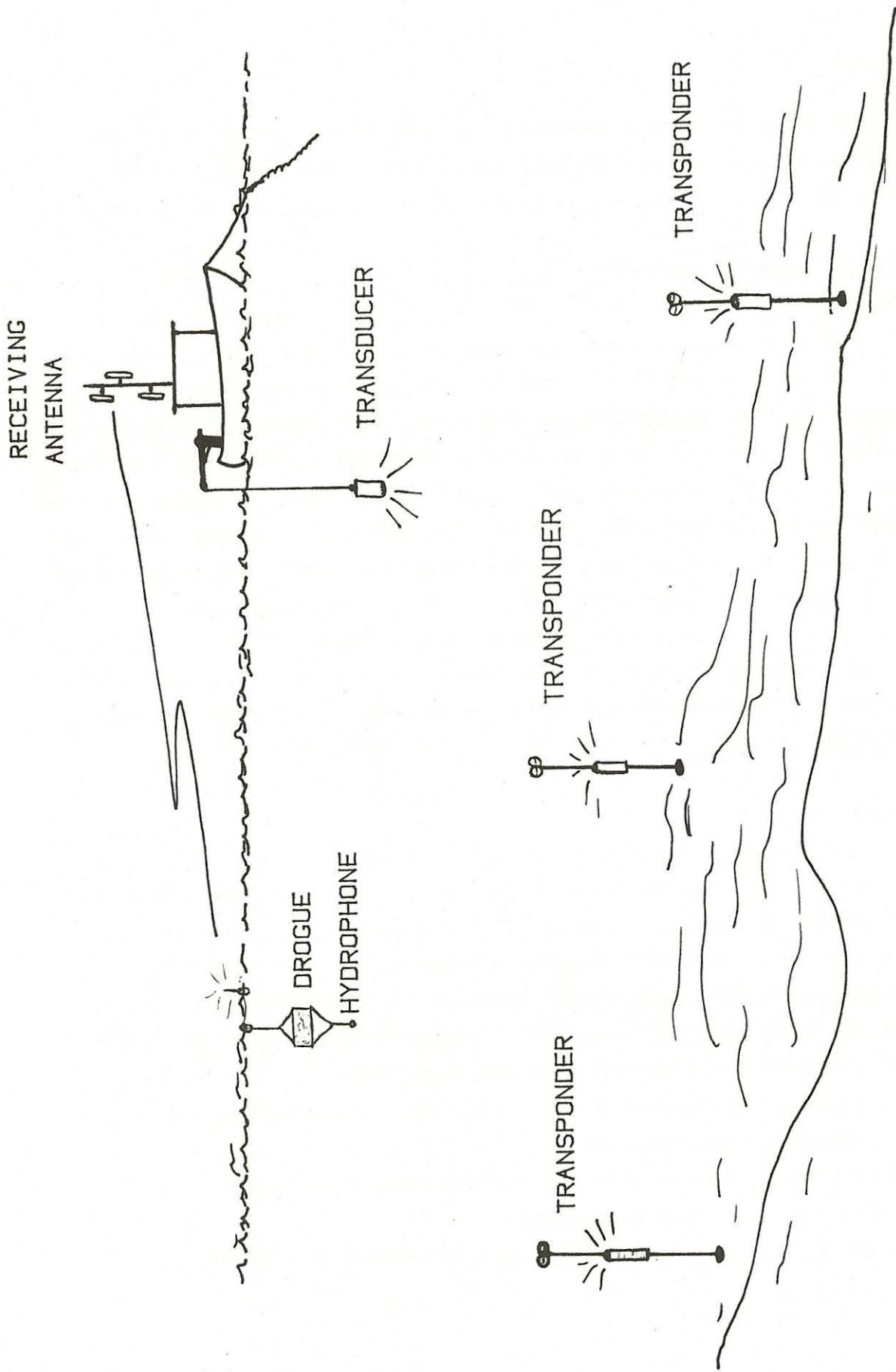


Figure 21: Geometry of the acoustic tracking system used in Lake Huron.

- a receiving antenna aboard ship
- a shipboard master timing clock, and minicomputer system which controls operation, processes incoming data, and displays computed positions
- a cassette tape recorder for data storage.

Two phases of navigation 'ship' and 'sonobuoy' are performed as separate cycles.

The ship cycle is initiated with the transmission of a pulse (7.5 khz, 10 msec) from the ship's transducer. Immediately following the detection of this pulse each bottom transponder generates a reply pulse at a specific frequency (11.5, 12.5 and 13.5 khz). These reply pulses are detected by the ship's transducer. The acoustic round trip travel times between the ship and each bottom transponder are thus determined and logged by the shipboard computer. Slant range between the ship and each transponder is found by multiplying the one-way travel time by the average sound velocity of the water column. The position of the ship relative to the transponder net is computed using an operator selected pair of slant ranges together with the known depth of the ship's transducer, the previously measured length of the baseline between the chosen transponder pair, and the transponder depths. The third slant range, if available, is used to resolve the ambiguity as to which side of the baseline the ship is on. (Otherwise the side of the baseline is specified by the operator.)

The sonobuoy cycle also begins with a pulse transmission from the ship's transducer. The reply pulses from the bottom transponders are received at the drogue and transmitted (via radio) to the ship. Assuming the travel time from the drogue to the ship is negligible, the elapsed time between the initial pulse transmission and a reception at the ship is the acoustic travel time from the ship to the respective transponder to the drogue. The travel time from each transponder to the drogue is found by subtracting the ship to transponder travel time determined by the most recent ship cycle. These travel times are converted to slant ranges and used to calculate the position of the drogue with respect to the transponder net in the same manner as for the ship position during the ship cycle. Ship and drogue positions are displayed in real time on an x-y plotter.

The baseline lengths between transponders and transponder depths are determined by a survey in which travel times are collected from a number of locations and analyzed using a least-squares technique. Geographic positioning of the transponder net is accomplished using the ship's navigation system, as will be discussed in section 3f.

The procedure of alternating between ship and sonobuoy cycles yields a drogue position one to two times a minute. The normal practice is to track each drogue for about five minutes at a time. The present system can concurrently track 16 drogues, each transmitting at a different frequency. Constant attention is required. The operator must, among other duties, select which drogue is to be tracked and the transponder pair to be used for position calculation. An unpublished report on the system operation and the computer programs used has been prepared by Loud (1981).

3c. Acoustic Drogue Assembly

The acoustic drogue assembly, recently developed at W.H.O.I., consists of: a drogue made from matted packing material, waterproofed sonobuoy electronics enclosed within the drogue, attached hydrophone, and float-antenna assembly. The drogues have been designed to drift either submerged at a specific depth or with the top face just at the water's surface.

Typical assemblies of submerged drogues are shown in Figure 22. The drogue is constructed of a wire mesh (1" x 2") frame formed into a block with a padding of 5 cm thick, densely entwined, synthetic horsehair (material also used for sighted drogue construction, see section 2a) fastened to the exterior. Ethafoam strips are attached to the interior of the wire frame for positive buoyancy. With appropriate counterweights the drogue constitutes a slightly negative buoyant, stable body with extremely high drag. The drogue depth is specified as the distance between the center of the support float, which is presumed to be at the water's surface, and the center of the drogue. The dimensions of the drogues that were used depended on the weather conditions: larger drogues were deployed during rough weather.

The float-antenna assembly for submerged drogues consists of a support float for the drogue connected by 1.3 m of antenna wire (RG-174/U) to an an-

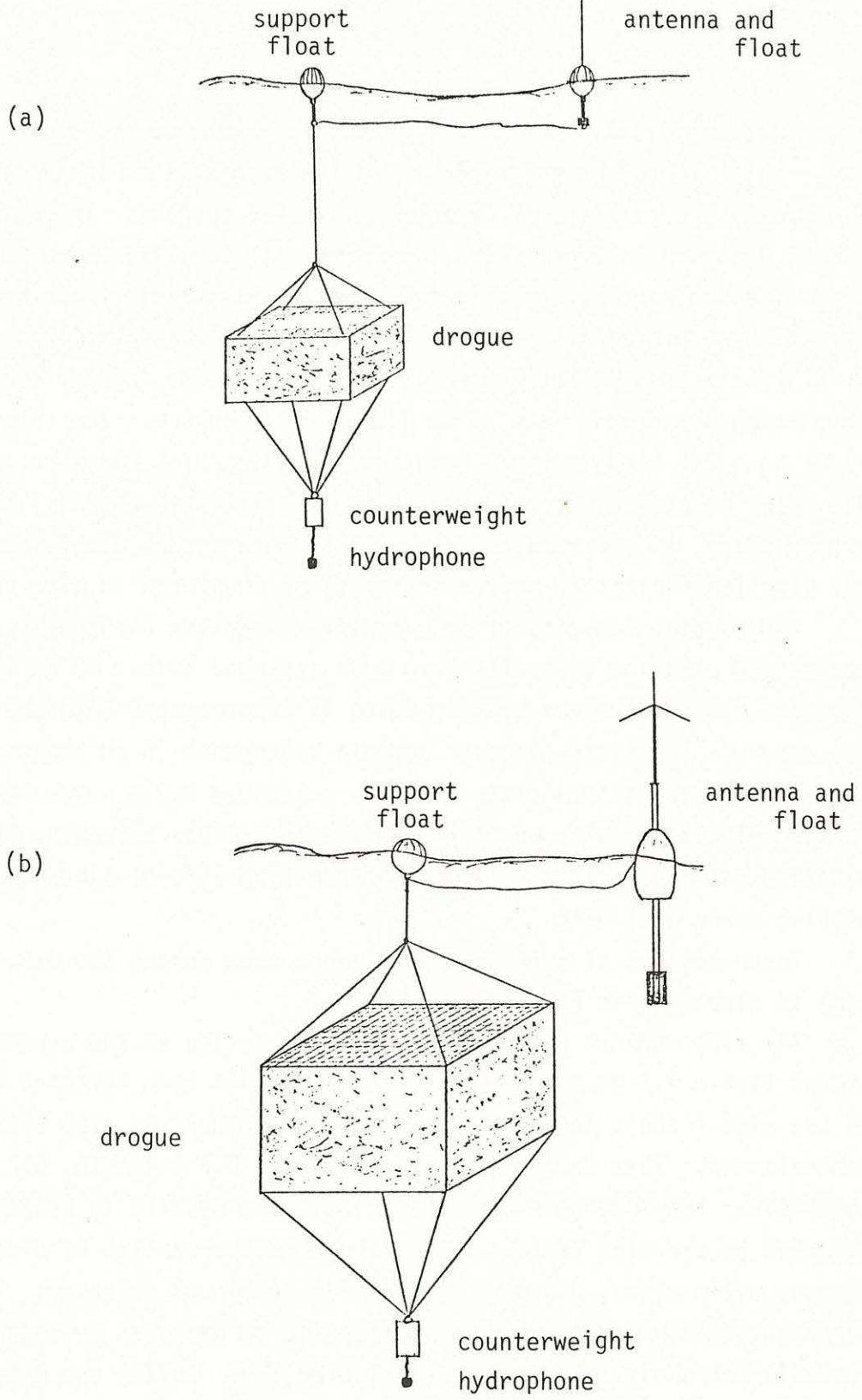


Figure 22: Assemblies of submerged drogues: (a) calm weather drogue; (b) rough weather drogue.

tenna bearing float. The assembly used in calm weather is displayed in Figure 22a. Both floats are made from 10 cm diameter x 15 cm long copper floats and drift with approximately 7 cm above the water surface. The antenna carrying float, designed to freely ride the waves, is stabilized by a 10 cm long rod with attached zinc counterweights. The VHF electronics have been modified to permit the use of a 1/4 wave antenna (0.16 cm diameter x 41 cm length).

The assembly for use in rough weather is shown in Figure 22b. The float supporting the drogue is a 15 cm diameter PVC sphere. The antenna supporting float is a PVC "lobster pot" buoy through which 3/4" EMT pipe, with appropriate steel counterweights, is inserted. The 1/4 wave antenna, with built-in ground plane, is extended above the float by a wooden dowel inserted into the EMT pipe (to facilitate better transmission when used in high waves).

The electronics consist of a modified Magnavox AN/SS041B sonobuoy. The boards and alkaline batteries have been packaged into a 46 cm long by 13 cm diameter sealed aluminum housing which is incorporated into the interior of the drogue. The piezo-electric ceramic hydrophone (5 cm length, 4.5 cm dia.) has an omni-directional pattern and is suspended 0.3 m below the counterweight by its original compliance cable and shock absorber assembly. The present alkaline battery package provides an operating life of nine hours at a transmitting power of 1 watt.

Three designs of surface drogues were used during the experiments. Each type is displayed in Figure 23.

The slab surface drogue is of the same design as the submerged drogue except that a 2.5 cm thick sheet of ethafoam has been fastened to the interior of the wire frame's top side. During calm weather the slab shown in Figure 23a was released. This drogue is of dimensions: 0.7 m length, 0.7 m width, 0.3 m thickness. The antenna and support floats are mounted in ethafoam rings and attached to the wire frame. During rough weather a slab of dimensions: 0.9 m length, 0.9 m width, 0.6 m thickness (Fig. 23b) was released. The manufacturer's sonobuoy package (80 cm length x 12 cm diameter cylinder with a folded monopole antenna) is mounted within the drogue. During the experiments both of these slabs drifted with the top side slightly above the water surface. As will be discussed in section 3h this resulted in excessive wind drag on the drogue.

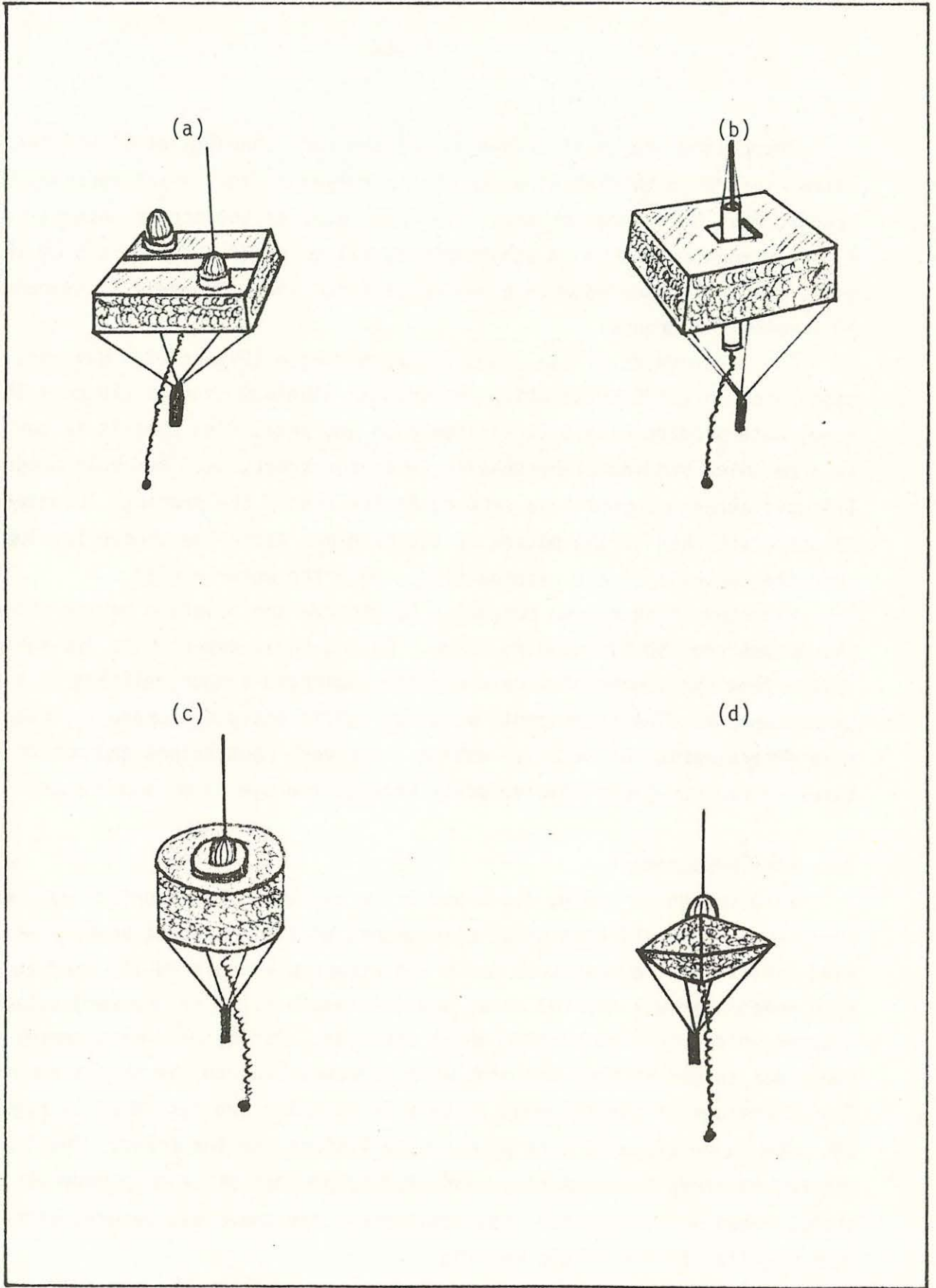


Figure 23: Surface drogue assemblies: (a) calm weather slab; (b) rough weather slab; (c) cylinder; (d) diamond.

The cylindrical surface drogue (Figure 23c) consists of a cylinder (41 cm diameter x 28 cm thickness) of synthetic horsehair into which sonobuoy electronics have been incorporated. The lower half of the copper antenna bearing float is mounted within an ethafoam ring (21 cm outer diameter x 5 cm thickness) which is inserted within the horsehair. The hydrophone is suspended 10 m below the drogue.

The electronics of the diamond-shaped drogue (Figure 23d) have been encapsulated in a BUD Corporation rectangular aluminum chassis (28 cm x 18 cm x 5 cm) waterproofed with G.E. silicon glue and seal. The chassis is surrounded by 5 cm thick padding of horsehair. A copper float, used for both drogue and 1/4 wave antenna support, is secured to the top of the padding. Counterweights, attached to the bottom of the padding, cause the drogue to float with just the top half of the antenna float above the water surface.

Experiments have been conducted to observe the relative motion between the drogue and the surrounding water. During these experiments dye was released from the center of a calm weather submerged drogue drifting in a near-shore current. The experiments were not sufficiently elaborate for quantitative determination of relative motion. However, photographs and motion pictures showed no appreciable velocity between the dye plume and drogue.

3d. Wind Measurement

Wind speeds at 1.0 m, 4.3 m and 6.7 m above the lake surface were measured aboard the R/V Coot using climatronic WM-III recording anemometers. The wind direction at a height of 6.7 m was recorded using a WM-III wind vane. Each anemometer was mounted on an arm (of length 1.7 m or greater) attached to a tower which could be pivoted about its base. During wind measurement the tower was turned so that the arms were perpendicular to the ship's length. The dimensions of the assembly in this orientation are displayed in Figure 24. The upper two arms were permanently fastened to the tower. The lowest arm was attached for measuring winds during periods of calm to moderate lake state. When not in use for wind measurement the tower was secured with the arms parallel to the ship's heading.

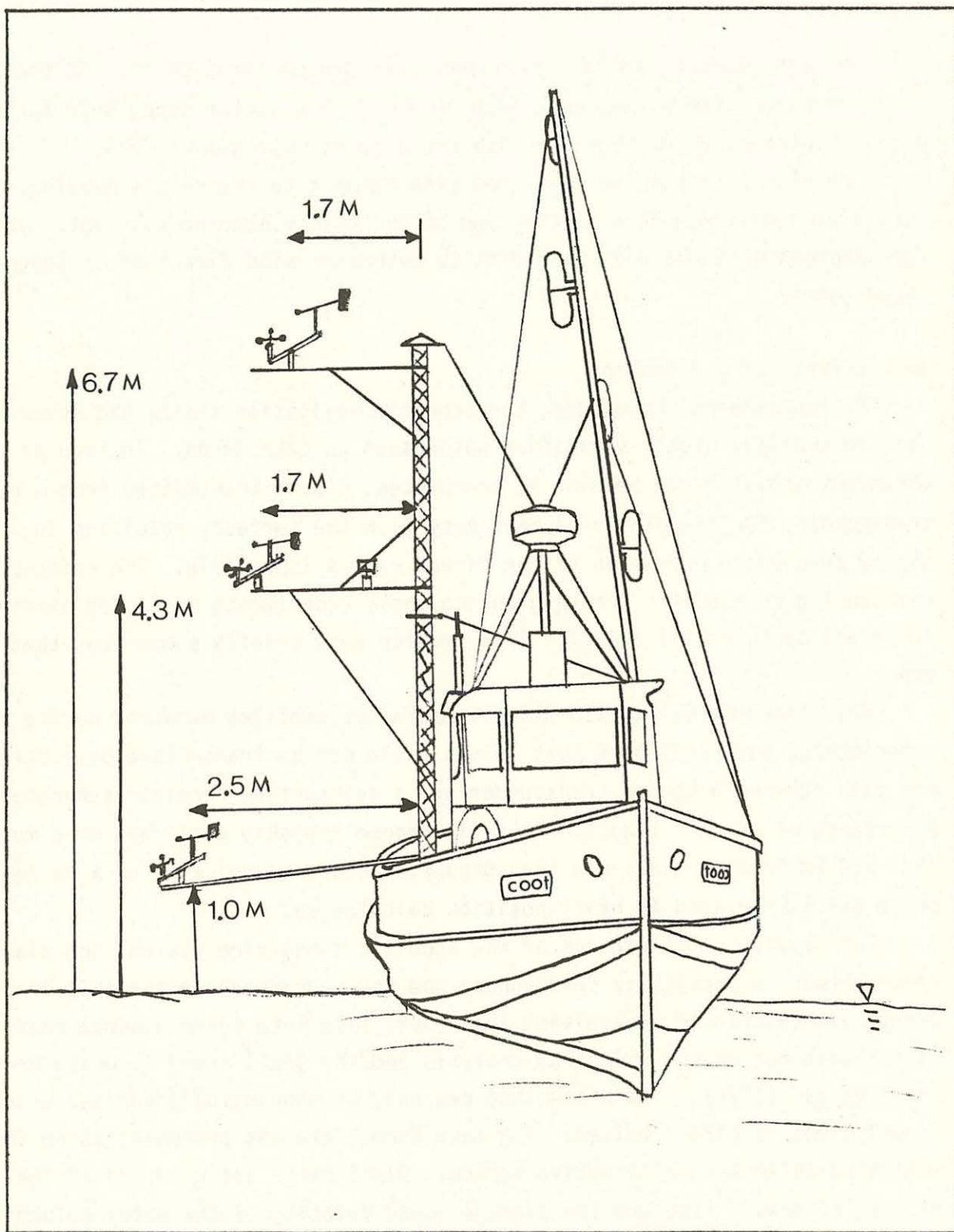


Figure 24: R/V Coot as equipped during the experiments. Distances of the anemometers from the water and tower are shown. The antenna tower on the port side is for receiving the acoustic drogue transmission.

The wind speeds and direction were recorded on strip chart. At the operator's request, the values were also recorded on cassette tape, once during each navigation cycle, together with the acoustic navigation data.

The wind direction was measured with respect to the ship's heading. During wind measurement a written log of the ship's heading was kept. This was combined with the wind vane data to determine wind direction in geographic coordinates.

3e. Effects of Ray Bending

To the authors' knowledge, the acoustic navigation system had never been used in shallow, highly stratified water such as Lake Huron. In such an environment acoustic ray bending is pronounced. Sound transmitted from a bottom transponder, for example, will bend away from the surface, resulting in a shadow zone where reception of the direct ray is impossible. The effects of ray bending on acoustic tracking during these experiments have been examined in detail by Churchill (1981). This section very briefly summarizes that report.

Ray diagrams, calculated using temperature profiles measured during the experiments, have indicated that pulses could not be transmitted by a direct ray path between a bottom transponder and a nearsurface receiver separated by a distance of greater than 1.4 km. All drogue and ship positions were more than 1.4 km from at least one transponder. Thus, a travel time of a reflected pulse was likely used in every position calculation.

For previous applications of the acoustic navigation system, the slant range between a particular transponder and the hydrophone of the ship or a drogue was calculated by applying the travel time into formula whose coefficients were determined using ray analysis and the local sound velocity profile [Hunt et al. (1974)]. Such a method can only be meaningfully applied using travel times of direct pulses. The Lake Huron data was processed using the most straightforward alternative method. Slant range was computed as the product of travel time and the average sound velocity of the water column; which is equivalent to assuming that the pulses traveled in a straight line at constant velocity.

Prior to the experiments a simple model was developed to predict the error in slant range due to receiving reflected pulses and assuming straight line travel. For the conditions encountered in Lake Huron the error values were approximately 2 percent. The error associated with drogue velocity determination was predicted to be about 1 percent.

Ship cycle travel times recorded during the experiments, combined with ray diagrams, have strongly suggested that pulses transmitted between the ship's transducer and a transponder, which was greater than 1.2 km from the ship, traveled by ray paths trapped below the thermocline. The error in slant range and velocity determination of such rays (due to assuming straight line travel) was shown to be from 1 to 2 percent. Because these presumed errors were very small, no attempt was made to correct for slant range error.

Shortly after the second transponder deployment on July 14, the reception range between the ship and the transponder was measured by steaming away from it until the reply pulse was not consistently detected. The range of 8 km was about equal to that noted during the experiment at DWD-106 [Churchill *et al.* (1981)]. During the drogue tracking experiments, roughly one month later, the reception range was approximately 4 km. During these experiments the mixed layer was about 14 m deep, whereas on July 14, the mixed layer was only 4 m deep.

As previously stated, pulses transmitted between the ship's transducer and a transponder separated by more than 1.2 km likely traveled by ray paths reflected at the thermocline and bottom. Because of the shallower mixed layer, a ray trapped below the thermocline on July 14 traveled a longer horizontal distance between bottom reflections and reflected at a smaller grazing angle than did a similar ray during the acoustic drogue experiments. The signal attenuation due to bottom reflection would thus have been less for thermocline reflected pulses on July 14. Churchill (1981) presents a rough calculation which indicates that the increased bottom reflection signal loss due to increased mixed layer depth during the drogue tracking experiments approximately accounted for the difference between the reception range measured during the experiments and on July 14.

Again, this section is only a brief summary of the report by Churchill (1981) which deals, in detail, with the problems and findings concerning ray bending.

3f. Determination of Transponder Position

Each transponder was suspended about 15 m above the bottom by glass ball flotation which was attached to the transponder by 15 m of line. 200 m of cable connected the transponder's anchor to a second anchor which supported a marker buoy used for eventual retrieval. Transponders were deployed on July 11, 14, and 15.

During July 15 and 16, travel times were measured at a number of locations in the vicinity of the transponder net. These were used by program SWURV for calculating relative transponder locations. SWURV, whose theory and operation is described in Hunt et al. (1974), determines transponder locations so as to minimize the sum of the squares of the difference between the slant ranges calculated from the travel times and those calculated using the ship and transponder positions. Computed and printed also are the standard error of the slant ranges and the survey error, which is the sum of the variances of the transponder locations normalized by the slant range standard error.

For the survey of July 15 and 16, the slant range and survey errors were 11.7 m and 10,860 m respectively. Although this survey error was unsatisfactory the transponder locations were used for real time processing during drogue tracking. A more systematic survey, for determining transponder locations to be used for data reprocessing, was conducted on August 13. The error of this survey was 10^6 m; again extremely high, mostly due to variances of the transponder depths. The minimization algorithm appeared to have difficulty with the shallow transponder depths. With successive iterations the depths decreased, tending towards the ship's transducer depth. This problem was circumvented by modifying SWURV to treat the transponders' depths as constants (their values were measured using the ship's depth finder). The slant range standard error and survey error resulting from use of the modified program were 11.5 m and 6.5 m respectively. The calculated transponder positions were used for data reprocessing as will be described in section 3g.

The geographic orientation of the net was determined as follows. On July 18, the Coot was tracked while steaming in a straight line from station 8 to 9 (Figure 1). After the ship was turned about, a compass bearing was taken on the line from station 9 to 8. The Coot then steamed back to station 8 while being tracked. The net was orientated such that the bearing of the ship track matched the compass measurement (+ the local magnetic deviation).

3g. Data Analysis

Initially, drogue and ship positions were calculated by a deterministic formula using two of the three available travel times. Despite the effort made in determining transponder locations (section 3f), drogue positions calculated using different pairs of travel times differed significantly, often by more than 100 m. Because of this, it was decided to employ a nonlinear regression method, which used all three travel times, for computing drogue and ship positions. Each position calculated by this method minimizes the following formula:

$$(14) \quad S S = \sum_{i=1}^3 (S L_i - s r_i)^2$$

where $S L_i$ is the slant range between transponder i and the drogue or ship hydrophone, as determined from the travel time. $s r_i$ is the computed slant range, given by:

$$s r_i = [(X_{sd} - X_{t_i})^2 + (Y_{sd} - Y_{t_i})^2 + (Z_{sd} - Z_{t_i})^2]^{1/2}$$

where:

X_{sd} and Y_{sd} are the east and north position components of the ship or drogue. Z_{sd} is the known depth of the hydrophone of the drogue or ship. X_{t_i} , Y_{t_i} , Z_{t_i} are the coordinates of transponder i .

The minimization was done by subroutine LSQF which was created by Dr. Woollcott Smith as part of program SWURV (Hunt et al., 1974). Drogue positions calculated using this method had less scatter about the apparent trajectory than did corresponding positions calculated using only two travel times.

The square root of SS defines the slant range standard error for the particular fix. Values of the slant range standard error were used to identify and reject questionable fixes. The average value was approximately 40 m for drogue fixes and 10 m for ship fixes.

For the experiment at DWD-106, drogue velocity components were calculated as the slopes of linear regressions relating position component with time. For such a calculation each drogue is assumed to travel in a straight line at constant speed. This assumption is valid for the drogue track of the August 14 experiment (Figure 27). However, drogue trajectories during all other experiments were markedly curved (Figures 25, 29, 31, and 33). Drogue velocities of these experiments were determined from quadratic regressions relating position component with time.

East position component, for example, was fit, by least-squares, to the following formula:

$$(15) \quad x_d = B_{2x} t^2 + B_{1x} t + B_{0x}$$

where t is the time since the release of the drogue.

At a particular time, the eastward velocity component is:

$$(16) \quad u_d = 2 B_{2x} t + B_{1x}$$

The standard error of this velocity is given by:

$$(17) \quad \text{ST ERR } (u_d) = [V(u_d)]^{1/2}$$

where $V(u_d)$ is the variance of u_d which is given by:

$$V(u_d) = 4 t^2 V(B_{2x}) + V(B_{1x}) + 4 t \text{ cov}(B_{1x}, B_{2x})$$

The variances and covariances of the regression coefficients were determined using the variance-covariance matrix according to a method described by Draper and Smith (1966).

The variance-covariance matrix is given by:

$$(18) \begin{bmatrix} V(B_0) & \text{cov}(B_0, B_1) & \text{cov}(B_0, B_2) \\ \text{cov}(B_0, B_1) & V(B_1) & \text{cov}(B_1, B_2) \\ \text{cov}(B_0, B_2) & \text{cov}(B_1, B_2) & V(B_2) \end{bmatrix} = [T'T]^{-1} \frac{SSR}{n-3}$$

where:

SS = sum of squares about the regression equation (15)

n = number of positions

T is a matrix of the times (since the release of the drogue) of each fix, given by:

$$T = \begin{bmatrix} 1 & t_1 & t_1^2 \\ 1 & t_2 & t_2^2 \\ 1 & t_3 & t_3^2 \\ \vdots & \vdots & \vdots \\ 1 & t_n & t_n^2 \end{bmatrix}$$

The necessary terms of the $[T'T]^{-1}$ matrix were calculated by Cramer's rule.

3h. Results

Drogue tracking experiments were conducted on five days from August 12 to August 21. Drogues were released and tracked from the R/V Coot (15 m LOA) which was moored at Flag station 8 (Figure 1). After completion of tracking, drogue retrieval from the Coot was accomplished with the aid of the navigation system.

Ship and drogue positions of each experiment are shown in Figures 25, 27, 29, 31, and 33. East and north components of position, velocity and velocity standard error, calculated at specific times from least squares regressions of position components vs. time [equations (15)-(18)], are listed in Tables A23-A27 of the Appendix. The corresponding velocity vectors together with the wind velocity measured at 6.7 m are displayed in Figures 26, 28, 30, 32 and 34. Temperature and current meter profiles, measured at Flag station 8 during acoustic drogue tracking, are listed in Table A28 in the Appendix.

As noted in section 3g, all drogue tracks, except for those of August 14, are markedly curved. Most drogues curved clockwise. For a particular time period, the rate of rotation of a drogue's velocity vector may be defined by:

$$R = \frac{\theta_2 - \theta_1}{t_2 - t_1}$$

where θ_2 and θ_1 are the bearings of drogue velocity at times t_2 and t_1 . For clockwise rotation, the time necessary for a 360° rotation at the rate, R (given in deg/s), is simply:

$$(19) \quad T_R = \frac{1}{10} \frac{t_2 - t_1}{\theta_2 - \theta_1} \text{ hr}$$

These times have been calculated from the velocities of all drogues which curved clockwise and are listed in Table 4. They may be compared with the inertial period, which at the Lake Huron latitude is 17 hr (keep in mind, however, that drogues were tracked for 1/4 inertial period or less).

A summary of each drogue tracking experiment follows.

On August 12, a surface slab of 30 cm mean depth and three submerged slabs were released. The wind was moderate from the north, but the lake state was relatively high (1 m or more). As can be seen in Figure 25, the surface slab was tracked to the south (windward) of the other drogues. The motion of this drogue may have been influenced by the wind as will be demonstrated by an

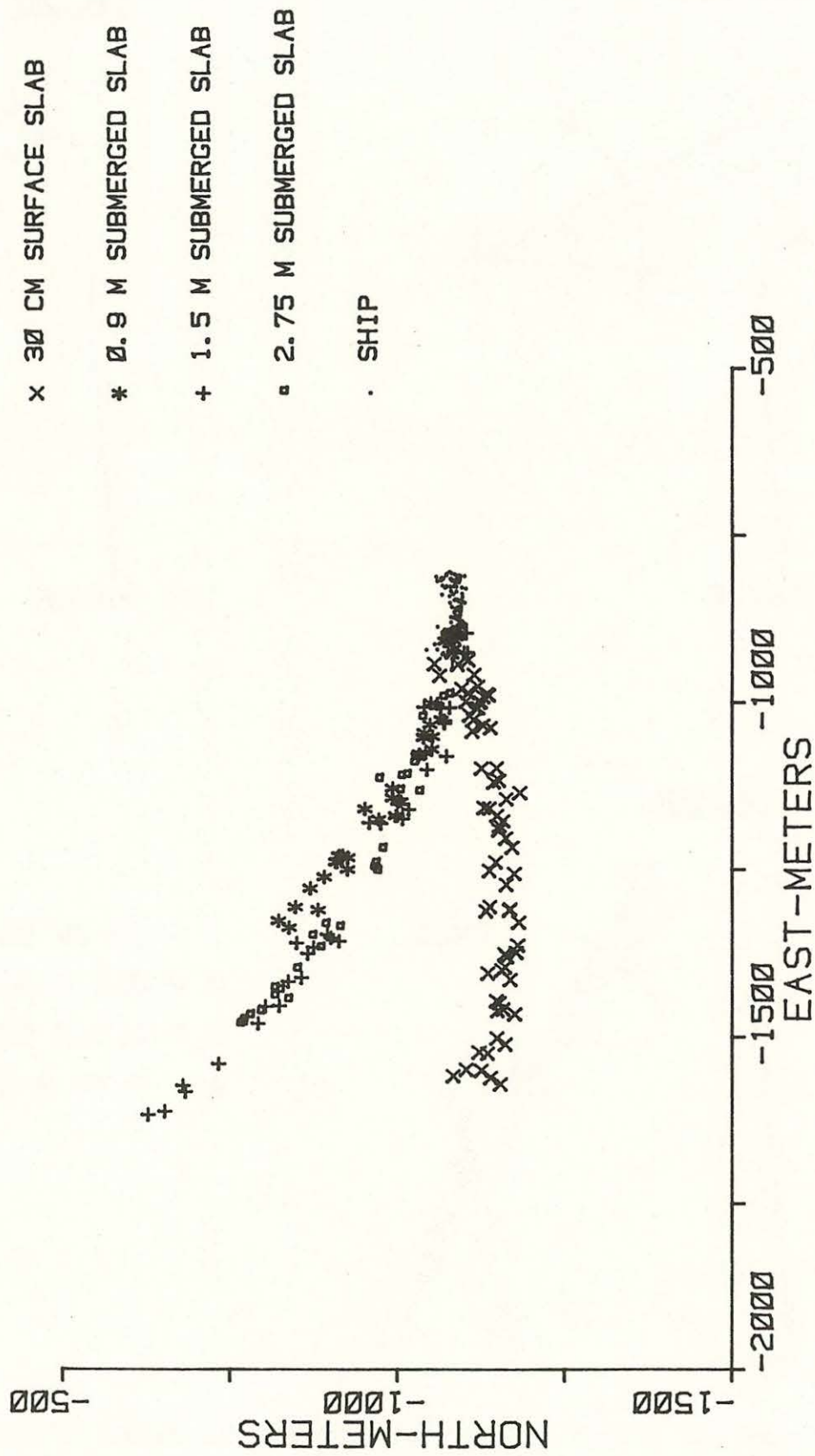
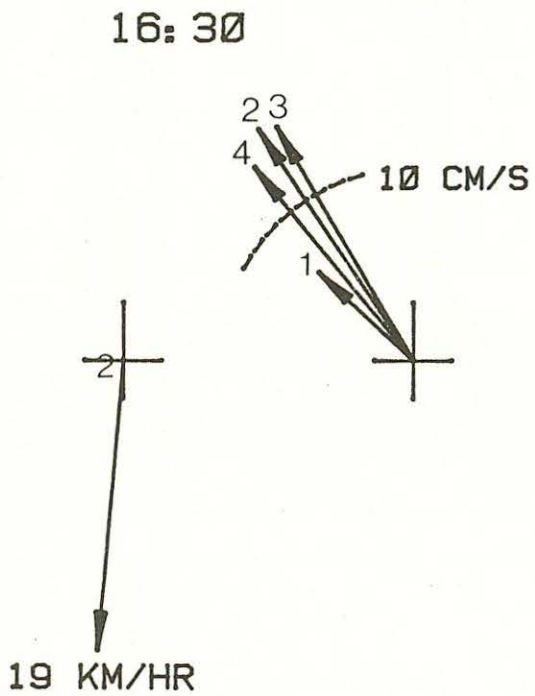
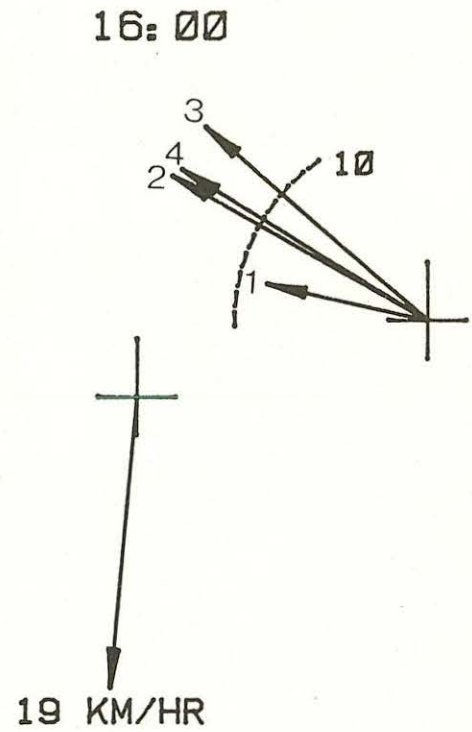
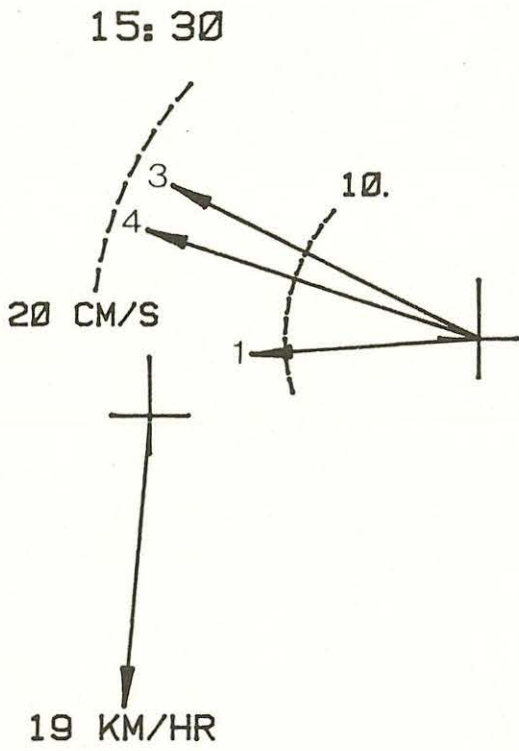


Figure 25: Drogue and ship positions of the August 12 experiment.



- 1 - 30 CM SUR. SLAB
- 2 - 0.9 M SUBM. SLAB
- 3 - 1.5 M SUBM. SLAB
- 4 - 2.75 M SUBM. SLAB

Figure 26: Drogue and wind velocities of the August 12 experiment.

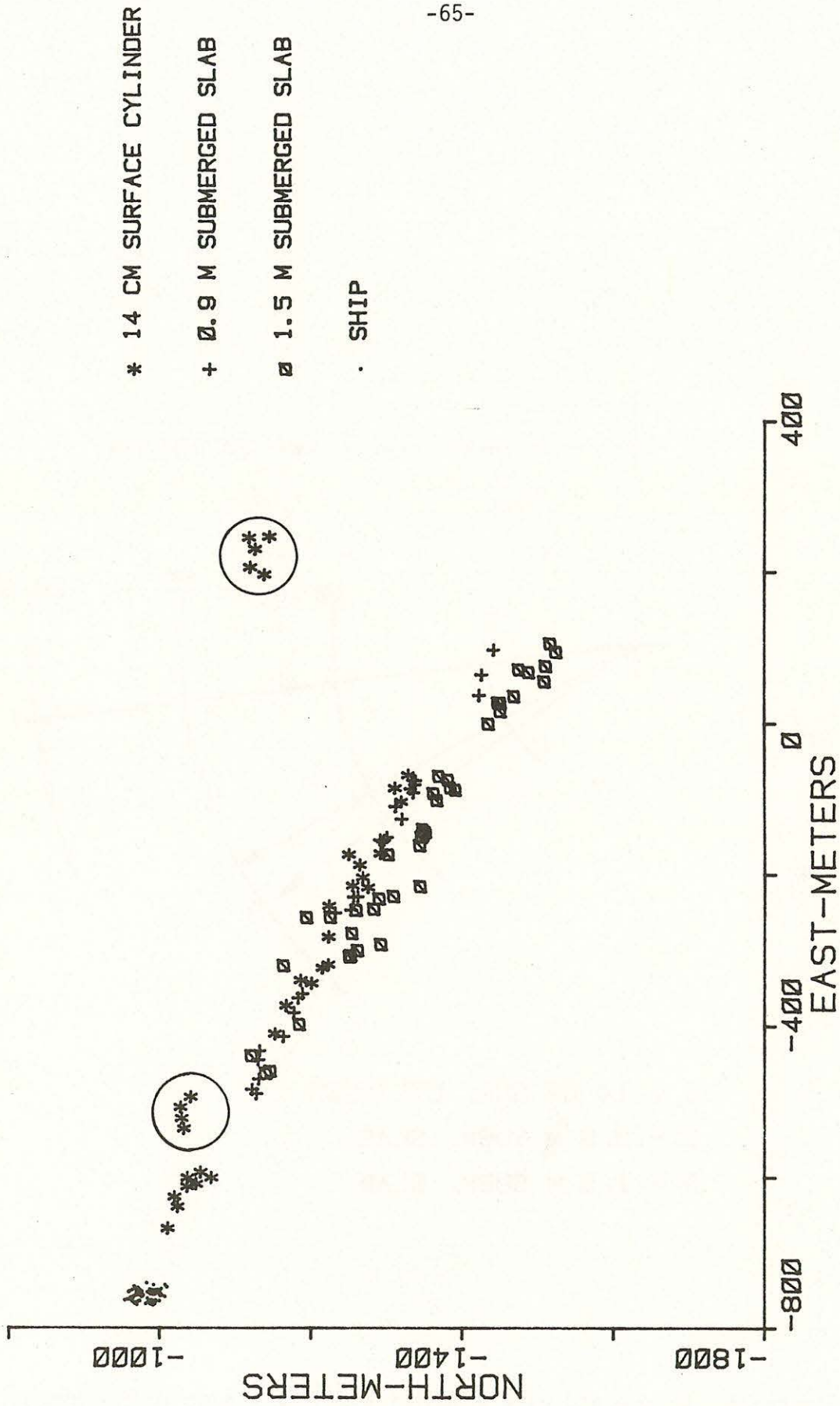
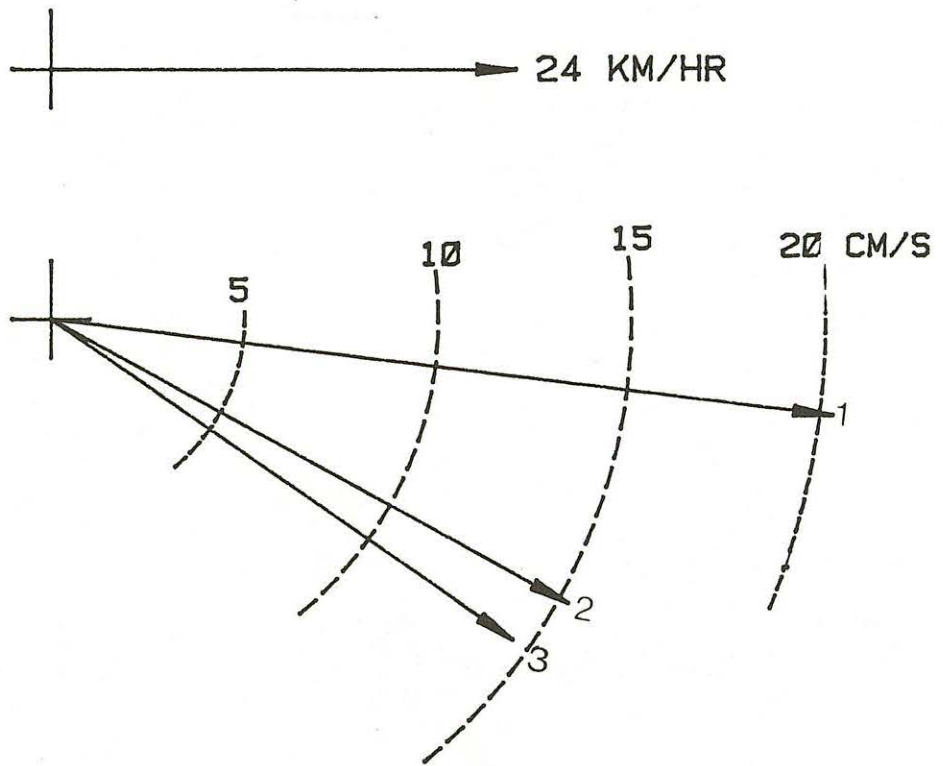


Figure 27: Drogue and ship positions of the August 14 experiment.



- 1 - 14 CM SUR. CYLINDER
- 2 - Ø.9 M SUBM. SLAB
- 3 - 1.5 M SUBM. SLAB

Figure 28: Drogue and wind velocities of the August 14 experiment.

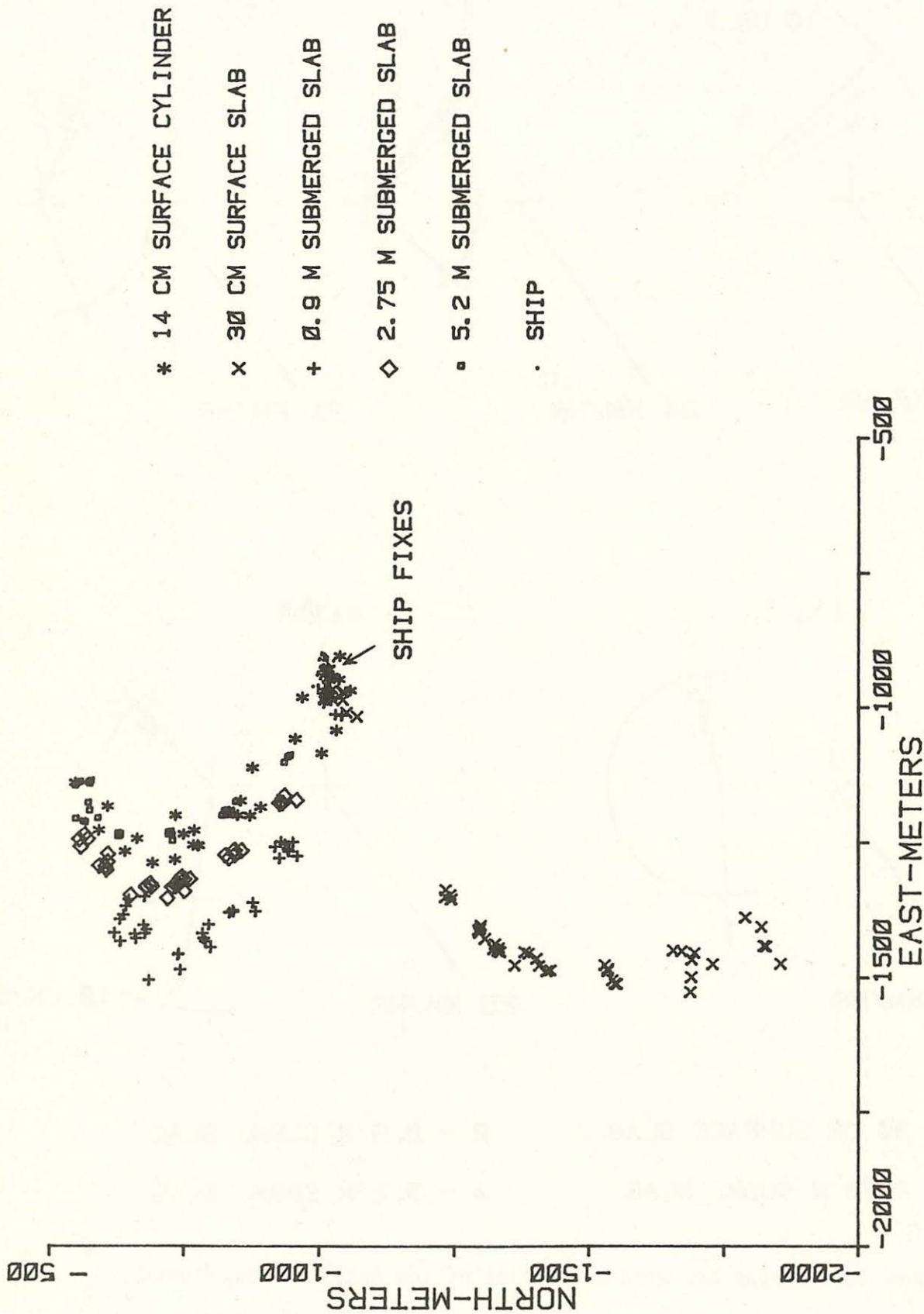
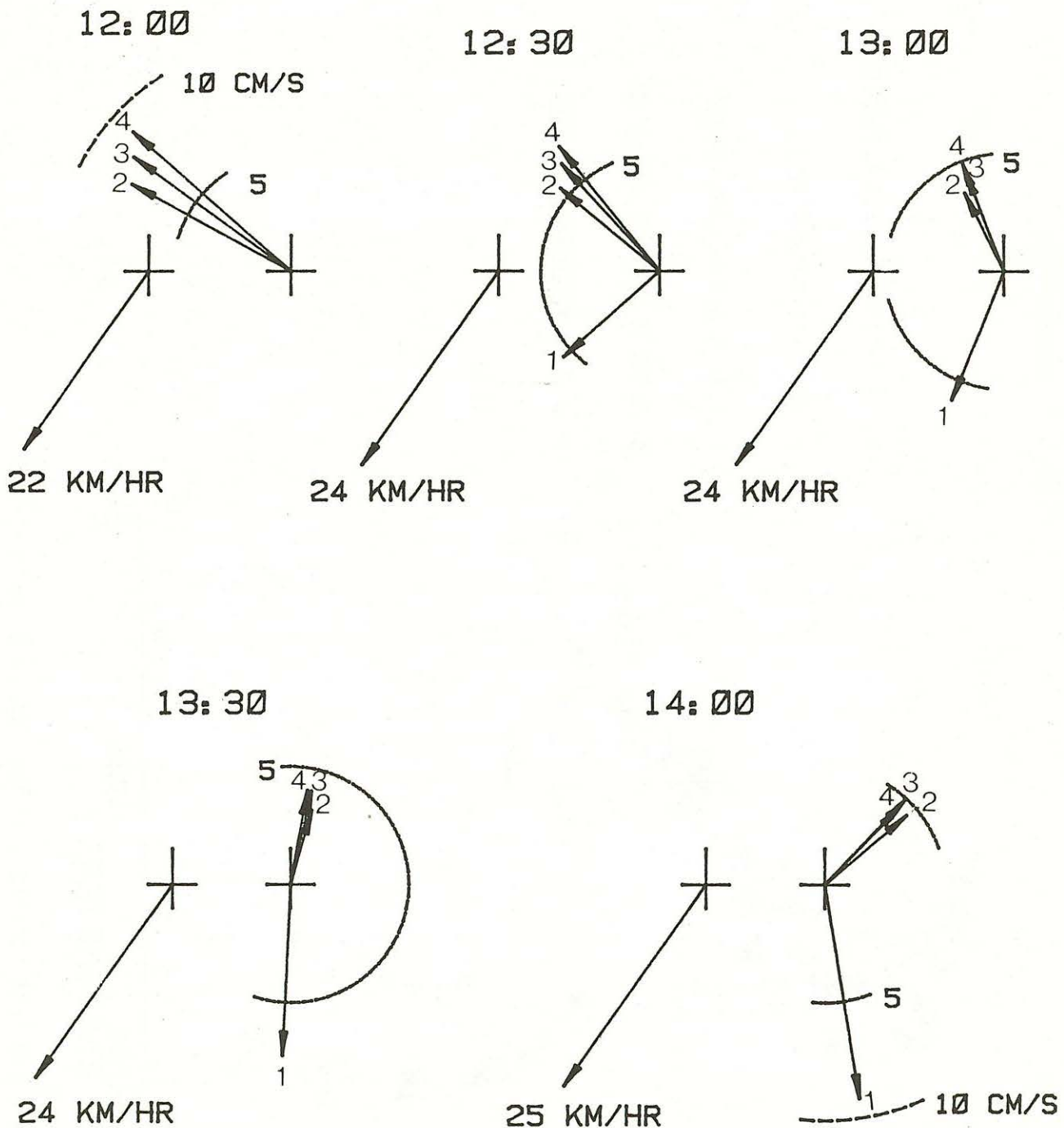


Figure 29: Drogue and ship positions of the August 15 experiment.



1 - 30 CM SURFACE SLAB
3 - 2.75 M SUBM. SLAB

2 - 0.9 M SUBM. SLAB
4 - 5.2 M SUBM. SLAB

Figure 30: Drogue and wind velocities of the August 15 experiment.

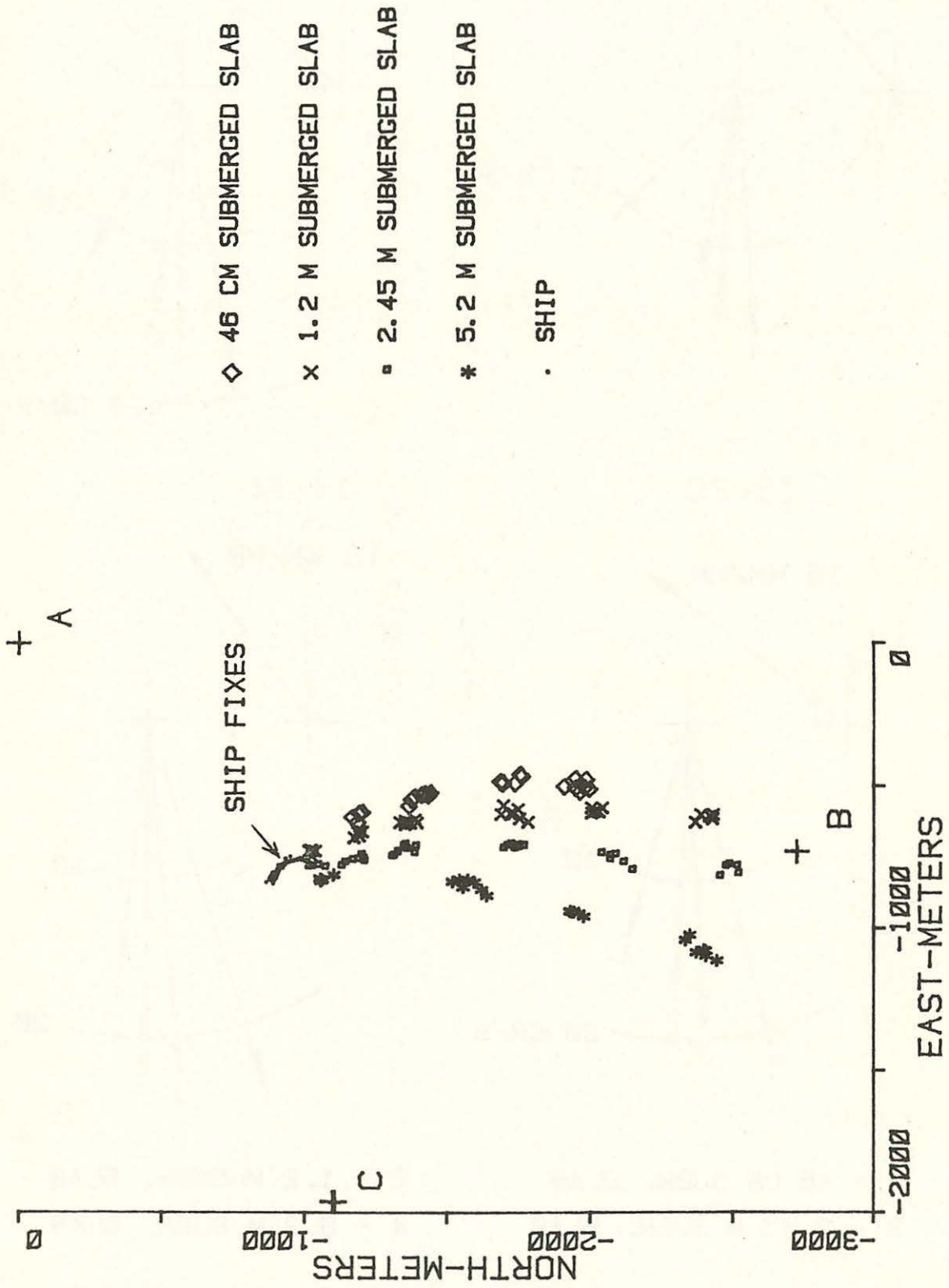


Figure 31: Drogue and ship positions of the August 20 experiment.

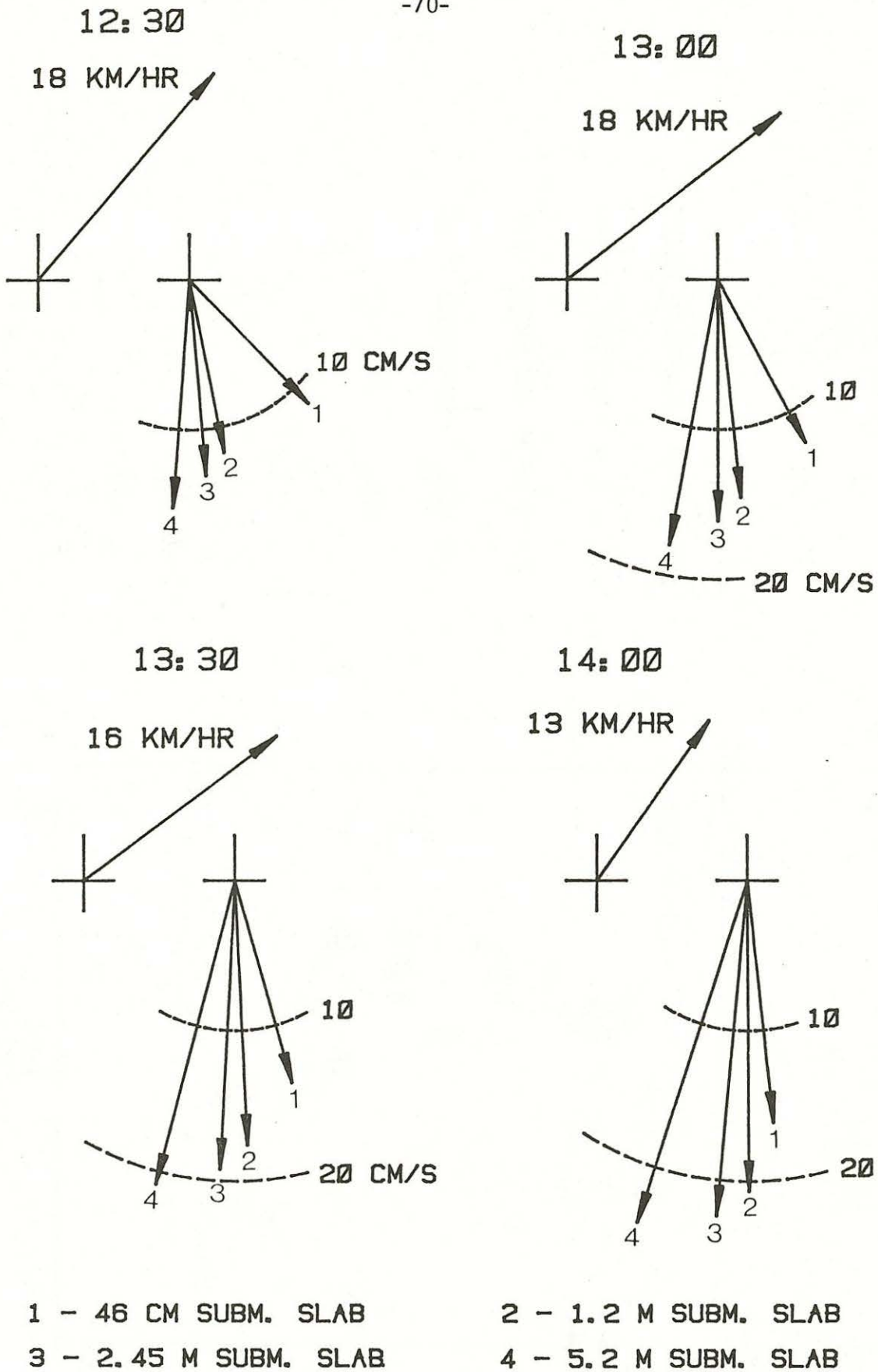


Figure 32: Drogue and wind velocities of the August 20 experiment.

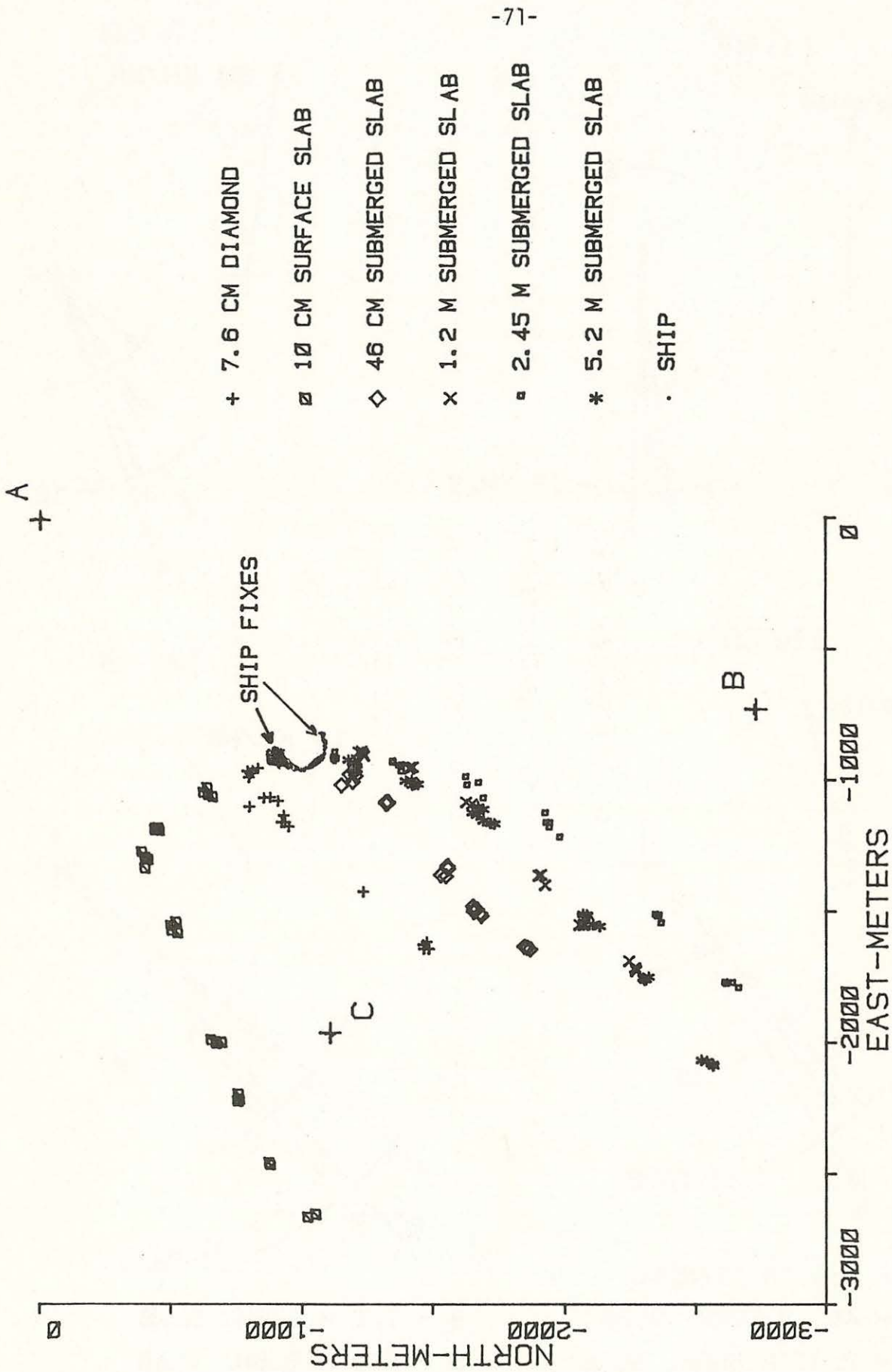


Figure 33: Drogue and ship positions of the August 21 experiment.

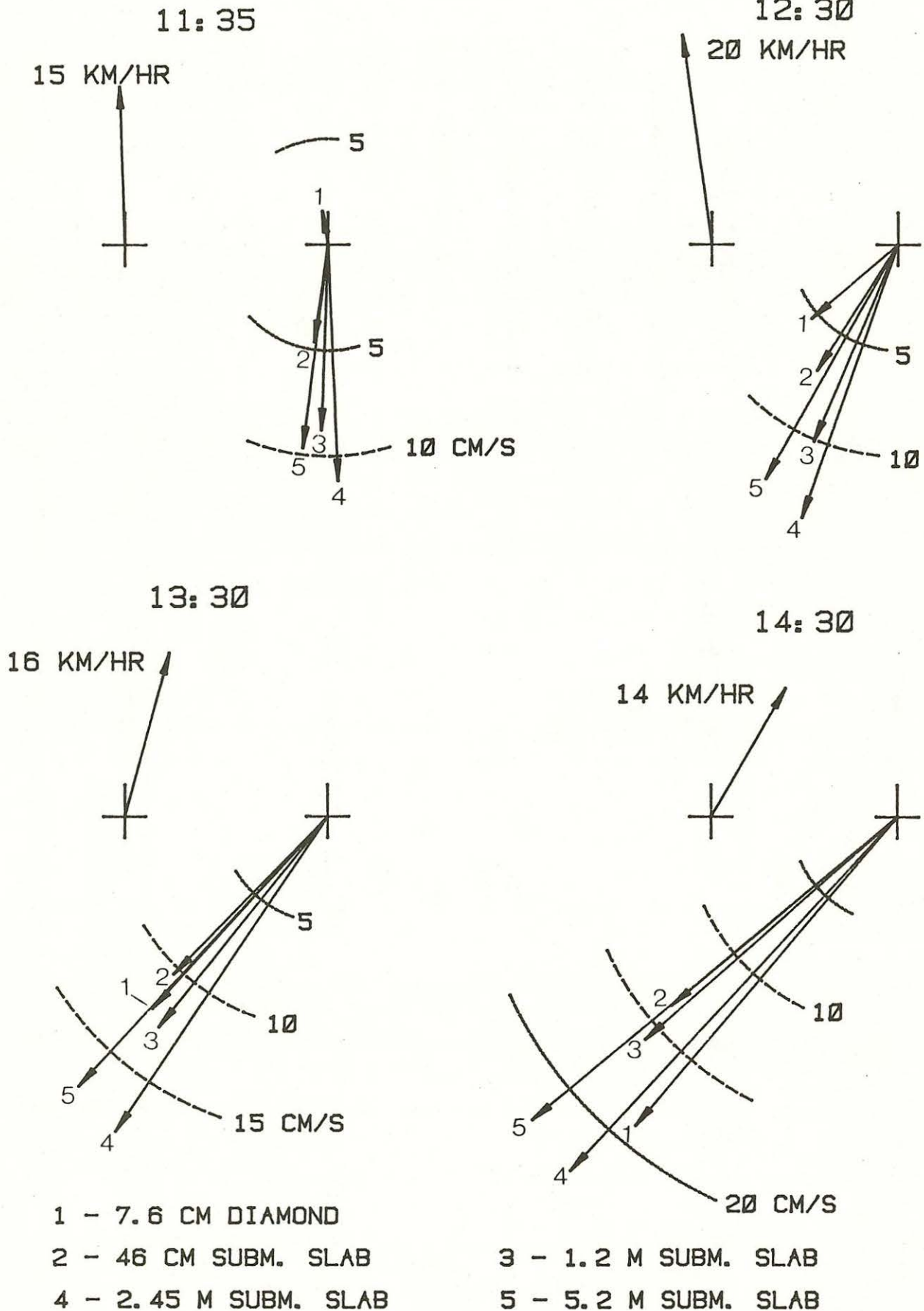


Figure 34: Drogue and wind velocities of the August 21 experiment.

Table 4

Rotation Periods Calculated by Equation 19 from the
Velocities of Acoustic Drogues which Curved Clockwise

A) AUGUST 12			
DROGUE (MEAN DEPTH)	θ_1 - DEG ($t_1 = 15:45$)	θ_2 - DEG ($t_2 = 16:30$)	T_R - HR
30 cm Surface Slab	273.0	313.2	6.7
0.9 m Submerged Slab	288.4	326.2	7.1
1.5 m Submerged Slab	303.4	329.7	10.3
2.75 m Submerged Slab	294.3	320.6	10.3
B) AUGUST 15			
DROGUE (MEAN DEPTH)	θ_1 - DEG ($t_1 = 12:00$)	θ_2 - DEG ($t_2 = 14:00$)	T_R - HR
0.9 m Submerged Slab	298.9	49.4	6.5
2.75 m Submerged Slab	306.2	43.0	7.4
5.2 m Submerged Slab	311.6	43.6	7.8
C) AUGUST 20			
DROGUE (MEAN DEPTH)	θ_1 - DEG ($t_1 = 12:30$)	θ_2 - DEG ($t_2 = 14:00$)	T_R - HR
46 cm Submerged Slab	136.2	173.7	14.4
1.2 m Submerged Slab	168.7	179.6	49.5
2.45 m Submerged Slab	175.2	185.2	54.0
5.2 m Submerged Slab	184.1	197.8	39.4
D) AUGUST 21			
DROGUE (MEAN DEPTH)	θ_1 - DEG ($t_1 = 11:35$)	θ_2 - DEG ($t_2 = 14:30$)	T_R - HR
46 cm Submerged Slab	188.0	230.1	25.0
1.2 m Submerged Slab	182.0	228.5	22.5
2.45 m Submerged Slab	177.5	222.6	23.3
5.2 m Submerged Slab	187.0	230.2	24.3

ensuing experiment. As shown in Figure 26, the velocities of the submerged drogues were initially perpendicular to the wind. They rotated clockwise at a somewhat greater than inertial rate.

On August 13, data was collected to examine the effect of the ship's transducer depth on acoustic tracking. The results are discussed by Churchill (1981).

On August 14, a surface cylinder and two submerged drogues of mean depths 0.9 m and 1.5 m were tracked while simultaneous sighted drogue experiments were conducted at station 7. The designated VHF channels on which the drogues transmitted to the ship were: 14 cm cylinder - ch 5, 0.9 m slab - ch 10, 1.5 m slab - ch 9 (channels labelled 1-16 correspond to frequencies of 162.25 - 173.50 mhz in steps of 0.75 mhz per channel). On two occasions, the cylinder was tracked while the ship's receiver was erroneously set to channel 4. The positions associated with channel 4, which are circled in Figure 27, are markedly out of line with those associated with channel 5. The drogue clearly could not have traveled by the path outlined by both sets of fixes. The velocity necessary to travel from the last channel 5 fix to the ensuing channel 4 fix is 74 cm/s. The drogue was retrieved in the vicinity of the last channel 4 fixes. The channel 5 associated positions were nearly coincident with those of the 0.9 m slab. It is our hypothesis that the signal received on channel 5 was actually "splash" from the 0.9 m drogue transmission on channel 10; and, for some reason, the cylinder's sonobuoy was actually transmitting on channel 4.

The August 14 drogue tracks were nearly straight lines. For this reason, linear regressions were used for velocity determination. Only the circled positions of Figure 27 were included in the regressions which determined the cylinder's velocity. The acoustic drogue velocities are in close agreement with those of the sighted drogue experiments given in Tables A18-A19 and Figure 13.

On August 15 drogues of the following mean depth and channel number were tracked: 14 cm cylinder - ch 5, 30 cm surface slab - ch 16, 0.9 m slab - ch 10, 2.75 m slab - ch 12, 5.2 m slab - ch 14. The signal from the cylinder began to squeal shortly after release. As can be seen in Figure 29, the track

of the cylinder was nearly identical to that of the 5.2 m drogue. At any time the locations of the two drogues, as determined by the least squares regression equations of position as a function of time, were within 50 m (Table A25). The cylinder was, however, retrieved significantly west of the 5.2 m drogue. It is thus likely that the pulses received on channel 5 were actually "splash" from the signal of the 5.2 m drogue on channel 14. Because the track of the cylinder is suspect its velocity has not been included in Figure 30.

With the exception of the surface slab all drogues initially traveled perpendicular to the wind and curved clockwise. The velocity of the surface slab was initially parallel to the wind and rotated counterclockwise. The motion of this drogue was likely influenced by wind because the shallower cylindrical drogue was retrieved north (upwind) of the release location. The velocity of the slab can be thought of as being comprised of two components, that due to wind drag and that due to water drag. Because of the steady wind during tracking the wind drag velocity component would have been nearly constant. The acceleration of the surface slab would thus have been mostly due to the acceleration of the water drag component, and should be roughly equal to the acceleration of the submerged drogues. The surface slab and all submerged drogues did accelerate to the southeast by about the same amount.

The hodograph at 1200 EDT on August 15 (Figure 30) shows a well-defined relative velocity between the 0.9 m, 2.75 m and 5.2 m drogues. This velocity is directed at 180° , about 35° to the left of the wind. As the experiment progressed all drogue velocities rotated clockwise at a somewhat greater than inertial rate. The relative velocity direction, however, changed very little.

During these first three drogue tracking sessions the lake state was relatively high and large slabs (0.9 x 0.9 x 0.6 m) were deployed. The wind was recorded on strip chart, not on magnetic tape, and the ship headings were sparsely noted. The wind directions of Figures 26, 28, and 30 are accurate to 20° . During the final two tracking experiments (August 20 and 21) the lake was relatively calm and smaller slabs (0.68 x 0.68 x 0.3 m) were deployed. Anemometer data was recorded both on strip chart and magnetic tape, and the ship's heading was frequently noted. The reported wind directions are accurate to 10° .

On August 20, four submerged drogues and a surface cylinder were released. The signal from the cylinder (on channel 12) began to squeal shortly after deployment; no meaningful fixes were obtained. Hodographs of the submerged slabs (Figure 32) indicate that as the experiment progressed all drogue velocities increased in magnitude and rotated clockwise at a slower than inertial rate. At all times the relative velocity was roughly aligned with the wind.

The wind speed and direction recorded by the top anemometer during the August 20 experiment are shown in Figure 35 together with the shear between the top and mid-anemometers.

On August 21, a surface slab, a surface diamond, and four submerged slabs were tracked. The drogues were released from 1000 to 1100 EDT. As shown in Figure 36, during this time the wind was strong and from the south. Both surface drogues initially move windward while all submerged drogues traveled against the wind. The surface slab moved at a greater speed in the wind direction than did the shallower diamond. This slab was of the same design as that deployed on August 12 and 15 and its velocity is likewise suspect of excessive wind drag. Its velocity has thus not been included in the hodographs of Figure 34. From 1100 to 1200 EDT the wind considerably increased. The surface drogues, however, continued to accelerate opposite to the wind direction.

A relative velocity, roughly parallel with the wind direction, is defined by velocities labeled 1-4 (7.6 cm - 2.45 m) of the 1135 and 1230 hodographs in Figure 34. At 1330 and 1430 the relative velocity is defined only by vectors labeled 2-4. By those times the 7.6 cm drogue (vector No. 1) was approximately 1 km from the submerged drogues, as indicated by Table A27. Also, the velocity of the 7.6 cm drogue rotated counterclockwise with time, whereas the submerged drogues' velocities rotated clockwise.

As on August 20, the submerged drogues' velocities increased in magnitude and rotated clockwise at a less than inertial rate, while the relative velocity profile remained nearly unchanged. The coincident current meter profiles of Tables A28e and A28f showed a similar rate of increase and rotation.

The velocity profile of sighted drogue run 2 (Figure 14) which commenced at 1120 at station 6 is significantly different from the nearly concurrent

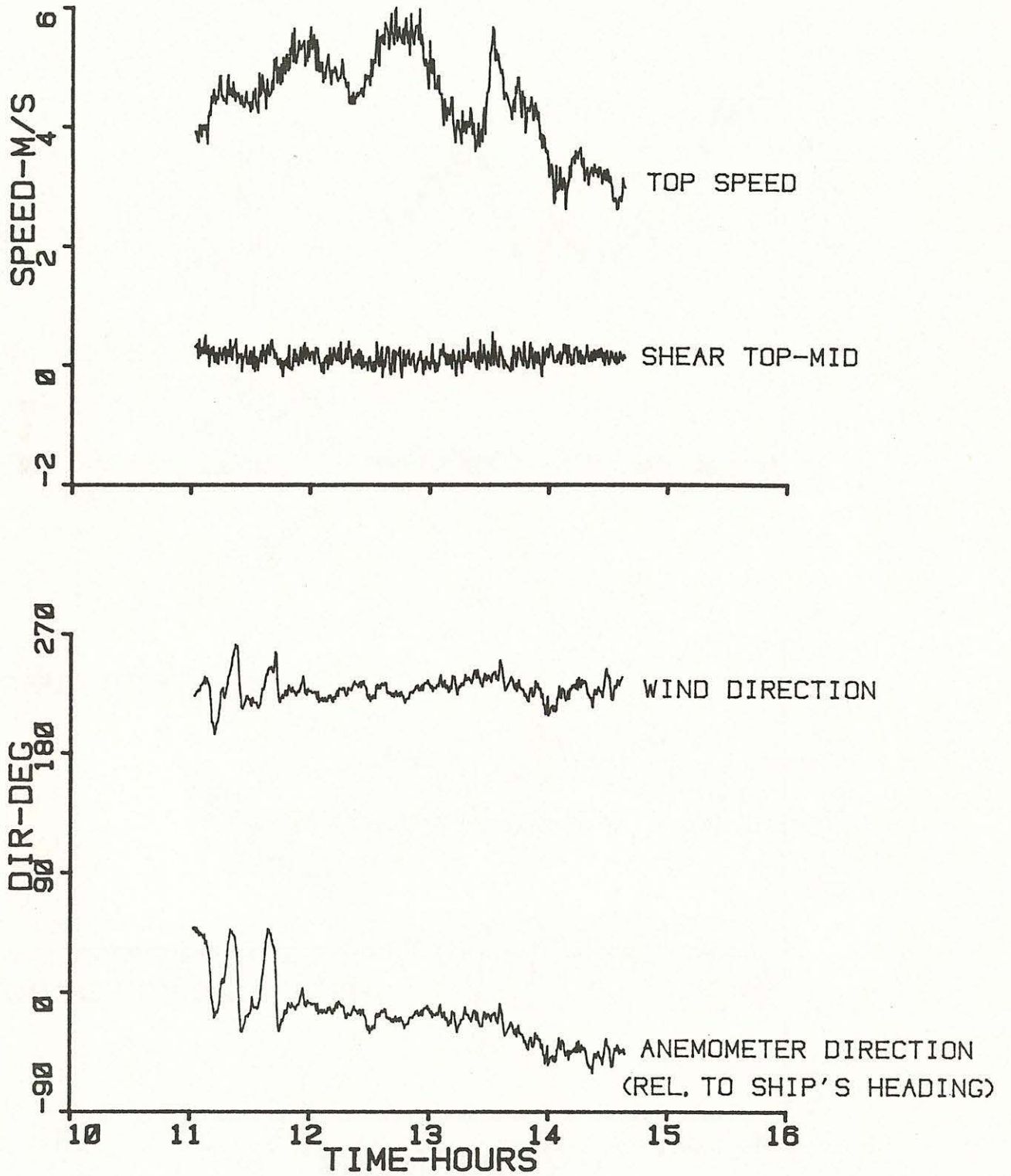


Figure 35: Wind data recorded during the August 20 drogue tracking experiment. The top and mid-anemometers were 6.7 m and 4.3 m, respectively, above the lake surface.

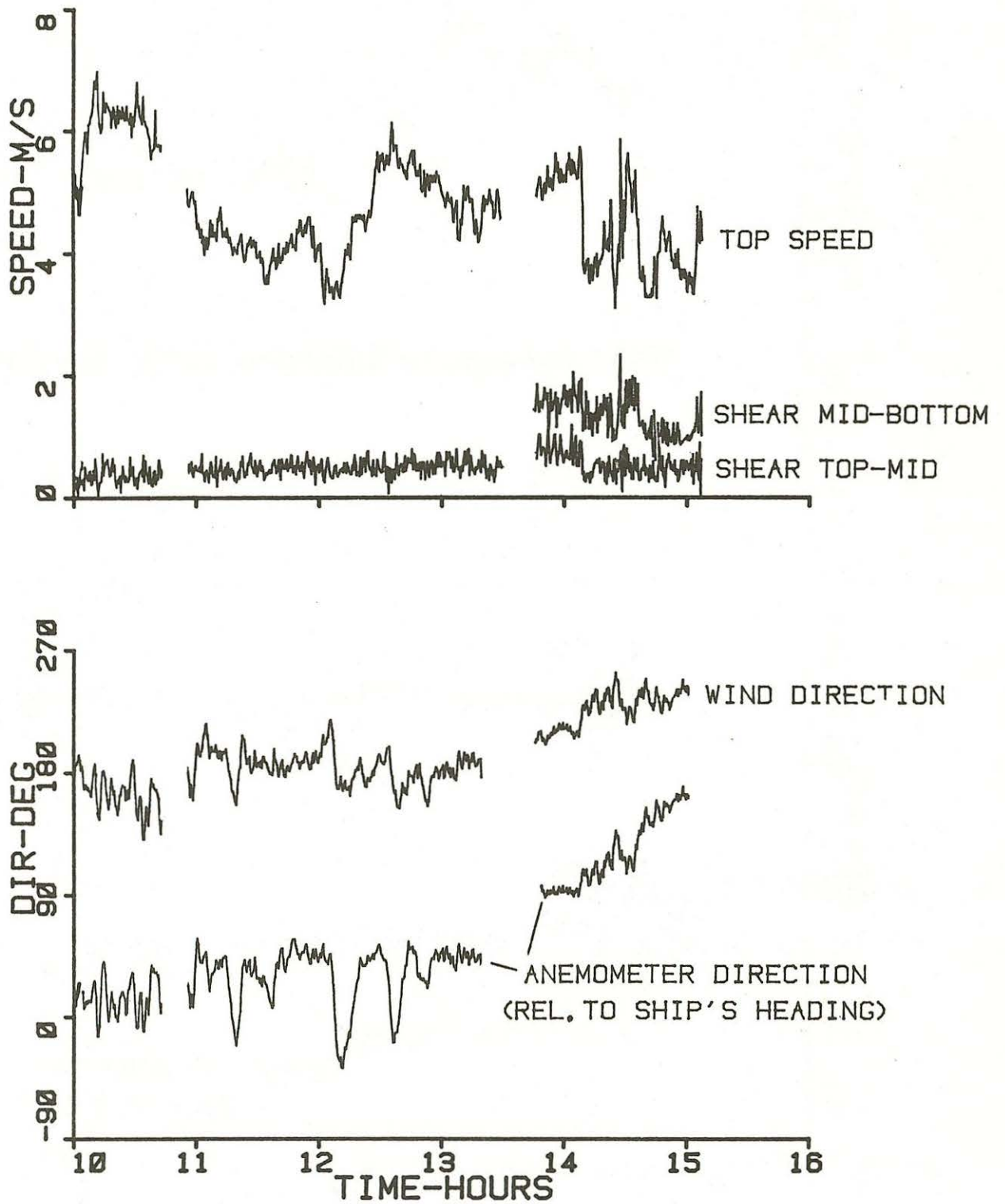


Figure 36: Wind data recorded during the August 21 drogue tracking experiment. The top, mid- and bottom anemometers were 6.7 m, 4.3 m and 1.0 m above the lake surface. Gaps in the records are due to interruptions of data recording after an end of file mark was put on the cassette tape data.

acoustic drogue profile at 1135 (Figure 34). Sighted drogue velocities were to the north and northeast and rotated clockwise with increasing depth. Only the shallowest acoustic drogue velocity was to the north, all others were to the south, and the velocities rotated counterclockwise with increasing depth. The sighted drogue velocity profile of run 2, which started at 1310, was markedly different from the run 1 profile, but similar to the 1135 acoustic drogue profile.

The above observations can be explained by assuming that during run 1 there was a front between the sighted drogues at station 6 and the acoustic drogues near station 8. The passage of the front over station 6 at some time between runs 1 and 2 would account for the difference between the two sighted drogue profiles and the similarity between the second sighted drogue profile and the acoustic drogue profile at 1135.

The wind speed, direction and the shear between the top and mid anemometers, recorded during the August 21 experiment, is displayed in Figure 36. During the final 1 1/2 hours of tracking the wind speed from the bottom anemometer was recorded. The shear between the mid and bottom anemometers is also displayed in Figure 36. Note that the top to mid shear is nearly constant throughout the experiment except for a brief "high spot" from 1345 to 1410. This corresponded to a time when the wind was broadside to the ship, and was thus likely due to the influence of the ship. At all other times, however, the shear was independent of the angle between the wind and the ship's heading. It, therefore, appears that the shear between the top and mid anemometer was only affected by the ship's presence when the wind was nearly broadside to the ship. Note that the shear during both the August 20 and August 21 experiments was independent of wind speed. During the August 21 experiment, the lake state was slightly greater and, as would be expected, so was the shear.

During August 21, from the start of tracking at 1000 until 1400, the ship location changed very little (maximum speed 1 cm/s). From 1400 to 1500 the ship moved at a relatively high speed (~ 12 cm/s) in a counterclockwise arc about the mooring (likely the result of a shift in wind direction shown in Figure 36). During this period, the slant range standard errors of the ship

and drogue fixes were roughly a factor of 2 higher than those of fixes from 1000 to 1400. The accuracy of the navigation system thus appears to significantly worsen with increasing ship speed.

3i. Discussion

The acoustic drogue velocities clearly consist of two components. Using the terms of section 2i these are: A sub-current which varied slowly with depth (compared with the deepest drogue depth of 5.2 m) and rotated clockwise with time; and, a surface layer-current which was directed roughly parallel with the wind and waves.

Within 12 hours of the August 12 and August 15 experiments, the wind had shifted dramatically (Figure 16). These experiments were characterized by a rough lake surface, sub-currents rotating at high frequency, and relatively low nearsurface shear. The winds were more steady prior to the August 20 and 21 experiments. During these experiments the lake state was moderate. The sub-current rotated at low frequencies and were directed roughly alongshore, in the direction of previous strong winds. The surface currents of August 20 and 21 were particularly well-defined and of approximate magnitude expected for Stokes' drift [as calculated using equation (13) and a typical spectrum]. The shears of August 12 and 15 were lower than expected for Stokes drift (considering the rough lake surface). The nearsurface dynamics of these experiments may have been further complicated due to the sudden wind shift, as suggested by the high frequency of the sub-currents.

As evidenced by these experiments the nearsurface velocity field is extremely complicated. Just recently have theories been advanced which collectively consider the effects of waves, Reynolds stresses and inertial currents [Craik and Leibovich (1976), Leibovich (1977), and Huang (1979)]. Field measurements are necessary to test these theories and to provide insight for future models. These experiments have demonstrated that the acoustic and visual drogue tracking techniques can be employed to measure nearsurface Lagrangian velocities unobtainable using conventional current meters. Future drogue tracking experiments combined with precise measurement of the wave field should provide additional understanding of nearsurface dynamics.

4. MEASUREMENTS OF WATER VELOCITY AND TEMPERATURE STRUCTURE PRIOR TO AND FOLLOWING A COASTAL UPWELLING

On August 16 observations of nearshore surface temperature indicated that a coastal upwelling had occurred, the result of strong north and northwest winds during August 15 and 16, and possibly during August 12 (see Figure 16). This section reports on measurements of water velocity and temperature structure four days prior to and 12 days following the upwelling.

Acoustic drogue experiments were conducted during the strong NW wind events of August 12 and August 15. The results are given in Tables A23 and A25 and Figures 26 and 30. As noted in section 3h, all drogue velocities (sub-currents) rotated clockwise at a greater than inertial rate (keep in mind, however, that drogues were tracked for 1/4 inertial period at most). Particularly noteworthy is that on August 15 the drogue velocities directed offshore (at 12:00 in Figure 30) were about 5 cm/s faster than velocities of the same depth directed longshore (at 13:30) or onshore (at 14:00). Figure 26 indicates that the drogue velocities of August 12 also decreased in magnitude as they rotated away from the offshore direction.

During August 14 the wind shifted briefly towards the north and northeast. The velocities of acoustic and sighted drogues tracked on that day were all onshore (Tables A18, A19 and A24 and Figures 13 and 28).

By August 17 the wind had diminished to a slight breeze. On the morning of August 17 two crews set out from Baie Du Doré to study the upwelled front. One crew, aboard a fast outboard, was to follow the progress of the front (which could be identified by a slick of scum and debris, and an approximate temperature difference of 2°C), and make temperature and current meter measurements in the front's vicinity. The other crew departed in two boats. It was their duty to carry out sighted drogue experiments on either side of the front. Measurements were made at moored flag stations labeled 1-10 in Figure 1. Throughout the day the wind was very slight (< 5 cm/s).

The onshore speed of the front appeared to vary. At approximately 12:00 it was estimated to be moving at roughly 300 m/hr. The temperature profiles to be presented are thus subject to some error due to movement of the isotherms during measurement (the magnitude probably isn't very great though).

Water velocity vectors and temperature structure measured at three stations from 9:30 to 10:45 are displayed in Figure 37. Note the reversal in current direction between 5 m and 20 m depth. Current meter and temperature measurements taken between 12:00 and 14:00 are displayed in Figure 38. The velocity field, which does not appear to be consistent with the shoreward movement of the front, is characterized by significant clockwise rotation of vectors with depth and time, and counterclockwise rotation with increasing offshore distance.

Sighted drogues were tracked on the shoreward side of the front at flag station 4 during the morning of August 17. During the afternoon sighted drogues were tracked on the lakeward side of the front at station 5. The averaged velocities of these experiments are displayed in Figure 39 and listed in Tables A29 and A30 of the Appendix.

During the morning experiment bearing of the 1.8 m drogues was approximately 120° counterclockwise from that of the surface slabs. After tracking was completed the slabs drifted into the slick and were retrieved significantly to the south (counterclockwise) of their last bearing.

During the afternoon experiment there was no perceptible wind and the lake was glassy calm. As shown in Figure 39 all velocities were approximately to the southwest (as were the nearsurface current meter measured velocities shown in Figure 37), and the relative velocity was directed onshore.

It should be noted that although the slick in Figure 39 is depicted as being midway between stations 4 and 5, during tracking at station 4 the slick was about 250 m offshore from station 4; during tracking at station 5 the slick was more than 1 km shoreward of station 5.

At 15:30, while the sighted drogue crew was returning to camp, they encountered the slick in the vicinity of site S shown in Figure 1. 10.2 cm slabs were deployed on either side of the slick. They converged on the slick cyclonically as shown in the following diagram:

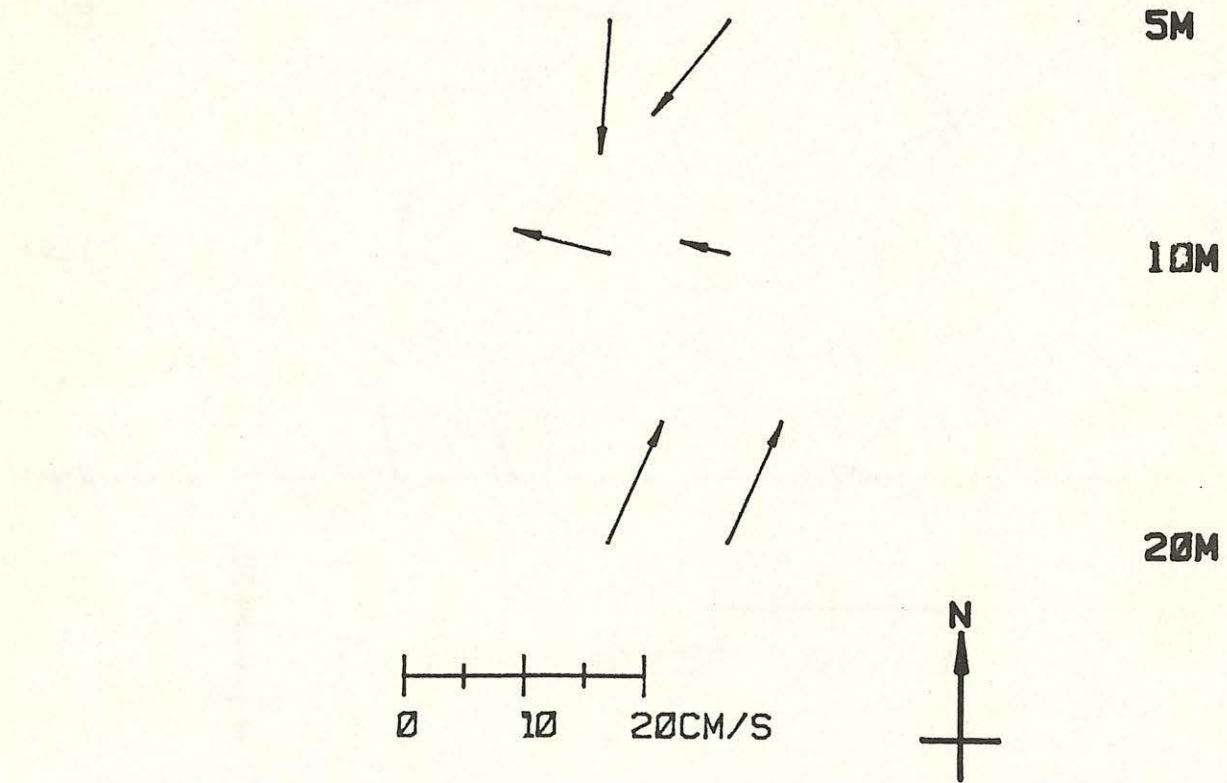
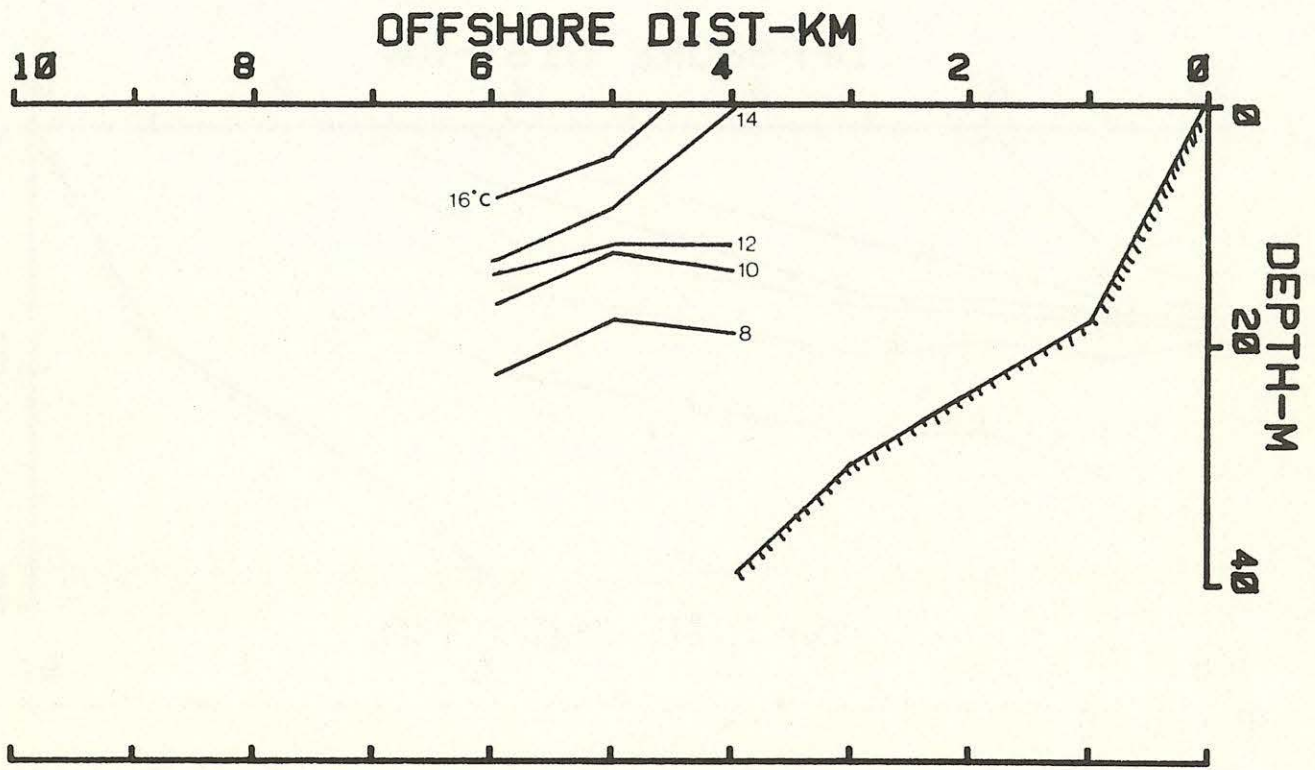


Figure 37: Temperature profile and horizontal velocities at 3 depths from measurements taken from 9:30 to 10:45 EDT on August 17. The offshore distance axis corresponds to stations 1-10 in Figure 1. Although shown parallel to the east-west axis in the lower graph, it is actually orientated at 285°.

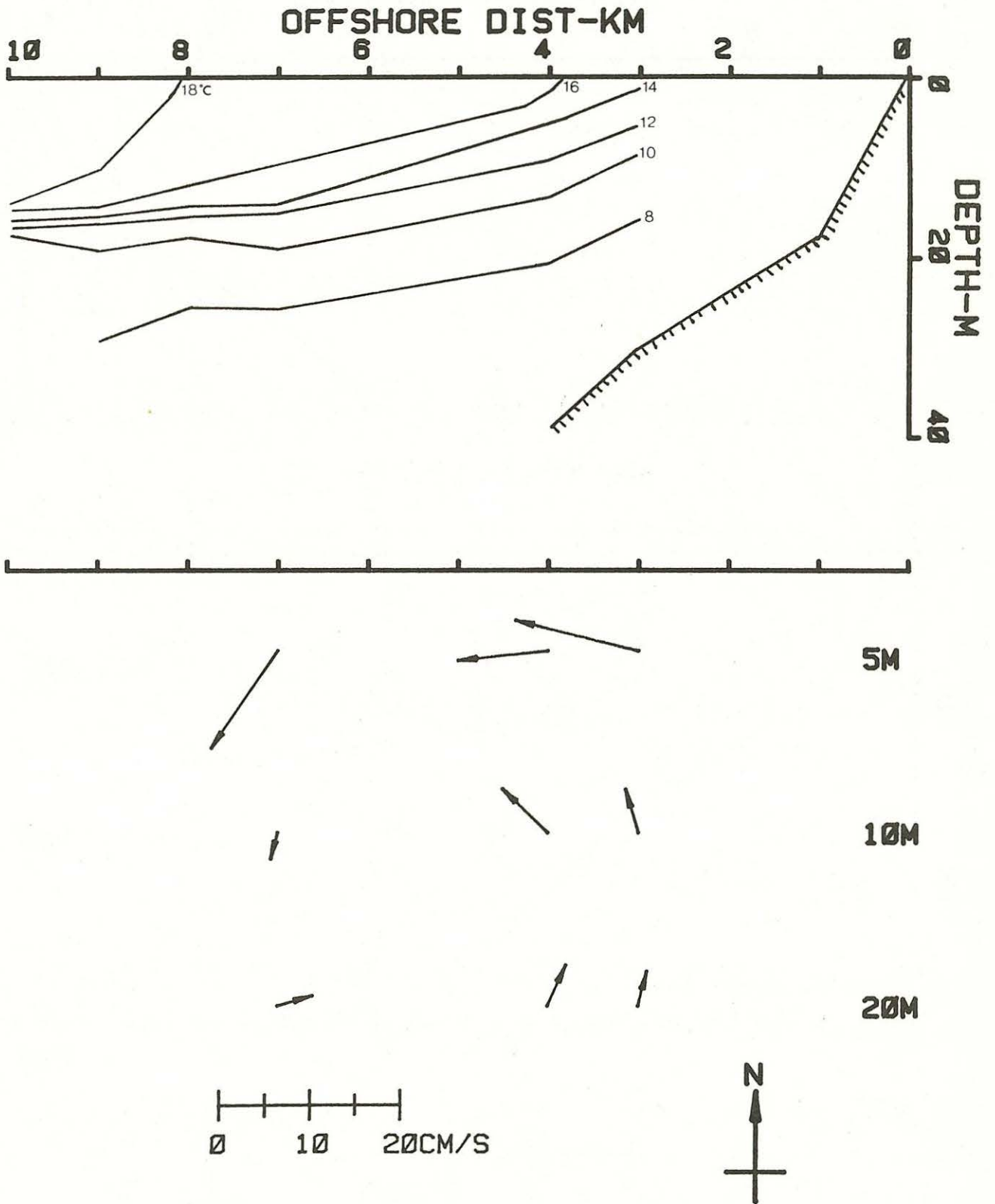


Figure 38: Temperature profile and horizontal velocities at 3 depths from measurements taken from 12:00 to 14:00 EDT on August 17.

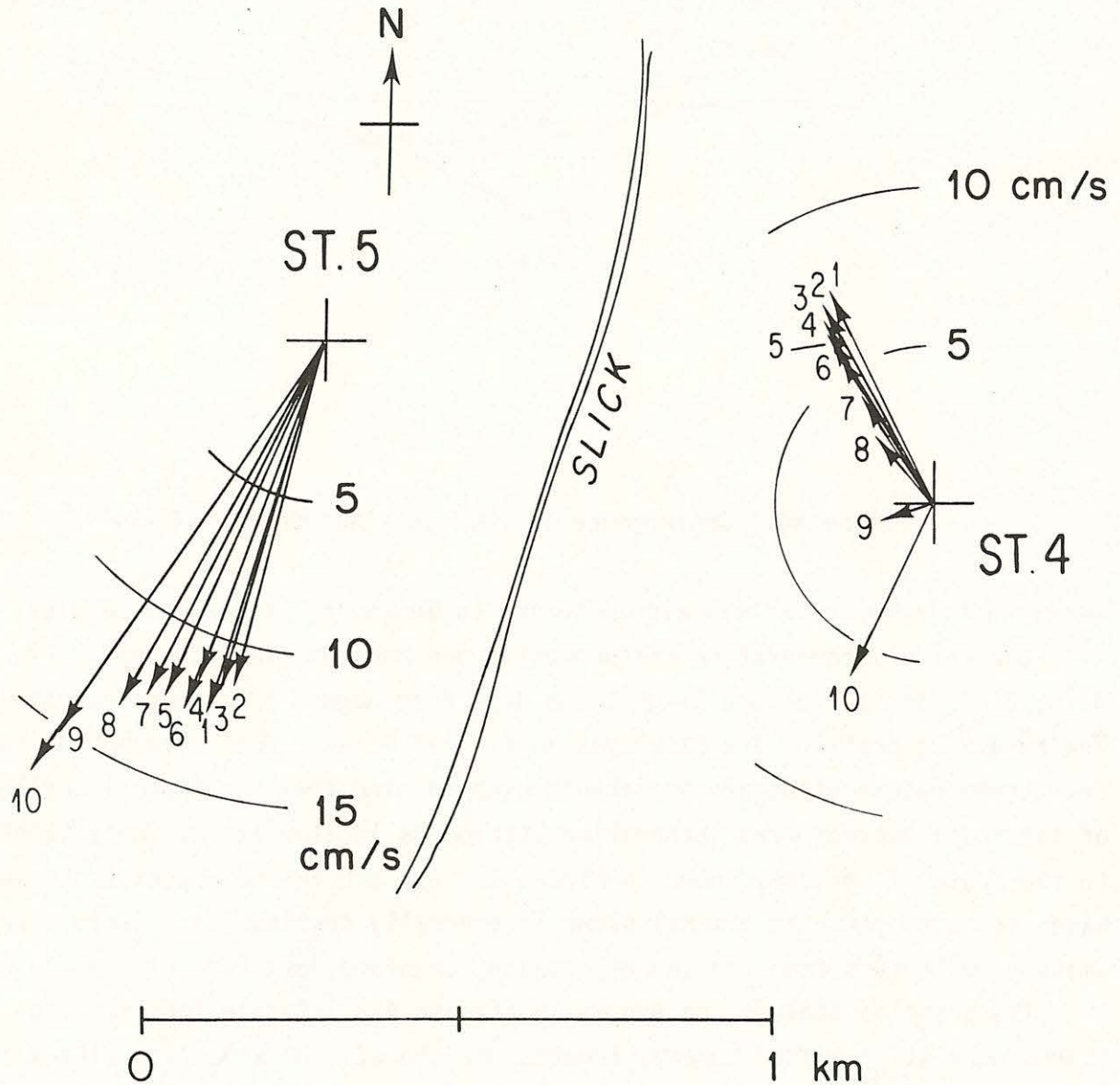


Figure 39: Hodographs of sighted drogue velocities, labeled according to Table 2. Measurements were conducted on August 17 on either side of the upwelled front.

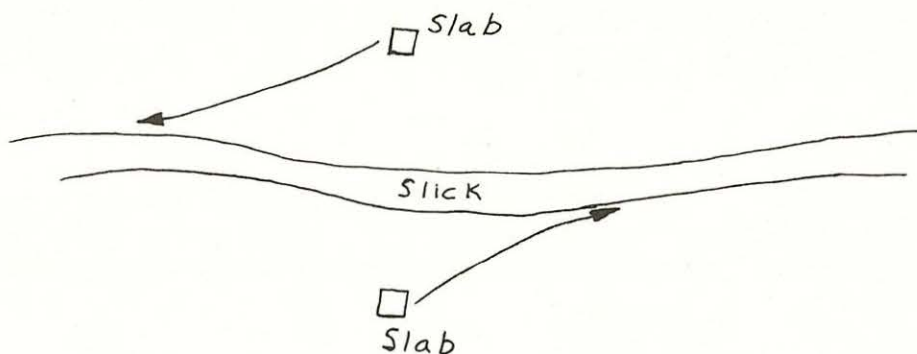


Figure 40: Convergence of 10.2 cm slabs on the slick.

Debris within the slick was also observed to be moving in cyclonic eddies.

Current and temperature measurements were made at flag stations 1, 2, 3, 4, 5, 6, 8, and 10 (Figure 1) on seven days from August 18 through August 28. The resulting profiles are displayed in Figures 41-47. When viewing the near-shore temperature structure one should keep in mind that the thermal outflow of the Bruce Nuclear Power Generating Station is located at the shore slightly to the south of the dome shown in Figure 1. Dye and thermal studies, however, have indicated that the thermal plume is generally confined to a strip approximately 500 meters from the shore [Csanady, Crawford, and Pade (1970)].

The profiles measured on August 18 (Figure 41) indicate that the isotherms were still tilted upwards towards the shore. The water velocities at 5 m and 10 m were in approximate geostrophic equilibrium with the pressure field as deduced from the isotherms. These are equivalent to the sub-currents discussed in sections 2i and 3i. The coastal velocities at 20 m were directed offshore suggesting downward movement of the isotherms near the coast.

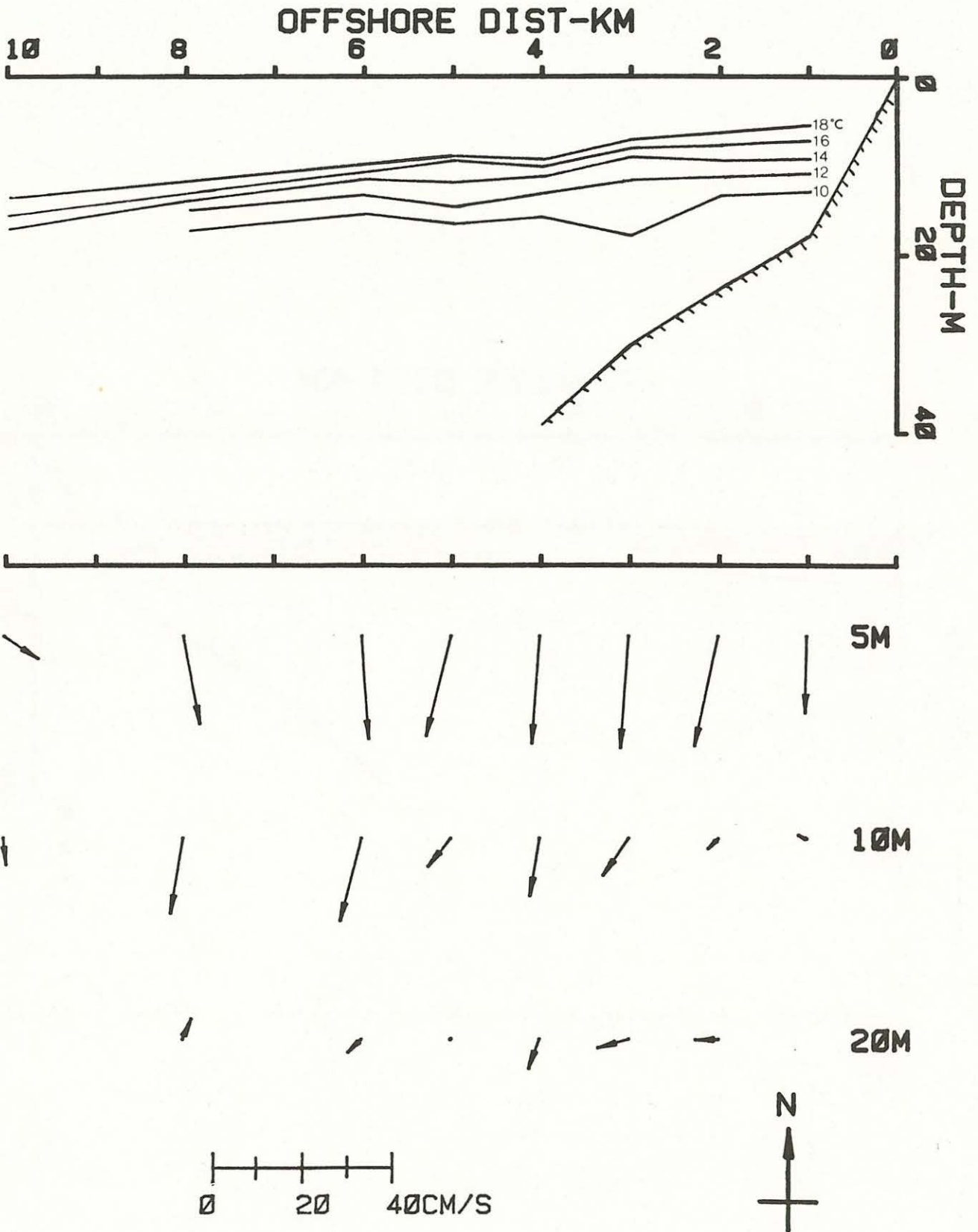


Figure 41: Temperature profile and horizontal velocities at 3 depths from measurements taken from 9:30 to 13:30 EDT on August 18.

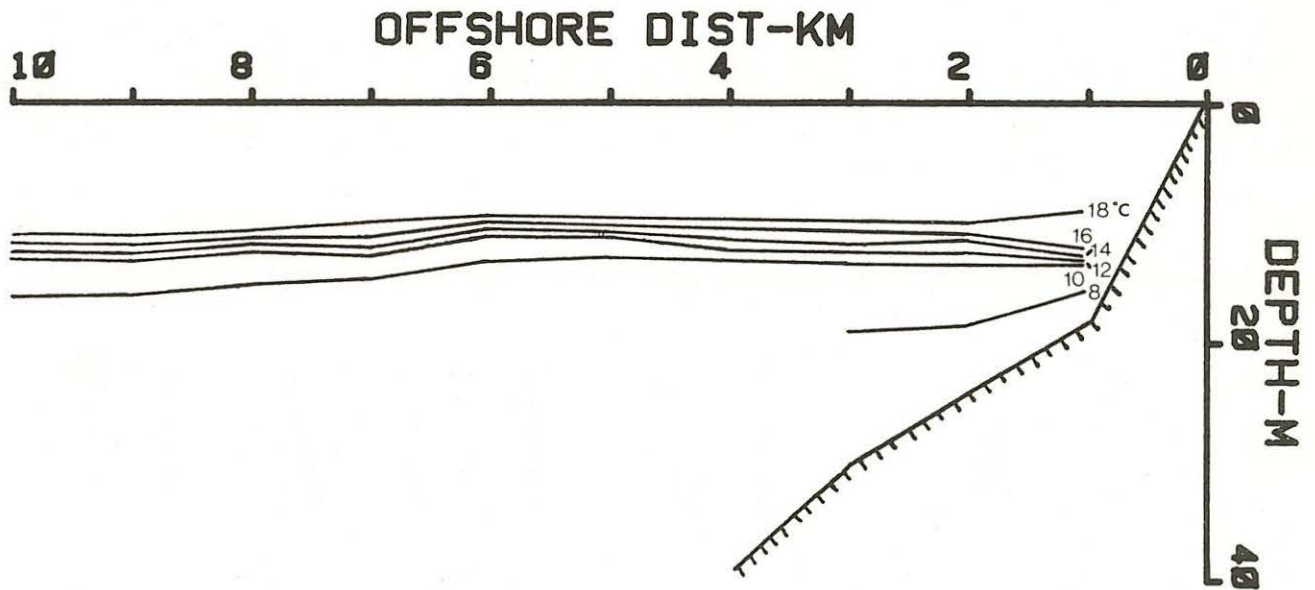


Figure 42: Temperature profile from measurements taken from 9:40 to 12:00 EDT on August 19. No current meter measurements were made.

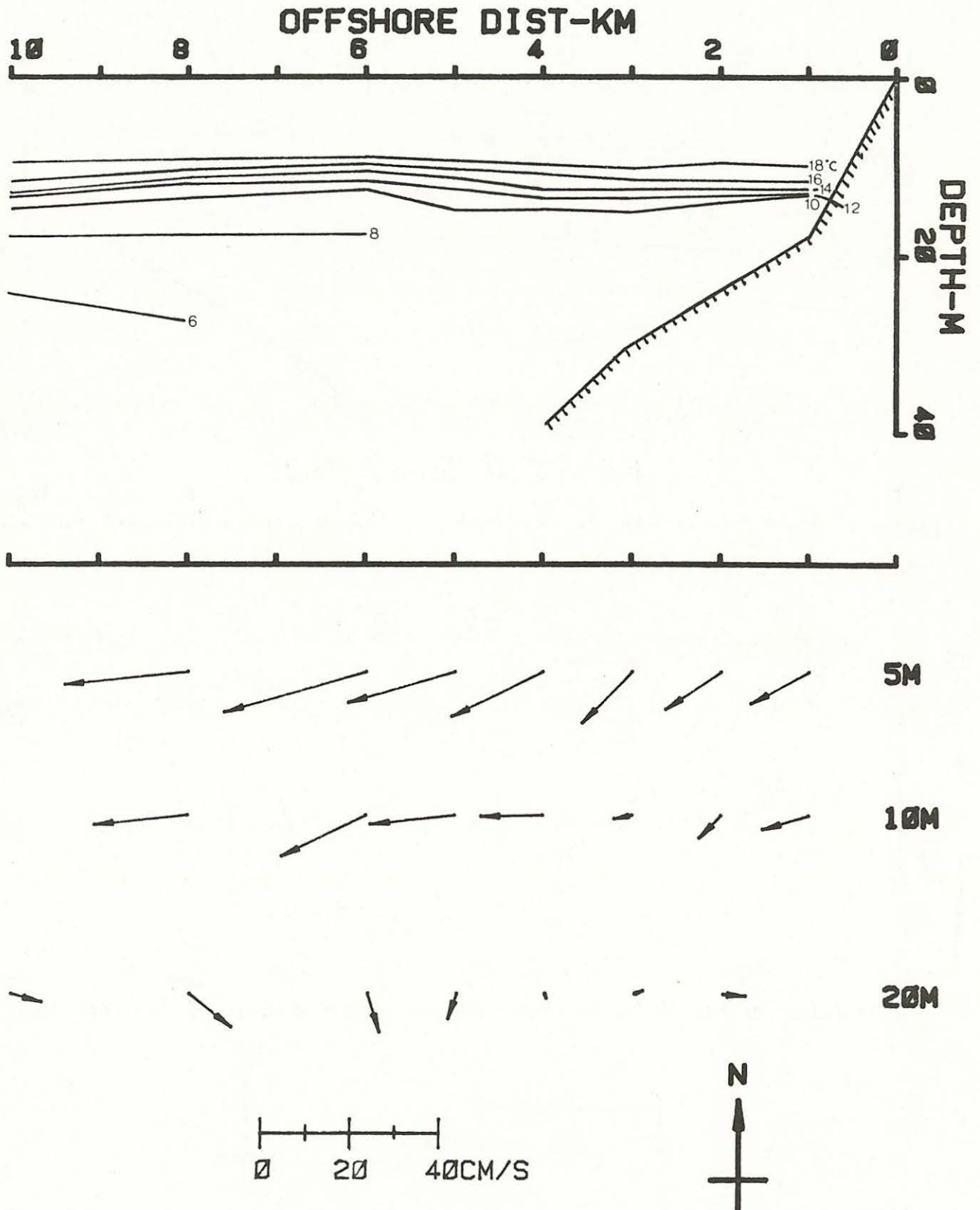


Figure 43: Temperature profile and horizontal velocities at 3 depths from measurements taken from 9:10 to 11:20 EDT on August 22.

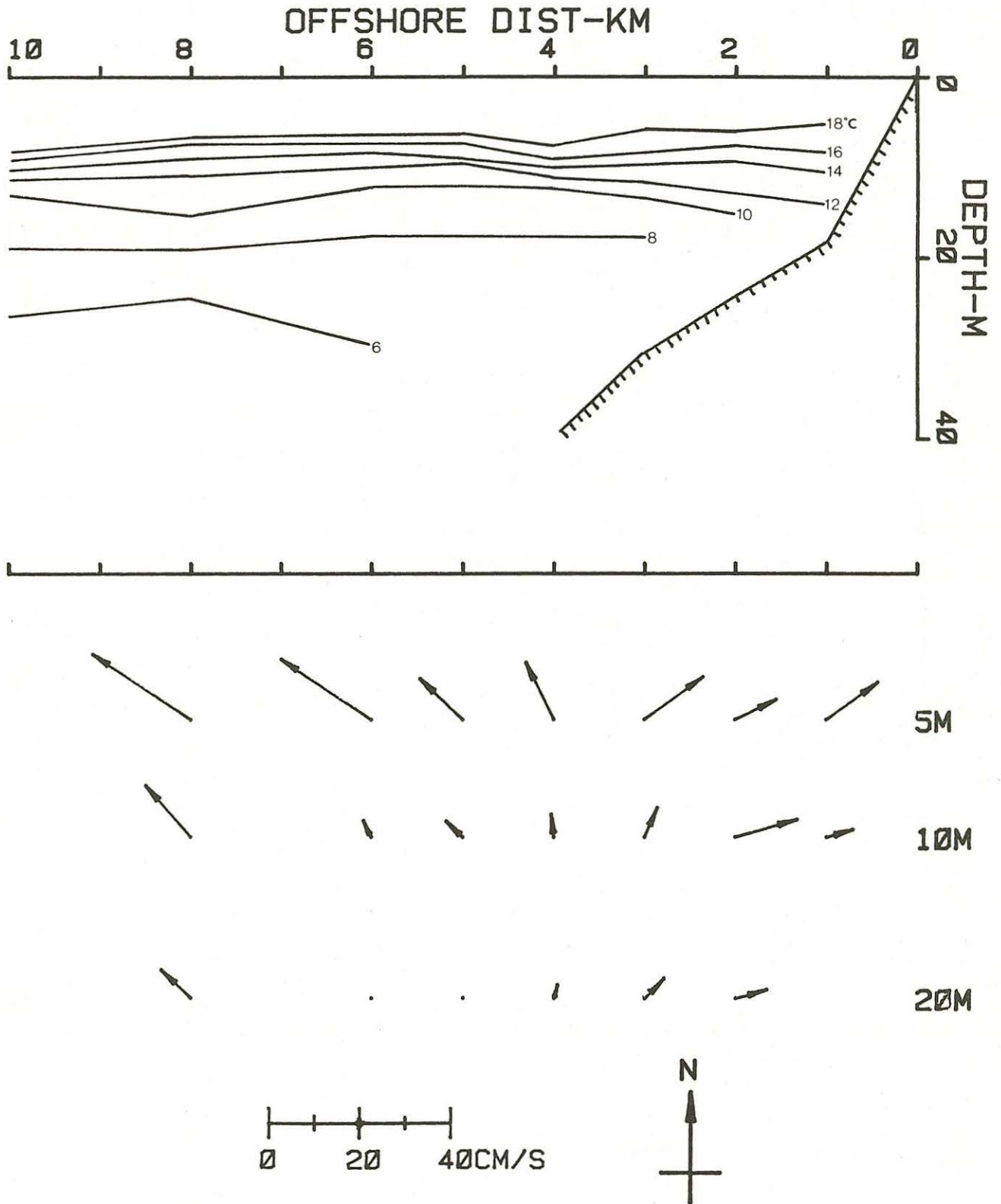


Figure 44: Temperature profile and horizontal velocities at 3 depths from measurements taken from 9:00 to 11:30 on August 23.

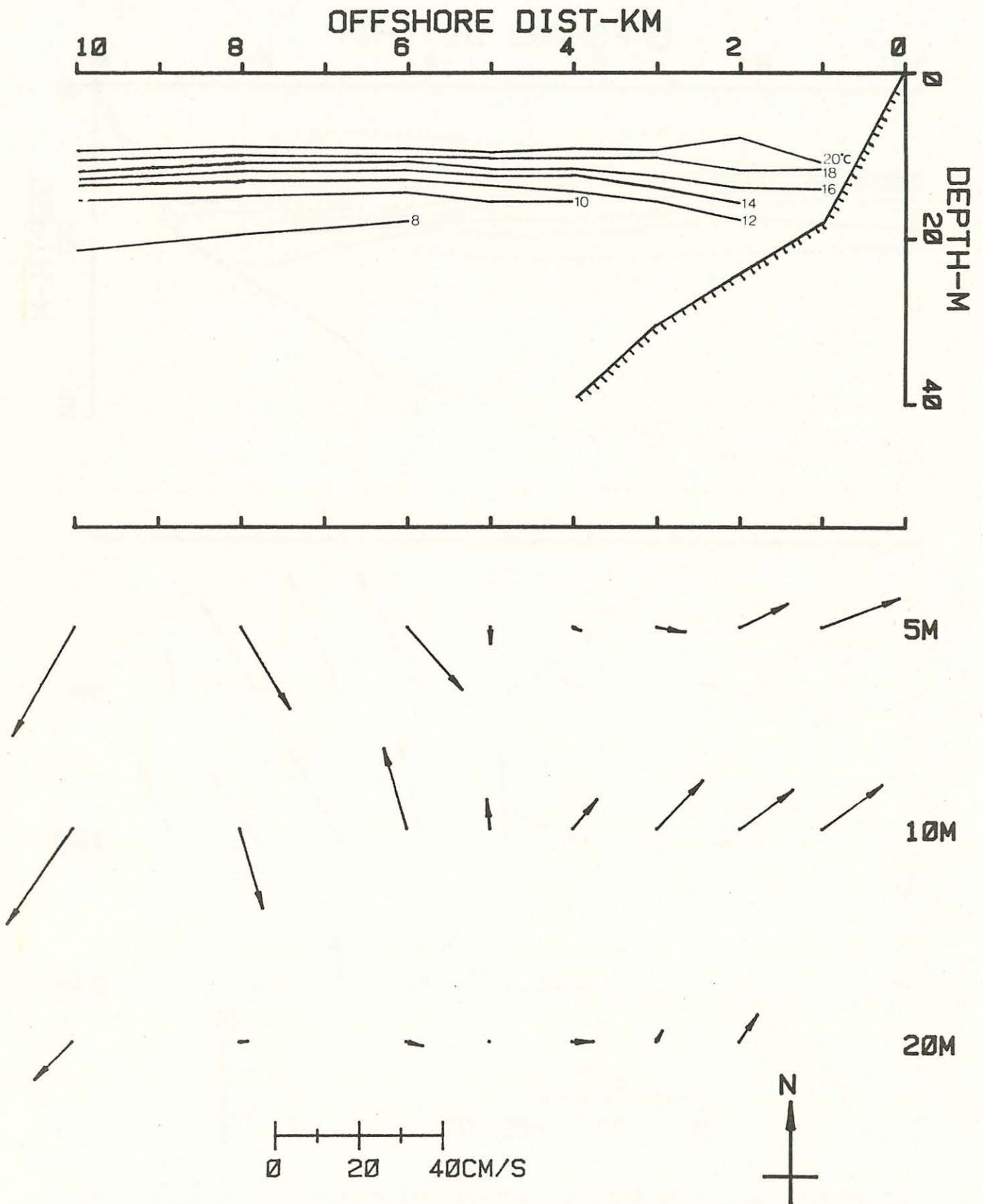


Figure 45: Temperature profile and horizontal velocities at 3 depths from measurements taken from 9:20 to 11:30 EDT on August 26.

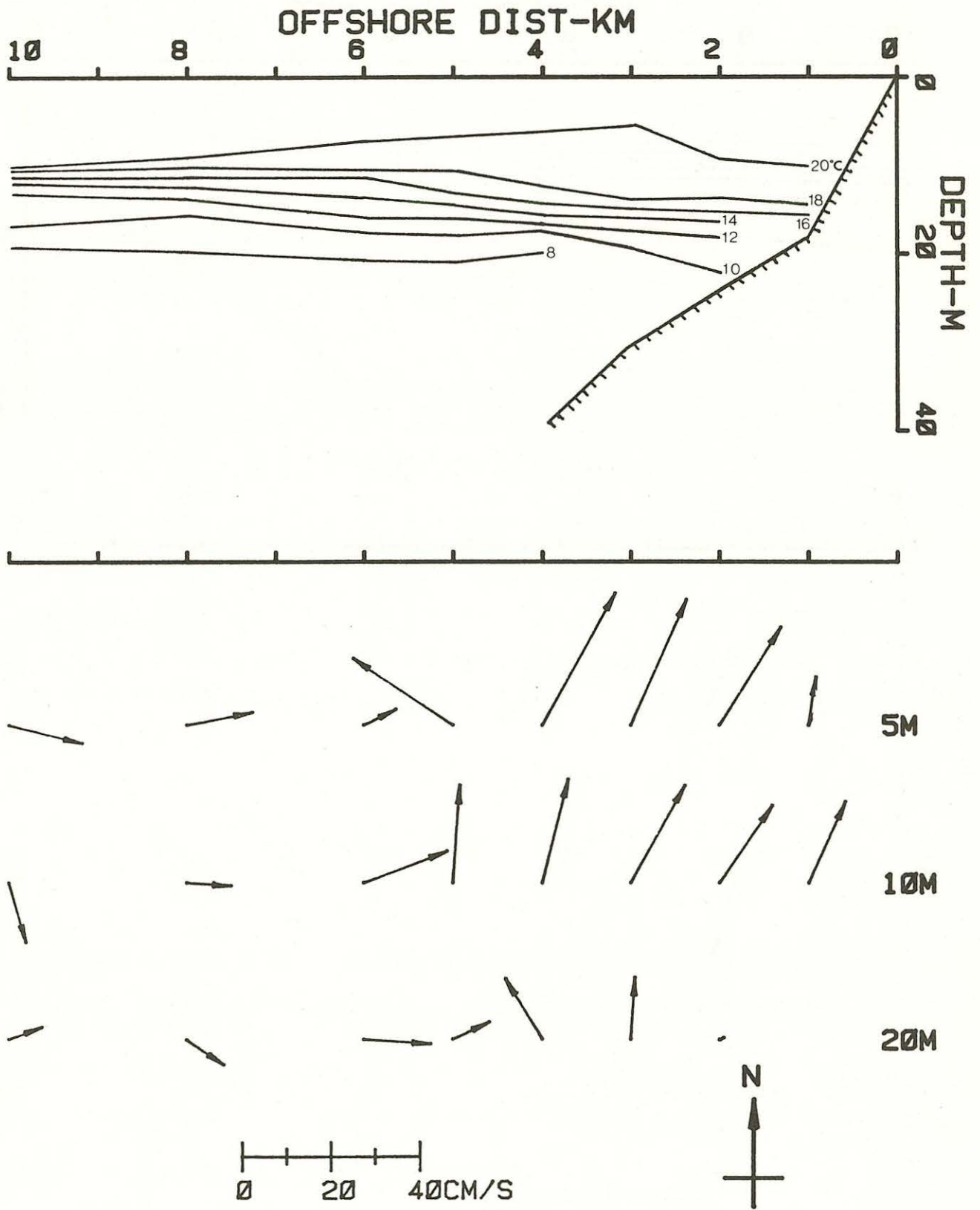


Figure 46: Temperature profile and horizontal velocities at 3 depths from measurements taken from 9:30 to 13:20 EDT on August 27.

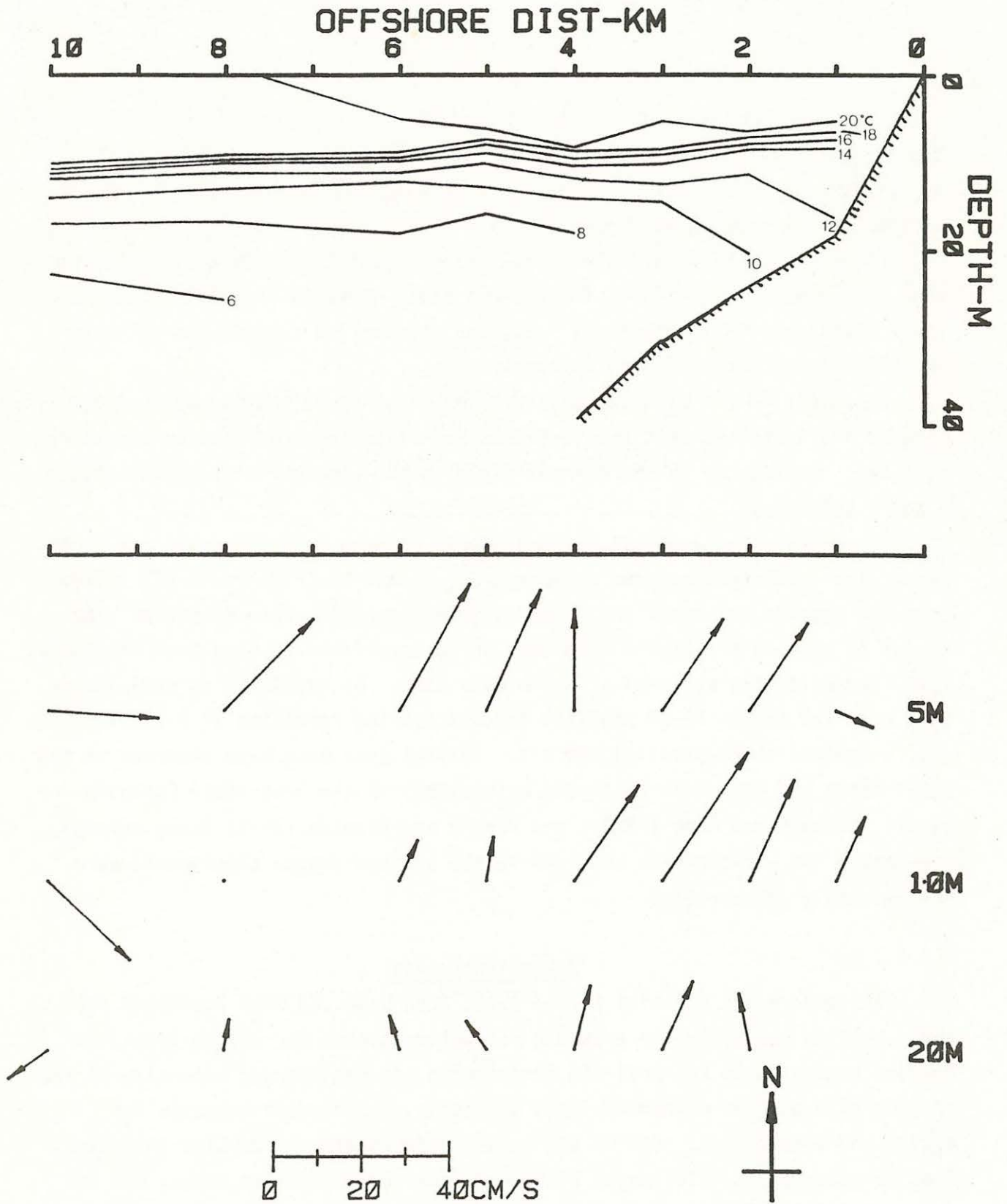


Figure 47: Temperature profile and horizontal velocities at 3 depths from measurements taken from 9:15 to 12:50 EDT on August 28.

By August 19, three days after the initial observation of the upwelling, the isotherms were nearly horizontal as shown by Figure 42. During that three day period wind forcing on the lake surface was relatively slight as indicated by the low wind speeds of Figure 16.

Figure 43 displays profiles measured on August 22 during a strong northwest wind event (Figure 16). The current field suggests that the generation of an upwelling was in progress; i.e., the nearsurface current was offshore and the deeper current flowed onshore.

By August 23 the wind had abated. The temperature profile of that day (Figure 44) indicates that the isotherms had tilted upwards towards the shore slightly. Noteworthy in the current field is the apparent divergence between 3 and 4 kilometers.

The winds from August 24 through August 28 were from the south and southwest. The isotherms measured on August 26, 27 and 28 (Figures 45-47) tilted downward towards the coast and progressively separated close to shore. The August 26 profile displays a northeast current confined to 4 km from the coast. This flow evidently extended offshore with time. By August 28 it had widened to 8 km. The August 26-28 profiles demonstrate the formation of a coastal jet, a coastal shore-parallel current. Coastal jets have been observed in the Great Lakes and have been described extensively in the literature [Csanady (1981), Csanady and Pade (1968), and Murthy and Blanton (1975) among others]. Presumably the sub-currents observed in the sighted drogue experiments were predominantly jet currents.

Acknowledgements

The authors are grateful to Ken Peal, John Loud and Stan Rosenblad for their work on modifying the acoustic navigation system for drogue tracking. Special thanks go to Ken Peal who contributed his engineering expertise at the project site and who responded, most helpfully, to frequent requests for advice and suggestions. Useful advice was also obtained from Lincoln Baxter, Stan Bergstrom, Jim McCullough, Ping-Tung Shaw, Dr. Woollcott Smith, and Dr. Robert Spindel. Paul-Andre Bolduc of the Marine Environmental Data Service generously supplied us with copies and explanations of wave field data from

Lake Huron. We are especially grateful to the principal investigator, Dr. Gabriel Csanady.

All those who participated in the project at Lake Huron did so with dedication and enthusiasm. These individuals include: John Craft, Capt. John Crew, Bill Henley, Mike Kingston, Reed Payne and Joel Pecchioli.

This work was supported by the Department of Energy contract DE-AC02-79EV10005 and National Oceanic and Atmospheric Administration contract 03-5-022-26.

References

- Alofs, D. J., and R. L. Reisbig, 1972. An experimental evaluation of oil slick movement caused by waves. J. Phys. Oceanogr., 2, 439-443.
- Brown, M. B., editor, 1977. Biomedical Computer Programs P-Series, Univ. of Calif. Press, Berkley, California.
- Bye, John A. T., 1967. The wave drift current. J. Mar. Res., 25, 95-102.
- Churchill, J. H., 1981. Tracking near surface drogues using an acoustic travel time technique in shallow, highly stratified water, problems and observations. W.H.O.I. Technical Report, WHOI-81-37. Woods Hole Oceanographic Institution, Woods Hole, Massachusetts.
- Churchill, J. H., and B. H. Pade, 1980. Measurement of nearsurface current in Cape Cod Bay using sighted drogues. W.H.O.I. Technical Report, WHOI-80-8. Woods Hole Oceanographic Institution, Woods Hole, Massachusetts.
- Churchill, J. H., B. H. Pade and K. R. Peal, 1981. Water velocity measurement from nearsurface to 110 m depth at deep water dumpsite#106 using acoustically tracked drogues and conventional current meters. W.H.O.I. Technical Report, WHOI-81-11. Woods Hole Oceanographic Institution, Woods Hole, Massachusetts.
- Craik, A. D. D., and S. Leibovich, 1976. A rational model for Langmuir circulations. J. Fluid Mech., 73, 401-426.
- Csanady, G. T., 1978. Turbulent interface layers. J. Geophys. Res., 83, 2329-2342.
- Csanady, G. T., 1979. A developing turbulent surface shear layer model. J. Geophys. Res., 84, 4944-4948.

- Csanady, G. T., 1981. Circulation in the coastal ocean, Part 1. EOS Transactions, 62, 9-11.
- Csanady, G. T., and B. Pade, 1968. The coastal jet project. Report No. PR36. Great Lakes Institute, University of Toronto.
- Csanady, G. T., W. R. Crawford and B. Pade, 1970. Thermal plume study at Douglas Point Lake Huron, 1970. Environmental Fluid Mechanics Lab, University of Waterloo, Waterloo, Ontario.
- Draper, N. R., and H. Smith, 1966. Applied Regression Analysis, John Wiley and Sons, New York.
- Ekman, V. W., 1905. On the influence of the earth's rotation on ocean-currents. Arkiv. Math. Astr. Ocean Phys., 2(11).
- Huang, N. E., 1979. On surface drift currents in the ocean. J. Fluid Mech., 91, 191-208.
- Hunt, M. M., et al., 1974. An acoustic navigation system. W.H.O.I. Technical Report, WHOI-74-6. Woods Hole Oceanographic Institution, Woods Hole, Massachusetts.
- Jones, I. S. F., and B. C. Kenney, 1977. The scaling of velocity fluctuations in the mixed layer. J. Geophys. Res., 82, 1392-1396.
- Kirwan, A. D., et al., 1979. Analysis of surface current response to wind. J. Phys. Oceanogr., 9, 401-412.
- Lange, Philipp, and H. Huhnerfuss, 1978. Drift response of monomolecular slicks to wave and wind action. J. Phys. Oceanogr., 8, 142-150.
- Leibovich, S., 1977. On the evolution of the system of wind drift currents and Langmuir circulations in the ocean. Part 1. Theory and averaged current. J. Fluid Mech., 79, 715-743.
- Longuet-Higgins, M. S., 1952. On the statistical distribution of the heights of sea waves. J. Mar. Res., 11, 245-265.
- Loud, J. F., 1981. SHACK. 2, SHIN. 2 program documentation. Woods Hole Oceanographic Institution. Unpublished manuscript.
- Murthy, C. R., and J. O. Blanton, 1975. Coastal zone climatological studies of the Laurentian great lakes. Proceedings Second World Congress, International Water Resources Association, New Delhi, 5, 431-448, December.

- Peal, K. R., 1974. Acoustic navigation system operating and service manual. W.H.O.I. Technical Report, WHOI-74-4. Woods Hole Oceanographic Institution, Woods Hole, Massachusetts.
- Phillips, O. M., 1958. The equilibrium range in the spectrum of wind generated waves. J. Fluid Mech., 4, 426-434.
- Simpson, J. H., 1969. Observations of the directional characteristics of sea waves. Geophys. J. R. Ast. Soc., 17, 93-120.
- Spindel, R. C., S. B. Davis, K. C. MacDonald, R. P. Porter, and J. D. Phillips, 1974. Microearthquake survey of median valley of the Mid-Atlantic Ridge at 36°30'N, Nature, 248, 577-579.
- Spindel, R. C., and R. P. Porter, 1974. Precision tracking system for sonobuoys. IEEE Ocean 74 Symposium, Halifax, Nova Scotia, 2, 162-165.

-A1-

APPENDIX

SIGHTED DROGUE, ACOUSTIC DROGUE AND
CURRENT METER MEASURED VELOCITIES

Table A1

Averaged Drogue Speeds, Bearings and Error Parameters for
July 23 Run 5

MEAN DEPTH	TYPE	# OF SGHT	SPEED CM/S	ST DEV CM/S	BEARING DEG	ST DEV DEG	$\overline{ERR^2}$ CM/(S DEG)
Confetti		1	15.91	--	156.0	--	.29
1.2 cm	Slab	3	12.07	.09	155.3	1.2	.25
2.5 cm	Slab	3	9.79	.30	164.0	0.0	.17
3.8 cm	Slab	3	9.36	.54	164.7	2.3	.15
5.1 cm	Slab	2	10.02	.23	167.0	1.4	.16
10.2 cm	Slab	3	8.76	.76	172.7	2.3	.12
20.0 cm	Subm	3	6.31	.69	182.7	2.3	.09
30.0 cm	Subm	3	5.82	.36	187.0	0.0	.09
60.0 cm	Subm	4	5.45	.52	200.3	2.5	.04
120.0 cm	Subm	2	5.47	1.20	205.0	1.4	.55

Wind: 23 km/hr from 339.

Wave Height: 2-4 ft

Bearings from Grebe taken while standing on deck

Location: Site P; starting time: 16:10 EDT

Table A2

Averaged Drogue Speeds, Bearings and Error Parameters for
July 24 Run 2

MEAN DEPTH	TYPE	# OF SGHT	SPEED CM/S	ST DEV CM/S	BEARING DEG	ST DEV DEG	$\overline{ERR^2}$ CM/(S DEG)
Confetti		2	27.98	2.99	36.5	3.5	.23
1.2 cm	Slab	4	25.81	1.28	30.0	2.2	.37
2.5 cm	Slab	4	25.11	.62	28.3	1.5	.38
3.8 cm	Slab	4	24.79	.96	29.3	1.5	.35
5.1 cm	Slab	4	25.26	1.18	29.0	2.4	.37
10.2 cm	Slab	4	23.07	.73	29.8	2.2	.32
20.0 cm	Subm	4	21.81	3.70	26.5	1.7	.37
30.0 cm	Subm	4	21.25	2.54	27.3	1.3	.33
60.0 cm	Subm	4	19.53	1.67	30.0	2.8	.27
120.0 cm	Subm	4	18.98	1.27	26.8	2.1	.26
180.0 cm	Subm	4	17.98	1.03	27.3	2.5	.25

Wind: 20 km/hr from 205.

Wave Height: 1 ft, increasing

Bearings from Grebe taken while standing on the bow

Location: Site Q; starting time: 15:40 EDT

Table A3

Averaged Drogue Speeds, Bearings and Error Parameters for
July 25 Run 2

MEAN DEPTH	TYPE	# OF SGHT	SPEED CM/S	ST DEV CM/S	BEARING DEG	ST DEV DEG	$\overline{\text{ERR}^2}$ CM/(S DEG)
1.2 cm	Slab	3	25.25	1.94	46.0	5.2	.40
2.5 cm	Slab	3	23.67	.89	47.0	2.7	.37
3.8 cm	Slab	3	23.79	1.09	49.0	1.0	.36
5.1 cm	Slab	3	22.87	.65	46.0	0.0	.36
10.2 cm	Slab	3	20.93	3.05	37.0	0.0	.43
20.0 cm	Subm	3	19.89	.64	49.6	.6	.31
30.0 cm	Subm	3	19.42	1.45	56.0	0.0	.26
60.0 cm	Subm	3	18.16	1.10	58.7	.6	.24
120.0 cm	Subm	3	17.34	1.71	62.7	.6	.22
180.0 cm	Subm	3	17.07	.95	59.3	.6	.25

Wind: 20 km/hr from 211.

Wave Height: 2 ft, increasing slowly

Bearings from Grebe taken while standing on deck

Location: Site P; starting time: 11:10 EDT

Table A4

Averaged Drogue Speeds, Bearings and Error Parameters for
July 25 Run 3

MEAN DEPTH	TYPE	# OF SGHT	SPEED CM/S	ST DEV CM/S	BEARING DEG	ST DEV DEG	$\overline{\text{ERR}^2}$ CM/(S DEG)
1.2 cm	Slab	3	26.44	1.67	48.0	1.7	.38
2.5 cm	Slab	3	24.57	.72	52.7	2.3	.32
3.8 cm	Slab	3	24.63	.63	53.7	.6	.32
5.1 cm	Slab	3	23.14	.73	55.3	.6	.28
10.2 cm	Slab	3	21.91	1.14	58.0	0.0	.25
20.0 cm	Subm	3	18.28	.85	60.0	1.0	.26
30.0 cm	Subm	3	18.02	.87	64.0	0.0	.21
60.0 cm	Subm	3	18.28	1.88	68.3	.6	.19
120.0 cm	Subm	3	17.09	.60	68.7	2.3	.20
180.0 cm	Subm	3	17.68	1.66	70.0	0.0	.19

Wind: 24 km/hr from 224.

Wave Height: 2-3 ft, increasing slowly

Bearings from Grebe taken while standing on deck

Location: Site P; starting time: 11:45 EDT

Table A5

Averaged Drogue Speeds, Bearings and Error Parameters for
July 29 Run 1

MEAN DEPTH	TYPE	# OF SGHT	SPEED CM/S	ST DEV CM/S	BEARING DEG	ST DEV DEG	$\overline{ERR^2}$ CM/(S DEG)
1.2 cm	Slab	3	18.81	.30	63.3	.6	.25
2.5 cm	Slab	3	17.97	.45	65.3	.6	.25
3.8 cm	Slab	3	18.19	.35	66.3	.6	.25
5.1 cm	Slab	3	17.72	.35	68.3	.6	.24
10.2 cm	Slab	3	17.38	.41	68.6	.6	.24
20.0 cm	Subm	3	16.43	.14	72.0	0.0	.25
30.0 cm	Subm	3	16.00	.32	73.3	1.2	.27
60.0 cm	Subm	3	15.51	.34	75.0	1.0	.29
120.0 cm	Subm	3	14.22	.59	72.6	2.1	.34
180.0 cm	Subm	3	13.16	.60	71.3	2.5	.40

Wind: very slight from about 226.

Wave Height: < 1 ft

Bearings from Grebe taken while standing on the bow

Location: Station 4; starting time: 14:30 EDT

Table A6

Averaged Drogue Speeds, Bearings and Error Parameters for
July 29 Run 2

MEAN DEPTH	TYPE	# OF SGHT	SPEED CM/S	ST DEV CM/S	BEARING DEG	ST DEV DEG	$\overline{ERR^2}$ CM/(S DEG)
Confetti		2	16.10	1.24	64.5	3.5	.50
1.2 cm	Slab	3	16.53	1.04	65.0	2.6	.32
2.5 cm	Slab	3	16.56	.58	65.7	1.5	.31
3.8 cm	Slab	3	15.73	.80	66.0	3.0	.28
5.1 cm	Slab	3	15.38	1.26	65.3	2.5	.29
10.2 cm	Slab	3	14.66	1.38	65.7	1.5	.30
20.0 cm	Subm	5	15.14	.57	68.2	1.1	.22
30.0 cm	Subm	5	14.96	.50	71.0	1.0	.21
60.0 cm	Subm	5	13.95	.08	73.2	.8	.19
120.0 cm	Subm	5	12.13	.34	73.4	2.0	.21
180.0 cm	Subm	5	11.42	.39	71.4	1.5	.25

Wind: very slight from about 226.

Wave Height: < 1 ft

Bearings from Grebe taken while standing on the bow

Location: Station 4; starting time: 15:10 EDT

Table A7

Averaged Drogue Speeds, Bearings and Error Parameters for
July 30 Run 1

MEAN DEPTH	TYPE	# OF SGHT	SPEED CM/S	ST DEV CM/S	BEARING DEG	ST DEV DEG	$\overline{ERR^2}$ CM/(S DEG)
1.2 cm	Slab	3	10.16	.69	146.7	3.1	.09
2.5 cm	Slab	3	8.97	.90	148.7	1.5	.09
3.8 cm	Slab	3	8.77	.31	148.3	.6	.09
5.1 cm	Slab	3	8.84	.88	151.3	1.2	.08
10.2 cm	Slab	3	7.57	1.54	156.0	2.0	.15
20.0 cm	Subm	1	5.93	--	164.0	--	.02
30.0 cm	Subm	1	4.08	--	174.0	--	.04
60.0 cm	Subm	1	2.41	--	212.0	--	.08
120.0 cm	Subm	1	2.54	--	209.0	--	.08
180.0 cm	Subm	1	2.68	--	206.0	--	.08

Wind: 17 km/hr from 324.

Wave Height: 2-3 ft, with long swells

Bearings from Grebe taken while standing on deck

Location: Station 4; starting time: 11:00 EDT

Table A8

Averaged Drogue Speeds, Bearings and Error Parameters for
July 30 Run 2

MEAN DEPTH	TYPE	# OF SGHT	SPEED CM/S	ST DEV CM/S	BEARING DEG	ST DEV DEG	$\overline{ERR^2}$ CM/(S DEG)
Confetti		1	6.42	--	132.0	--	.25
1.2 cm	Slab	4	5.61	.43	127.8	4.3	.14
2.5 cm	Slab	4	5.44	.22	135.0	6.8	.15
3.8 cm	Slab	4	5.01	.67	136.0	3.3	.16
5.1 cm	Slab	4	4.43	.57	142.7	3.1	.16
10.2 cm	Slab	1	3.60	--	146.0	--	.17
20.0 cm	Subm	4	--	--	179.3	3.4	--
30.0 cm	Subm	4	--	--	211.0	2.0	--
60.0 cm	Subm	3	4.73	.72	236.0	3.5	.22
120.0 cm	Subm	4	4.50	.80	241.8	3.1	.22
180.0 cm	Subm	4	4.32	1.22	251.3	3.1	.23

Wind: 12 km/hr from 316.

Wave Height: 2-3 ft, with long swells

Bearings from Grebe taken while standing on deck

Location: Station 4; starting time: 12:00 EDT

Table A9

Averaged Drogue Speeds, Bearings and Error Parameters for
July 31 Run 1

MEAN DEPTH	TYPE	# OF SGHT	SPEED CM/S	ST DEV CM/S	BEARING DEG	ST DEV DEG	$\overline{ERR^2}$ CM/(S DEG)
Confetti		1	36.73	--	10.0	--	.84
1.2 cm	Slab	3	33.13	.83	10.0	0.0	.57
2.5 cm	Slab	3	31.56	.70	7.3	1.2	.8
3.8 cm	Slab	3	31.37	.20	7.7	2.3	.7
5.1 cm	Slab	3	29.57	1.04	10.0	0.0	.51
10.2 cm	Slab	3	28.74	.46	11.0	0.0	.49
20.0 cm	Subm	3	27.64	1.10	12.0	0.0	.47
30.0 cm	Subm	2	26.09	.25	15.0	0.0	.48
60.0 cm	Subm	3	24.64	1.17	17.0	0.0	.41
120.0 cm	Subm	3	25.29	1.87	14.0	0.0	.47
180.0 cm	Subm	3	24.88	2.00	14.0	0.0	.51

Wind: 26 km/hr from 184.

Wave Height: 2 ft

Bearings from Grebe taken while standing on deck

Location: Station 4; starting time: 9:35 EDT

Table A10

Averaged Drogue Speeds, Bearings and Error Parameters for
July 31 Run 2

MEAN DEPTH	TYPE	# OF SGHT	SPEED CM/S	ST DEV CM/S	BEARING DEG	ST DEV DEG	$\overline{ERR^2}$ CM/(S DEG)
Confetti		2	33.28	1.66	3.0	0.0	.54
1.2 cm	Slab	3	31.19	.88	3.3	.6	.50
2.5 cm	Slab	2	30.67	.48	5.5	.7	.46
3.8 cm	Slab	2	30.08	.30	7.0	2.8	.44
5.1 cm	Slab	2	28.61	1.84	3.5	.7	.45
10.2 cm	Slab	2	27.74	1.10	6.5	.7	.40
20.0 cm	Subm	2	26.49	.18	11.0	1.4	.34
30.0 cm	Subm	2	26.17	.34	13.0	1.4	.32
60.0 cm	Subm	2	25.58	.36	13.5	.7	.33
120.0 cm	Subm	2	25.06	1.46	13.5	.7	.34
180.0 cm	Subm	2	26.78	1.60	13.0	1.4	.36

Wind: 25 km/hr from 174.

Wave Height: 2 ft

Bearings from Grebe taken while standing on deck

Location: Station 4; starting time: 10:20 EDT

Table A11

Averaged Drogue Speeds, Bearings and Error Parameters for
July 31 Run 3

MEAN DEPTH	TYPE	# OF SGHT	SPEED CM/S	ST DEV CM/S	BEARING DEG	ST DEV DEG	ERR ² CM/(S DEG)
1.2 cm	Slab	1	39.09	--	14.0	--	.25
2.5 cm	Slab	1	37.41	--	17.0	--	.21
3.8 cm	Slab	1	36.66	--	16.0	--	.21
5.1 cm	Slab	1	35.69	--	17.0	--	.20
10.2 cm	Slab	1	34.73	--	18.0	--	.18
20.0 cm	Subm	1	33.86	--	23.0	--	.12
30.0 cm	Subm	1	33.82	--	14.0	--	.22
60.0 cm	Subm	1	32.26	--	15.0	--	.20
120.0 cm	Subm	1	32.34	--	17.0	--	.18
180.0 cm	Subm	1	32.33	--	16.0	--	.20

Wind: 29 km/hr from 184.

Wave Height: 2 ft

Bearings from Grebe taken while standing on deck

Location: Station 4; starting time: 11:20 EDT

Table A12

Averaged Drogue Speeds, Bearings and Error Parameters for
July 31 Run 4

MEAN DEPTH	TYPE	# OF SGHT	SPEED CM/S	ST DEV CM/S	BEARING DEG	ST DEV DEG	ERR ² CM/(S DEG)
Confetti		2	45.05	.77	10.0	0.0	.46
1.2 cm	Slab	2	37.92	2.26	18.5	2.1	.30
2.5 cm	Slab	2	36.02	1.11	17.0	4.2	.30
3.8 cm	Slab	2	35.93	1.21	16.0	2.8	.32
5.1 cm	Slab	2	35.36	1.82	15.5	.7	.33
10.2 cm	Slab	2	33.85	2.44	21.0	2.8	.22
20.0 cm	Subm	2	33.21	3.63	22.0	0.0	.23
30.0 cm	Subm	2	33.43	2.96	24.0	0.0	.21
60.0 cm	Subm	2	32.74	1.33	23.5	3.5	.22
120.0 cm	Subm	2	31.60	3.19	23.0	0.0	.29
180.0 cm	Subm	2	31.67	2.94	25.0	0.0	.26

Wind: 25 km/hr from 184.

Wave Height: 2 ft

Bearings from Grebe taken while standing on deck

Location: Station 4; starting time: 12:00 EDT

Table A13

Averaged Drogue Speeds, Bearings and Error Parameters for
July 31 Run 5

MEAN DEPTH	TYPE	# OF SGHT	SPEED CM/S	ST DEV CM/S	BEARING DEG	ST DEV DEG	$\overline{ERR^2}$ CM/(S DEG)
1.2 cm	Slab	1	33.57	--	14.0	--	.24
2.5 cm	Slab	1	32.74	--	15.0	--	.23
3.8 cm	Slab	1	30.76	--	14.0	--	.24
5.1 cm	Slab	1	30.76	--	19.0	--	.20
10.2 cm	Slab	1	30.56	--	20.0	--	.20
20.0 cm	Subm	1	29.46	--	24.0	--	.20
30.0 cm	Subm	1	28.75	--	28.0	--	.25
60.0 cm	Subm	1	27.64	--	28.0	--	.33
120.0 cm	Subm	1	27.29	--	28.0	--	.35
180.0 cm	Subm	1	28.70	--	29.0	--	.39

Wind: 28 km/hr from 174.

Wave Height: 2 ft

Bearings from Grebe taken while standing on deck

Location: Station 4; starting time: 12:20 EDT

Table A14

Averaged Drogue Speeds, Bearings and Error Parameters for
August 6 Run 1

MEAN DEPTH	TYPE	# OF SGHT	SPEED CM/S	ST DEV CM/S	BEARING DEG	ST DEV DEG	$\overline{ERR^2}$ CM/(S DEG)
Confetti		1	32.49	--	38.0	--	1.09
1.2 cm	Slab	2	26.68	1.82	38.0	1.4	.67
2.5 cm	Slab	2	25.40	1.85	38.0	1.4	.66
3.8 cm	Slab	2	25.05	1.87	36.5	2.1	.67
5.1 cm	Slab	2	21.04	2.41	35.5	.7	.71
10.2 cm	Slab	2	22.50	2.76	34.5	2.1	.68

Wind: 10 km/hr from 214.

Wave Height: 2-4 ft, with long swells

Bearings from Grebe taken while standing on the milkbox, compass corr. applied

Location: Station 4; starting time: 10:00 EDT

Table A15

Averaged Drogue Speeds, Bearings and Error Parameters for
August 6 Run 2

MEAN DEPTH	TYPE	# OF SGHT	SPEED CM/S	ST DEV CM/S	BEARING DEG	ST DEV DEG	$\overline{ERR^2}$ CM/(S DEG)
1.2 cm	Slab	1	30.37	--	12.0	--	.73
2.5 cm	Slab	2	27.95	1.02	13.5	.7	.57
3.8 cm	Slab	2	26.72	.72	16.0	0.0	.52
5.1 cm	Slab	2	27.37	.75	17.5	2.1	.52
10.2 cm	Slab	2	23.94	1.64	19.0	0.0	.41
20.0 cm	Subm	2	23.02	.46	18.0	0.0	.40
30.0 cm	Subm	2	22.23	.09	18.0	0.0	.39
60.0 cm	Subm	2	20.31	.75	17.0	0.0	.37
120.0 cm	Subm	2	20.80	2.42	16.0	0.0	.40
180.0 cm	Subm	2	20.66	1.73	12.0	0.0	.43

Wind: 12 km/hr from 234.

Wave Height: 2-3 ft, with long swells

Bearings from Grebe taken while standing on the milkbox, compass corr. applied

Location: Station 4; starting time: 10:50 EDT

Table A16

Averaged Drogue Speeds, Bearings and Error Parameters for
August 6 Run 3

MEAN DEPTH	TYPE	# OF SGHT	SPEED CM/S	ST DEV CM/S	BEARING DEG	ST DEV DEG	$\overline{ERR^2}$ CM/(S DEG)
Confetti		1	28.24	--	22.0	--	1.15
1.2 cm	Slab	3	26.97	.73	18.3	4.7	.58
2.5 cm	Slab	2	26.38	.58	19.0	4.2	.43
3.8 cm	Slab	2	25.98	.49	21.0	2.8	.42
5.1 cm	Slab	2	24.62	.27	21.5	.7	.38
10.2 cm	Slab	2	23.82	.30	20.5	.7	.39
20.0 cm	Subm	2	23.29	.26	22.0	0.0	.37
30.0 cm	Subm	2	22.53	.09	20.0	0.0	.37
60.0 cm	Subm	2	20.49	.10	17.5	.7	.37
120.0 cm	Subm	2	19.87	.33	16.0	0.0	.38
180.0 cm	Subm	2	18.65	1.52	13.5	.7	.39

Wind: 17 km/hr from 200.

Wave Height: 2 ft, with long swells

Bearings from Grebe taken while standing on the milkbox, compass corr. applied

Location: Station 4; starting time: 11:40 EDT

Table A17

Averaged Drogue Speeds, Bearings and Error Parameters for
August 7 Run 1

MEAN DEPTH	TYPE	# OF SGHT	SPEED CM/S	ST DEV CM/S	BEARING DEG	ST DEV DEG	$\overline{ERR2}$ CM/(S DEG)
1.2 cm	Slab	2	36.83	1.85	36.0	0.0	.39
2.5 cm	Slab	2	35.68	.66	38.0	0.0	.37
3.8 cm	Slab	3	35.59	.48	38.0	0.0	.37
5.1 cm	Slab	2	34.87	.42	38.0	0.0	.38
10.2 cm	Slab	2	34.94	.54	39.0	0.0	.37
20.0 cm	Subm	2	33.33	.01	41.0	0.0	.36
30.0 cm	Subm	2	32.25	.29	40.0	0.0	.37
60.0 cm	Subm	2	31.28	.56	42.0	0.0	.38
120.0 cm	Subm	2	30.31	0.00	41.0	0.0	.41
180.0 cm	Subm	2	29.81	.45	41.0	0.0	.45

Wind: 18 km/hr from 191.

Wave Height: 2-3 ft

Bearings from Grebe taken while standing on the milkbox, compass corr. applied

Location: Station 4; starting time: 11:15 EDT

Table A18

Averaged Drogue Speeds, Bearings and Error Parameters for
August 14 Run 1

MEAN DEPTH	TYPE	# OF SGHT	SPEED CM/S	ST DEV CM/S	BEARING DEG	ST DEV DEG	$\overline{ERR2}$ CM/(S DEG)
1.2 cm	Slab	1	23.48	--	104.0	--	.31
2.5 cm	Slab	1	14.29	--	94.0	--	.55
3.8 cm	Slab	1	14.49	--	93.0	--	.49
5.1 cm	Slab	1	14.53	--	97.0	--	.51
10.2 cm	Slab	1	13.93	--	97.0	--	.53
20.0 cm	Subm	1	13.45	--	98.0	--	.54
30.0 cm	Subm	1	8.75	--	99.0	--	.88

Wind: 27 km/hr from 254.

Wave Height: 2-3 ft

Bearings from Grebe taken while standing on the milkbox, compass corr. applied

Location: Station 7; starting time: 10:40 EDT

Table A19

Averaged Drogue Speeds, Bearings and Error Parameters for
August 14 Run 2

MEAN DEPTH	TYPE	# OF SGHT	SPEED CM/S	ST DEV CM/S	BEARING DEG	ST DEV DEG	$\overline{ERR^2}$ CM/(S DEG)
1.2 cm	Slab	1	14.11	--	99.1	--	1.08
2.5 cm	Slab	1	14.55	--	100.0	--	.96
3.8 cm	Slab	1	13.91	--	103.0	--	1.09
5.1 cm	Slab	1	13.09	--	104.0	--	1.16
10.2 cm	Slab	1	15.49	--	109.0	--	1.51

Wind: 23 km/hr from 244.

Wave Height: 2-3 ft

Bearings from Grebe taken while standing on the milkbox, compass corr. applied

Location: Station 7; starting time: 11:35 EDT

Table A20

Averaged Drogue Speeds, Bearings and Error Parameters for
August 21 Run 1

MEAN DEPTH	TYPE	# OF SGHT	SPEED CM/S	ST DEV CM/S	BEARING DEG	ST DEV DEG	$\overline{ERR^2}$ CM/(S DEG)
1.2 cm	Slab	3	12.85	.56	7.0	3.5	.11
2.5 cm	Slab	3	12.37	.84	4.6	2.3	.09
3.8 cm	Slab	3	11.86	.20	8.0	1.7	.11
5.1 cm	Slab	3	11.96	.24	8.6	2.3	.11
10.2 cm	Slab	3	11.45	.48	9.0	0.0	.09
20.0 cm	Subm	3	10.44	.30	20.0	0.0	.12
30.0 cm	Subm	3	10.08	.20	19.3	2.1	.12
60.0 cm	Subm	3	9.45	.19	24.0	1.7	.12
120.0 cm	Subm	3	8.74	.31	30.3	3.8	.14
180.0 cm	Subm	3	8.31	.38	32.3	2.9	.14

Wind: 10 km/hr from 144.

Wave Height: 1 ft

Bearings from Grebe taken while standing on the bow

Location: Station 6; starting time: 11:20 EDT

Table A21

Averaged Drogue Speeds, Bearings and Error Parameters for
August 21 Run 2

MEAN DEPTH	TYPE	# OF SGHT	SPEED CM/S	ST DEV CM/S	BEARING DEG	ST DEV DEG	$\overline{ERR^2}$ CM/(S DEG)
1.2 cm	Slab	4	5.80	.17	334.5	.6	.08
2.5 cm	Slab	4	5.31	.42	333.0	.8	.10
3.8 cm	Slab	4	4.80	.23	333.0	1.4	.10
5.1 cm	Slab	4	3.98	.52	334.3	1.3	.13
10.2 cm	Slab	4	2.69	.57	335.0	0.0	.20
20.0 cm	Subm	3	2.64	.30	329.0	0.0	.07
30.0 cm	Subm	2	2.26	.18	324.0	0.0	.08
60.0 cm	Subm	1	1.63	--	298.0	--	.07
120.0 cm	Subm	1	1.69	--	216.0	--	.21
180.0 cm	Subm	1	3.62	--	189.0	--	.96

Wind: 16 km/hr from 154.

Wave Height: 1-2 ft

Bearings from Grebe taken while standing on the bow

Location: Station 6; starting time: 13:10 EDT

Table A22

Temperature and Current Meter Profiles Measured During Sighted Drogue Experiments

DEPTH M	a) JULY 23 10:00 EDT			b) JULY 24 14:00 EDT		
	SPEED CM/S	DIR DEG	TEMP °C	SPEED CM/S	DIR DEG	TEMP °C
1	*	*	18.8	*	*	19.8
2	5	327	18.8	18	*	19.8
3	5	325	18.8	15	25	19.8
4	13	18	18.8	15	25	19.5
5	17	15	18.8	18	25	19.5
6	20	15	18.5	16	13	19.0
7	20	5	18.0	15	13	18.6
8	20	5	17.9	15	45	17.0
9	23	26	17.9	10	40	16.7
10	23	26	17.8	7	15	16.5
12	18	*	16.7	9	55	16.0
14	20	18	14.8	12	35	14.0
16	22	*	12.5	10	65	10.7
18	10	39	9.6	7	72	8.7
20	3	49	8.9	8	75	7.8
22	4	45	8.7	4	50	7.8
24	2	*	8.2	2	50	7.8
26	3	*	7.8	3	65	7.8

Location - Site P
Wind Sp - 13 km/hr
Wind Dir - 335°

Location - Site Q
Wind Sp - 15 km/hr
Wind Dir - 224°

* Values unreliable or not available

Table A22
(Continued)

DEPTH M	c) JULY 24 16:00 EDT			d) JULY 25 10:00 EDT		
	SPEED CM/S	DIR DEG	TEMP °C	SPEED CM/S	DIR DEG	TEMP °C
1	*	*	19.8	*	*	17.0
2	16	35	19.8	13	75	17.0
3	17	45	19.8	23	75	17.0
4	15	45	19.7	13	70	17.0
5	18	30	19.7	17	*	17.0
6	17	30	18.9	12	80	17.0
7	12	35	17.5	12	75	17.0
8	8	35	17.1	12	85	17.0
9	18	35	16.7	8	80	16.8
10	12	30	16.4	8	65	16.6
12	6	55	15.9	8	305	15.4
14	9	35	11.9	18	325	12.5
16	15	65	9.3	20	5	10.0
18	9	85	7.8	9	5	8.8
20	6	65	7.8	15	55	8.2
22	6	45	7.8	12	35	8.1
24	3	15	7.7	10	5	8.0
26	3	5	7.4	12	25	8.0

Location - Site Q
Wind Sp - 20 km/hr
Wind Dir - 202°

Location - Site P
Wind Sp - 20 km/hr
Wind Dir - 220°

* Values unreliable or not available

Table A22
(Continued)

DEPTH M	e) JULY 29** 14:00 EDT	f) JULY 30** 10:30 EDT	g) JULY 31** 9:30 EDT	
	TEMP °C	TEMP °C	DIR DEG	TEMP °C
1	18.8	18.5	*	18.9
2	18.8	18.5	175	18.9
3	18.8	18.5	175	18.9
4	18.7	18.5	175	18.9
5	18.7	18.5	165	18.8
6	18.6	18.5	170	18.8
7	18.2	18.4	185	18.6
8	17.6	18.4	190	17.9
9	17.5	18.3	200	16.5
10	16.8	18.2	185	16.0
12	15.7	16.1	185	15.1
14	15.3	14.9	185	14.5
16	13.2	12.8	175	12.6
18	10.9	10.6	150	11.0
20	9.8	9.0	185	9.6
22	9.4	8.9	185	8.3
24	9.0	8.5	185	7.9
26	8.5	8.2	180	7.4
28	8.3	7.2	165	7.1
30	8.1	7.0	165	7.0

Location - Stat 4
Wind Sp - < 2 km/hr
Wind Dir - 226°

Location - Stat 4
Wind Sp - 19 km/hr
Wind Dir - 324°

Location - Stat 4
Wind Sp - 19 km/hr
Wind Dir - 177°

* Values unreliable or not available

** Current meter not functioning properly

Table A22
(Continued)

DEPTH M	h) AUGUST 6 9:30 EDT			i) AUGUST 7 11:00 EDT		
	SPEED CM/S	DIR DEG	TEMP °C	SPEED CM/S	DIR DEG	TEMP °C
1	*	*	20.0	*	*	20.8
2	15	40	20.0	*	*	20.8
3	20	40	20.0	30	40	20.8
4	22	45	20.0	24	35	20.8
5	20	35	20.0	32	50	20.8
6	20	35	20.0	27	52	20.8
7	20	40	20.0	26	45	20.7
8	20	25	20.0	20	45	20.6
9	17	25	20.0	24	45	20.5
10	17	35	20.0	18	25	20.5
12	18	40	20.0	12	23	19.9
14	22	25	20.0	0	-	17.4
16	15	25	20.0	0	-	14.6
18	27	20	19.9	*	*	12.6
20	20	13	16.8	*	*	11.9
22	16	45	12.2	0	-	11.1
24	11	70	11.1	0	-	9.5
26	9	105	10.2	0	-	8.1
28	0	-	9.4	0	-	7.5
30	0	-	9.0	0	-	7.1

Location - Stat 4
Wind Sp - 15 km/hr
Wind Dir - 234°

Location - Stat 4
Wind Sp - 22 km/hr
Wind Dir - 204°

* Values unreliable or unavailable

Table A22
(Continued)

j) AUGUST 21
10:00 EDT

DEPTH M	SPEED CM/S	DIR DEG	TEMP °C
1	*	*	17.7
2	12	350	17.7
3	12	305	17.7
4	10	305	17.7
5	6	315	17.7
6	4	305	17.7
7	4	305	17.7
8	8	275	17.5
9	10	245	17.5
10	10	255	17.5
12	15	255	17.3
14	8	305	12.5
16	5	300	11.9
18	3	330	11.4
20	4	300	10.0
22	4	245	9.2
24	7	245	8.2
26	0	-	8.0
28	0	-	7.9
30	0	-	7.2

Location - Stat 6
Wind Dir - 154°

* Values unreliable or unavailable

Table A23

August 12

Drogue Positions and Velocities (coordinate origin at transponder A)
 Calculated from Quadratic Regressions of Position Component as a Function of Time

DROGUE (MEAN DEPTH)	TIME (EDT)	# OF POS IN REG	EAST POS M	NORTH POS M	EAST VEL CM/S	STD ERR CM/S	NORTH VEL CM/S	STD ERR CM/S	SPEED CM/S	DIR DEG
30 cm Surf Slab	15:30	70	-1292	-1164	-11.72	0.02	-.83	0.02	11.75	266.0
0.9 m Subm Slab		36	Before Release							
1.5 m Subm Slab		39	-1209	-977	-15.82	0.06	7.97	0.05	17.72	296.7
2.75 m Subm Slab		37	-1028	-1054	-17.12	0.06	5.63	0.07	18.02	288.2
30 cm Surf Slab	16:00	70	-1472	-1155	-8.29	0.05	1.87	0.05	8.50	282.7
0.9 m Subm Slab		36	-1134	-998	-13.15	0.04	7.48	0.03	15.13	299.6
1.5 m Subm Slab		39	-1455	-815	-11.44	0.09	10.03	0.08	15.22	311.2
2.75 Subm Slab		37	-1296	-933	-12.68	0.02	7.82	0.03	14.89	301.7
30 cm Surf Slab	16:30	70	-1590	-1097	-4.87	0.09	4.58	0.10	6.68	313.2
0.9 m Subm Slab		36	-1324	-823	-8.00	0.14	11.97	0.13	14.40	326.2
1.5 m Subm Slab		39	-1621	-616	-7.06	0.19	12.98	0.17	14.01	329.7
2.75 m Subm Slab		37	-1484	-773	-8.23	0.08	10.01	0.10	12.96	320.6

Slab Dimensions: 90 cm x 90 cm x 60 cm
 Wave Height: 3-5 feet, decreasing

Table A24

August 14

Drogue Velocities Calculated from Linear Regressions of
 Position Component as a Function of Time

DROGUE (MEAN DEPTH)	TIMES (EDT)	# OF POS IN REG	EAST VEL CM/S	STD ERR CM/S	NORTH VEL CM/S	STD ERR CM/S	SPEED CM/S	DIR DEG
14 cm Surf Cylinder	10:40-12:05	9	20.18	0.23	-2.47	0.18	20.33	97.0
0.9 m Subm Slab	10:46-11:59	27	13.36	0.28	-7.38	0.18	15.26	118.9
1.5 m Subm Slab	10:43-11:58	40	11.93	0.30	-8.31	0.21	14.54	124.9

Slab Dimensions: 90 cm x 90 cm x 60 cm
 Wave Height: 2-3 feet

Table A25

August 15

Drogue Positions and Velocities Calculated from Quadratic Regressions
of Position Component as a Function of Time

DROGUE (MEAN DEPTH)	TIME (EDT)	# OF POS IN REG	EAST POS M	NORTH POS M	EAST VEL CM/S	STD ERR CM/S	NORTH VEL CM/S	STD ERR CM/S	SPEED CM/S	DIR DEG
14 cm Surf Cyl	12:00	29	-1131	-912	-6.13	0.07	5.51	0.06	8.25	312.0
30 cm Surf Slab		Time Before Release								
0.9 m Subm Slab		38	-1299	-903	-6.70	0.02	3.71	0.02	7.66	298.9
2.75 m Subm Slab		41	-1178	-909	-6.64	0.01	4.87	0.01	8.23	306.2
5.2 m Subm Slab		40	-1090	-936	-6.68	0.02	5.94	0.02	8.94	311.6
14 cm Surf Cyl	12:30	29	-1217	-817	-3.43	0.04	5.08	0.04	6.13	326.0
30 cm Surf Slab		40	-1413	-1288	-4.04	0.04	-3.64	0.03	5.43	228.0
0.9 m Subm Slab		38	-1397	-838	-4.17	0.01	3.51	0.01	5.46	310.1
2.75 m Subm Slab		41	-1275	-824	-4.13	0.01	4.56	0.01	6.15	317.8
5.2 m Subm Slab		40	-1188	-835	-4.22	0.01	5.28	0.01	6.76	321.4
14 cm Surf Cyl	13:00	29	-1254	-729	-.73	0.05	4.64	0.05	4.70	351.1
30 cm Surf Slab		40	-1469	-1370	-2.20	0.02	-5.44	0.02	5.87	202.0
0.9 m Subm Slab		38	-1450	-777	-1.64	0.01	3.32	0.01	3.70	333.6
2.75 m Subm Slab		41	-1327	-745	-1.62	0.01	4.25	0.01	4.55	339.1
5.2 m Subm Slab		40	-1242	-746	-1.76	0.01	4.63	0.01	4.95	339.2
14 cm Surf Cyl	13:30	29	-1243	-649	1.97	0.09	4.21	0.09	4.65	25.1
30 cm Surf Slab		40	-1492	-1484	-.36	0.02	-7.24	0.01	7.25	182.8
0.9 m Subm Slab		38	-1457	-719	.89	0.01	3.12	0.02	3.25	15.8
2.75 m Subm Slab		41	-1334	-671	.88	0.01	3.94	0.01	4.04	12.6
5.2 m Subm Slab		40	-1251	-668	.71	0.01	3.98	0.01	4.04	10.1
14 cm Surf Cyl	14:00	29	-1183	-578	4.68	0.14	3.77	0.13	6.01	51.1
30 cm Surf Slab		40	-1482	-1631	1.48	0.03	-9.05	0.03	9.17	170.7
0.9 m Subm Slab		38	-1418	-664	3.42	0.02	2.93	0.02	4.50	49.4
2.75 m Subm Slab		41	-1295	-603	3.39	0.01	3.64	0.02	4.97	43.0
5.2 m Subm Slab		40	-1216	-603	3.17	0.02	3.32	0.02	4.59	43.6

Slab Dimensions: 90 cm x 90 cm x 60 cm
Wave Height: 2 feet increasing to 4 feet

Table A26

August 20

Drogue Positions and Velocities Calculated from Quadratic Regressions
of Position Component as a Function of Time

DROGUE (MEAN DEPTH)	TIME (EDT)	# OF POS IN REG	EAST POS M	NORTH POS M	EAST VEL CM/S	STD ERR CM/S	NORTH VEL CM/S	STD ERR CM/S	SPEED CM/S	DIR DEG
46 cm Subm Slab	12:30	36	-768	-928	7.89	0.04	-8.22	0.04	11.39	136.2
1.2 m Subm Slab		51	-663	-1220	2.29	0.01	-11.48	0.02	11.71	168.7
2.45 m Subm Slab		48	-743	-1277	1.09	0.02	-13.02	0.02	13.07	175.2
5.2 m Subm Slab		31	-816	-1261	-1.09	0.02	-15.19	0.02	15.22	184.1
46 cm Subm Slab	13:00	36	-645	-1100	5.86	0.02	-10.83	0.02	12.31	151.6
1.2 m Subm Slab		51	-628	-1454	1.58	0.01	-14.53	0.01	14.62	173.8
2.45 m Subm Slab		48	-732	-1539	.06	0.01	-16.11	0.01	16.11	179.8
5.2 m Subm Slab		31	-854	-1557	-3.15	0.01	-17.69	0.01	17.97	190.1
46 cm Subm Slab	13:30	36	-558	-1318	3.82	0.01	-13.45	0.01	13.98	164.1
1.2 m Subm Slab		51	-606	-1743	.87	0.02	-17.59	0.02	17.61	177.2
2.45 m Subm Slab		48	-740	-1856	-.98	0.02	-19.19	0.02	19.21	182.9
5.2 m Subm Slab		31	-929	-1898	-5.21	0.03	-20.19	0.02	20.85	194.5
46 cm Subm Slab	14:00	36	-507	-1584	1.78	0.02	-16.06	0.02	16.16	173.7
1.2 m Subm Slab		51	-597	-2087	.16	0.03	-20.65	0.04	20.65	179.6
2.45 m Subm Slab		48	-767	-2229	-2.02	0.03	-22.27	0.03	22.36	185.2
5.2 m Subm Slab		31	-1042	-2284	-7.27	0.04	-22.70	0.04	23.83	197.8

Slab Dimensions: 68 cm x 68 cm x 30 cm
Wave Height: ~ 1 ft growing slowly

Table A27

August 21
 Drogue Positions and Velocities Calculated from Quadratic Regressions
 of Position Component as a Function of Time

DROGUE (MEAN DEPTH)	TIME (EDT)	# OF POS IN REG	EAST POS M	NORTH POS M	EAST VEL CM/S	STD ERR CM/S	NORTH VEL CM/S	STD ERR CM/S	SPEED CM/S	DIR DEG
10 cm Surf Slab	11:35	17	-1134	-462	-5.51	0.06	6.10	0.02	8.22	317.9
7.6 cm Diamond		19	-969	-788	-.27	0.04	1.57	0.06	1.59	350.1
46 cm Subm Slab		34	-929	-1008	-.65	0.03	-4.60	0.02	4.64	188.0
1.2 m Subm Slab		31	-870	-1052	-.31	0.03	-8.75	0.03	8.76	182.0
2.45 m Subm Slab		30	-915	-1116	.50	0.05	-11.16	0.06	11.17	177.5
5.2 m Subm Slab	37	-906	-1141	-1.17	0.03	-9.61	0.03	9.68	187.0	
10 cm Surf Slab	12:30	17	-1399	-429	-10.52	0.08	-4.10	0.03	11.29	248.7
7.6 cm Diamond		19	-1040	-820	-4.05	0.02	-3.49	0.03	5.35	229.2
46 cm Subm Slab		34	-1002	-1182	-3.78	0.01	-5.94	0.01	7.04	212.5
1.2 m Subm Slab		31	-940	-1350	-3.93	0.02	-9.30	0.02	10.09	202.9
2.45 m Subm Slab		30	-980	-1513	-4.48	0.03	-12.89	0.03	13.65	199.2
5.2 m Subm Slab	37	-1027	-1482	-6.18	0.01	-11.07	0.01	12.68	209.2	
10 cm Surf Slab	13:30	11	-2021	-681	-18.98	0.10	-6.72	0.18	20.13	250.5
7.6 cm Diamond		19	-1260	-1045	-8.17	0.02	-9.01	0.03	12.17	222.2
46 cm Subm Slab		34	-1199	-1422	-7.19	0.01	-7.40	0.01	10.32	224.2
1.2 m Subm Slab		31	-1153	-1695	-7.88	0.01	-9.89	0.01	12.64	218.6
2.45 m Subm Slab		30	-1239	-2011	-9.90	0.02	-14.79	0.03	17.80	213.8
5.2 m Subm Slab	37	-1348	-1909	-11.64	0.02	-12.66	0.01	17.20	222.6	
10 cm Surf Slab	14:30	11	-2565	-953	-11.25	0.08	-8.39	0.13	14.03	233.3
7.6 cm Diamond		19	-1629	-1469	-12.29	0.05	-14.53	0.07	19.04	220.2
46 cm Subm Slab		34	-1520	-1714	-10.61	0.03	-8.85	0.02	13.82	230.1
1.2 m Subm Slab		31	-1508	-2062	-11.83	0.03	-10.48	0.03	15.80	228.5
2.45 m Subm Slab		30	-1693	-2577	-15.33	0.05	-16.68	0.05	22.65	222.6
5.2 m Subm Slab	37	-1865	-2394	-17.10	0.03	-14.26	0.03	22.27	230.2	

Slab Dimensions: 68 cm x 68 cm x 30 cm
 Wave Height: 1 ft increasing to 2 ft

Table A28

Temperature and Current Meter Profiles Measured at Flag Station 8
During Acoustic Drogue Experiments

DEPTH M	a) AUGUST 12 16:00 EDT			b) AUGUST 14 11:30 EDT		
	SPEED CM/S	DIR DEG	TEMP °C	SPEED CM/S	DIR DEG	TEMP °C
1	*	*	21.0	*	*	20.0
2	22	310	21.0	8	115	20.0
3	26	305	21.0	10	105	20.0
4	28	310	21.0	12	145	20.0
5	20	307	21.0	10	145	20.0
6	19	307	21.0	10	143	20.0
7	20	310	20.9	9	145	19.8
8	12	325	20.0	5	123	19.8
9	6	323	19.8	6	155	19.8
10	6	15	19.5	3	185	19.8
12	6	300	12.2	2	215	19.8
14	6	295	11.4	2	275	19.5
16	14	328	9.1	9	340	17.0
18	8	328	7.9	14	35	12.0
20	7	20	7.7	17	45	10.8
22	2	15	7.2	14	55	9.0
24	10	15	7.0	10	50	7.7
26	4	20	6.2	8	45	7.1
28	2	47	6.1	5	45	6.8
30	5	45	5.8	8	15	6.6
35	*	*	5.3	8	15	6.0
40	-	-	-	4	15	5.2

* Values unavailable or unreliable

Table A28
(Continued)

DEPTH M	c) AUGUST 15 12:00 EDT			d) AUGUST 20 13:00 EDT		
	SPEED CM/S	DIR DEG	TEMP °C	SPEED CM/S	DIR DEG	TEMP °C
1	*	*	20.3	*	*	19.9
2	10	315	20.3	20	145	19.9
3	12	315	20.3	22	155	19.9
4	12	315	20.3	20	165	19.9
5	12	300	**	20	180	19.9
6	8	315		20	190	19.9
7	11	340		20	225	19.9
8	10	*		22	230	19.9
9	11	335		18	215	18.6
10	10	335		16	207	18.0
12	10	65		16	235	15.2
14	3	175		8	245	13.2
16	2	175		5	235	10.8
18	6	300		4	255	9.5
20	10	55		8	275	9.0
22	12	65		13	295	8.1
24	10	55		8	295	7.7
26	8	325		7	305	7.2
28	10	305		8	325	7.0
30	6	355		4	325	6.7
35	12	75		8	335	6.0

* Values unavailable or unreliable

** Temperature probe failed

Table A28
(Continued)

DEPTH M	e) AUGUST 21 11:30 EDT			f) AUGUST 21 14:30 EDT		
	SPEED CM/S	DIR DEG	TEMP °C	SPEED CM/S	DIR DEG	TEMP °C
1	*	*	18.4	*	*	19.2
2	10	185	18.4	18	255	19.2
3	11	165	18.4	20	237	19.2
4	14	190	18.4	20	240	19.2
5	13	185	18.4	21	240	19.1
6	10	190	18.4	22	245	18.9
7	10	200	18.2	19	255	18.8
8	10	215	18.1	20	255	18.3
9	10	205	18.1	16	260	18.1
10	11	215	18.0	20	275	17.9
12	11	225	17.7			
14	8	325	13.8			
16	8	305	13.1			
18	5	295	12.2			
20	6	265	10.0			
22	1	325	8.9			
24	3	5	8.0			
26	4	345	7.9			
28	1	295	7.7			
30	2	290	7.1			
35	5	255	6.8			
40	9	225	6.2			

* Values unavailable or unreliable

Table A29

Averaged Drogue Speeds, Bearings and Error Parameters for
August 17 Run 1

MEAN DEPTH	TYPE	# OF SGHT	SPEED CM/S	ST DEV CM/S	BEARING DEG	ST DEV DEG	$\overline{ERR^2}$ CM/(S DEG)
1.2 cm	Slab	3	7.35	.32	333.0	0.0	.06
2.5 cm	Slab	3	6.99	.23	329.7	1.2	.08
3.8 cm	Slab	3	6.56	.35	328.0	0.0	.08
5.1 cm	Slab	3	6.28	.40	327.0	1.7	.10
10.2 cm	Slab	3	5.73	.18	327.0	4.0	.12
20.0 cm	Subm	3	4.55	.47	327.0	0.0	.06
30.0 cm	Subm	3	4.05	.43	325.0	1.7	.09
60.0 cm	Subm	3	2.77	.16	318.0	0.0	.06
120.0 cm	Subm	1	1.61	--	254.0	--	.09
180.0 cm	Subm	1	5.88	--	205.0	--	.55

Wind: None

Waves: None

Bearings from Grebe taken while standing on the bow

Location: Station 4; starting time: 10:50 EDT

Table A30

Averaged Drogue Speeds, Bearings and Error Parameters for
August 17 Run 2

MEAN DEPTH	TYPE	# OF SGHT	SPEED CM/S	ST DEV CM/S	BEARING DEG	ST DEV DEG	$\overline{ERR^2}$ CM/(S DEG)
1.2 cm	Slab	5	12.08	.53	197.2	1.8	.21
2.5 cm	Slab	5	11.16	.25	194.4	.9	.23
3.8 cm	Slab	5	11.09	.38	196.4	.9	.22
5.1 cm	Slab	5	11.29	.28	200.0	0.0	.21
10.2 cm	Slab	5	12.15	.49	204.0	0.0	.21
20.0 cm	Subm	5	12.00	.29	200.4	2.2	.25
30.0 cm	Subm	5	12.34	.61	206.4	.9	.22
60.0 cm	Subm	5	13.10	.60	209.0	0.0	.24
120.0 cm	Subm	5	14.79	.78	213.8	.5	.20
180.0 cm	Subm	5	16.21	.82	214.0	.7	.20

Wind: None

Waves: None

Bearings from the Grebe taken while standing on the bow

Location: Station 5; starting time: 13:50 EDT

Woods Hole Oceanographic Institution

Distribution List

Library
Marine Physical Laboratory
Scripps Inst. of Oceanography
San Diego, CA 92152

Library
Rosensteil School of Marine
and Atmospheric Science
Univ. of Miami
10 Rickenbacker Causeway
Miami, FL 33146

Library
Dept. of Oceanography and
Meteorology
Texas A & M Univ.
College Station, TX 77843

Library, School of Science
Oregon State Univ.
Corvallis, OR 97331

Fisheries-Oceanography Library
151 Oceanography Teaching Bldg.
Univ. of Washington
Seattle, WA 98195

Library
Inst. of Marine Science
Univ. of Alaska
College, AK 99701

Florida Atlantic University
Library Acq./Serials
Boca Raton, FL 33431

Pell Marine Science Library
Graduate School of Oceanography
Univ. of Rhode Island
Kingston, RI 02881

Library
Inst. of Geophysics
Univ. of Hawaii
Honolulu, HI 96822

Marine Resources Reference Center
Mass. Inst. of Tech.
Cambridge, MA 02139

Chairman
Dept. of Earth & Planetary Sciences
Mass. Inst. of Tech.
Cambridge, MA 02139

Ms. Bettylou Rosen, Librarian
NOAA Miami Library
c/o Atlantic Oceanographic &
Meteorological Laboratory
15 Rickenbacker Causeway
Miami, FL 33140

M.I.T. Libraries
SER. JRL. Rm. 14E-210
Massachusetts Institute of Technology
Cambridge, MA U.S.A. 02139

Library
Chesapeake Bay Inst.
Johns Hopkins Univ.
Baltimore, MD 21218

Blue Hill Library
Harvard University
Pierce Hall - Oxford Street
Cambridge, MA 02138

Hancock Library of Bio. & Ocean.
Alan Hancock Laboratory
Univ. of Southern California
Los Angeles, CA 90007

Pearse Memorial Library
Duke Univ. Marine Laboratory
Beaufort, NC 28516

Library
Dept. of Oceanography
Florida State Univ.
Tallahassee, FL 32306

Library
Lamont-Doherty Geo. Observatory
Palisades, NY 10964

Library
Physical Oceanographic Lab.
Nova Univ.
8000 N. Ocean Drive
Dania, FL 33304

Library: Docs/Repts/Trans Sec.
Scripps Inst. of Oceanography
P.O. Box 2367
La Jolla, CA 92093

Library
Skidaway Inst. of Oceanography
P.O. Box 13687
Savannah, GA 31406-0687

Commanding Officer
U.S. Coast Guard Ocean. Unit
Bldg. 159 E Navy Yard Annex
Washington, DC 20390

Mrs. Shirley Robinson
Library
The Oceanic Institute
Makapuu Point
Waimanalo, Hawaii 96795

Virginia Institute of Marine Science
Attn: Janice Meadows, Asst. Librarian
Gloucester Point, VA 23062

REPORT DOCUMENTATION PAGE	1. REPORT NO. WHOI-81-91	2.	3. Recipient's Accession No.
4. Title and Subtitle ACOUSTICALLY AND VISUALLY TRACKED DROGUE MEASUREMENTS OF NEARSURFACE WATER VELOCITIES IN LAKE HURON, PLUS OBSERVATIONS OF A COASTAL UPWELLING		5. Report Date October 1981	
7. Author(s) J. H. Churchill and B.H. Pade		6.	
9. Performing Organization Name and Address Woods Hole Oceanographic Institution Woods Hole, Massachusetts 02543		8. Performing Organization Rept. No.	
12. Sponsoring Organization Name and Address The Department of Energy and The National Oceanic and Atmospheric Administration		10. Project/Task/Work Unit No.	
15. Supplementary Notes This report should be cited as: Woods Hole Oceanog. Inst. Tech. Rept. WHOI-81-91.		11. Contract(C) or Grant(G) No. (C) DE AC02-79EV10005 (G) 03-5-022-26	
16. Abstract (Limit: 200 words) During July and August of 1980 our research group measured nearsurface water velocity near the eastern coast of Lake Huron by tracking drogues using acoustic travel time and compass sighting techniques. The velocity fields appeared to consist of two components. These have been termed: a sub-current, which varied slowly with depth (compared to the deepest drogue depth of 5.2. m) and, in most cases, was apparently in geostrophic balance with the cross shore pressure gradient; and, a surface layer-current (defined by the relative velocity from deeper to shallower drogues) which decayed rapidly with depth and was directed nearly parallel with the wind and waves. There was, however, a direct dependence of relative velocity with estimated surface roughness, suggesting that Stokes drift may have been primarily responsible for the shear. The magnitudes of the observed relative velocities were approximately equal to Stokes drift magnitudes calculated from representative wave energy spectra. Also reported are measurements of current and temperature structure made prior to and following a coastal upwelling.		13. Type of Report & Period Covered Technical	
17. Document Analysis a. Descriptors 1. Acoustic and sighted drogue studies 2. Wind-driven currents 3. Nearsurface water velocities b. Identifiers/Open-Ended Terms c. COSATI Field/Group			
18. Availability Statement		19. Security Class (This Report) Unclassified	21. No. of Pages 122
		20. Security Class (This Page)	22. Price

<p>Woods Hole Oceanographic Institution WHOI-81-91</p> <p>ACOUSTICALLY AND VISUALLY TRACKED DROGUE MEASUREMENTS OF NEARSURFACE WATER VELOCITIES IN LAKE HURON, PLUS OBSERVATIONS OF A COASTAL UPWELLING by J.H. Churchill and B.H. Paade. 122 pages. Prepared for the Department of Energy under Contract DE AC02-79EV10005 and the National Oceanic and Atmospheric Administration under Contract 03-5-022-26.</p>	<p>Woods Hole Oceanographic Institution WHOI-81-91</p> <p>ACOUSTICALLY AND VISUALLY TRACKED DROGUE MEASUREMENTS OF NEARSURFACE WATER VELOCITIES IN LAKE HURON, PLUS OBSERVATIONS OF A COASTAL UPWELLING by J.H. Churchill and B.H. Paade. 122 pages. Prepared for the Department of Energy under Contract DE AC02-79EV10005 and the National Oceanic and Atmospheric Administration under Contract 03-5-022-26.</p>	<p>Woods Hole Oceanographic Institution WHOI-81-91</p> <p>ACOUSTICALLY AND VISUALLY TRACKED DROGUE MEASUREMENTS OF NEARSURFACE WATER VELOCITIES IN LAKE HURON, PLUS OBSERVATIONS OF A COASTAL UPWELLING by J.H. Churchill and B.H. Paade. 122 pages. Prepared for the Department of Energy under Contract DE AC02-79EV10005 and the National Oceanic and Atmospheric Administration under Contract 03-5-022-26.</p>	<p>Woods Hole Oceanographic Institution WHOI-81-91</p> <p>ACOUSTICALLY AND VISUALLY TRACKED DROGUE MEASUREMENTS OF NEARSURFACE WATER VELOCITIES IN LAKE HURON, PLUS OBSERVATIONS OF A COASTAL UPWELLING by J.H. Churchill and B.H. Paade. 122 pages. Prepared for the Department of Energy under Contract DE AC02-79EV10005 and the National Oceanic and Atmospheric Administration under Contract 03-5-022-26.</p>
<p>1. Acoustic and sighted drogue studies</p> <p>2. Wind-driven currents</p> <p>3. Nearsurface water velocities</p> <p>I. Churchill, J.H.</p> <p>II. Paade, B.H.</p> <p>III. DE AC02-79EV10005</p> <p>IV. 03-5-022-26</p> <p>This card is UNCLASSIFIED</p>	<p>1. Acoustic and sighted drogue studies</p> <p>2. Wind-driven currents</p> <p>3. Nearsurface water velocities</p> <p>I. Churchill, J.H.</p> <p>II. Paade, B.H.</p> <p>III. DE AC02-79EV10005</p> <p>IV. 03-5-022-26</p> <p>This card is UNCLASSIFIED</p>	<p>1. Acoustic and sighted drogue studies</p> <p>2. Wind-driven currents</p> <p>3. Nearsurface water velocities</p> <p>I. Churchill, J.H.</p> <p>II. Paade, B.H.</p> <p>III. DE AC02-79EV10005</p> <p>IV. 03-5-022-26</p> <p>This card is UNCLASSIFIED</p>	<p>1. Acoustic and sighted drogue studies</p> <p>2. Wind-driven currents</p> <p>3. Nearsurface water velocities</p> <p>I. Churchill, J.H.</p> <p>II. Paade, B.H.</p> <p>III. DE AC02-79EV10005</p> <p>IV. 03-5-022-26</p> <p>This card is UNCLASSIFIED</p>
<p>During July and August 1980 our research group measured nearsurface water velocities near the eastern coast of Lake Huron by tracking drogues using acoustic travel time and compass sighting techniques. The velocity fields appeared to consist of two components. These have been termed: a sub-current, which varied slowly with depth (compared to the deepest drogue depth of 5.2 m) and, in most cases, was apparently in geostrophic balance with the cross shore pressure gradient; and, a surface layer-current (defined by the relative velocity from deeper to shallower drogues) which decayed rapidly with depth and was directed nearly parallel with the wind and waves. There was no discernable relationship between wind speed and relative velocity. There was, however, a direct dependence of relative velocity with estimated surface roughness, suggesting that Stokes drift may have been primarily responsible for the shear. The magnitudes of the observed relative velocities were approximately equal to Stokes drift magnitudes calculated from representative wave energy spectra. Also reported are measurements of current and temperature structure made prior to and following a coastal upwelling.</p>	<p>During July and August 1980 our research group measured nearsurface water velocities near the eastern coast of Lake Huron by tracking drogues using acoustic travel time and compass sighting techniques. The velocity fields appeared to consist of two components. These have been termed: a sub-current, which varied slowly with depth (compared to the deepest drogue depth of 5.2 m) and, in most cases, was apparently in geostrophic balance with the cross shore pressure gradient; and, a surface layer-current (defined by the relative velocity from deeper to shallower drogues) which decayed rapidly with depth and was directed nearly parallel with the wind and waves. There was no discernable relationship between wind speed and relative velocity. There was, however, a direct dependence of relative velocity with estimated surface roughness, suggesting that Stokes drift may have been primarily responsible for the shear. The magnitudes of the observed relative velocities were approximately equal to Stokes drift magnitudes calculated from representative wave energy spectra. Also reported are measurements of current and temperature structure made prior to and following a coastal upwelling.</p>	<p>During July and August 1980 our research group measured nearsurface water velocities near the eastern coast of Lake Huron by tracking drogues using acoustic travel time and compass sighting techniques. The velocity fields appeared to consist of two components. These have been termed: a sub-current, which varied slowly with depth (compared to the deepest drogue depth of 5.2 m) and, in most cases, was apparently in geostrophic balance with the cross shore pressure gradient; and, a surface layer-current (defined by the relative velocity from deeper to shallower drogues) which decayed rapidly with depth and was directed nearly parallel with the wind and waves. There was no discernable relationship between wind speed and relative velocity. There was, however, a direct dependence of relative velocity with estimated surface roughness, suggesting that Stokes drift may have been primarily responsible for the shear. The magnitudes of the observed relative velocities were approximately equal to Stokes drift magnitudes calculated from representative wave energy spectra. Also reported are measurements of current and temperature structure made prior to and following a coastal upwelling.</p>	<p>During July and August 1980 our research group measured nearsurface water velocities near the eastern coast of Lake Huron by tracking drogues using acoustic travel time and compass sighting techniques. The velocity fields appeared to consist of two components. These have been termed: a sub-current, which varied slowly with depth (compared to the deepest drogue depth of 5.2 m) and, in most cases, was apparently in geostrophic balance with the cross shore pressure gradient; and, a surface layer-current (defined by the relative velocity from deeper to shallower drogues) which decayed rapidly with depth and was directed nearly parallel with the wind and waves. There was no discernable relationship between wind speed and relative velocity. There was, however, a direct dependence of relative velocity with estimated surface roughness, suggesting that Stokes drift may have been primarily responsible for the shear. The magnitudes of the observed relative velocities were approximately equal to Stokes drift magnitudes calculated from representative wave energy spectra. Also reported are measurements of current and temperature structure made prior to and following a coastal upwelling.</p>
<p>1. Acoustic and sighted drogue studies</p> <p>2. Wind-driven currents</p> <p>3. Nearsurface water velocities</p> <p>I. Churchill, J.H.</p> <p>II. Paade, B.H.</p> <p>III. DE AC02-79EV10005</p> <p>IV. 03-5-022-26</p> <p>This card is UNCLASSIFIED</p>	<p>1. Acoustic and sighted drogue studies</p> <p>2. Wind-driven currents</p> <p>3. Nearsurface water velocities</p> <p>I. Churchill, J.H.</p> <p>II. Paade, B.H.</p> <p>III. DE AC02-79EV10005</p> <p>IV. 03-5-022-26</p> <p>This card is UNCLASSIFIED</p>	<p>1. Acoustic and sighted drogue studies</p> <p>2. Wind-driven currents</p> <p>3. Nearsurface water velocities</p> <p>I. Churchill, J.H.</p> <p>II. Paade, B.H.</p> <p>III. DE AC02-79EV10005</p> <p>IV. 03-5-022-26</p> <p>This card is UNCLASSIFIED</p>	<p>1. Acoustic and sighted drogue studies</p> <p>2. Wind-driven currents</p> <p>3. Nearsurface water velocities</p> <p>I. Churchill, J.H.</p> <p>II. Paade, B.H.</p> <p>III. DE AC02-79EV10005</p> <p>IV. 03-5-022-26</p> <p>This card is UNCLASSIFIED</p>